

TECHNICAL REPORT STANDARD PAGE

1. Title and Subtitle
Prediction of Road Condition and Smoothness for Flexible and Rigid Pavements in Louisiana Using Neural Networks
2. Author(s)
Zhong Wu, Ph.D., P.E., and Yilong Liu, Ph.D.
3. Performing Organization Name and Address
Louisiana Transportation Research Center
4101 Gourrier Avenue Baton Rouge, LA 70808
4. Sponsoring Agency Name and Address
Louisiana Department of Transportation and Development
P.O. Box 94245
Baton Rouge, LA 70804-9245
5. Report No.
FHWA/LA.24/694
6. Report Date
March 2024
7. Performing Organization Code
LTRC Project Number: 21-1P
SIO Number: DOTLT1000376
8. Type of Report and Period Covered
Final Report
August 2020 – June 2023
9. No. of Pages
118
10. Supplementary Notes
Conducted in Cooperation with the U.S. Department of Transportation, Federal Highway Administration
11. Distribution Statement
Unrestricted. This document is available through the National Technical Information Service, Springfield, VA 21161.
12. Key Words
Pavement performance modeling, pavement management system, artificial neural network
13. Abstract

The Louisiana Department of Transportation and Development (DOTD) currently utilizes pavement performance prediction models in treatment selection and budget planning. These models are solely based on the non-linear curve-fitting regression of existing pavement condition data available in its pavement management system (PMS) database. The objective of the research was to develop short-term and long-term pavement performance prediction models to estimate future pavement condition and smoothness for flexible and rigid pavements using artificial neural network (ANN) modeling. To achieve the objective, two different pavement condition datasets were prepared— one each for short-term and long-term pavement performance prediction. The datasets were assembled based on DOTD’s PMS and other pavement project management data sources. A feedforward neural network technique was used in the training, validation, and testing of the ANN modeling. Specifically, this study developed three groups of ANN pavement performance prediction models: 17 individual neural network models for short-term federal-designated cracking percent prediction, 8 incremental ANN models for long-term asphalt overlay pavement performance prediction, and 5 ANN-based regression models for asphalt

pavement family curve generation. The developed short-term models will be used to support DOTD's prediction of 2- and 4-year performance target values for federal pavement condition assessment. On the other hand, the incremental long-term performance models can be utilized to forecast pavement condition even with limited historical performance records, which are insufficient for developing site-specific curves. The developed ANN-based family curves, which incorporate additional factors such as climate and traffic, may replace the current family curves used in DOTD's PMS with improved accuracy and flexibility.

Project Review Committee

Each research project will have an advisory committee appointed by the LTRC Director. The Project Review Committee is responsible for assisting the LTRC Administrator or Manager in developing acceptable research problem statements, requests for proposals, reviewing research proposals, overseeing approved research projects, and implementing findings.

LTRC appreciates the dedication of the following Project Review Committee Members in guiding this research study to fruition.

LTRC Administrator/Manager

Zhongjie “Doc” Zhang, Ph.D., P.E.

Pavement and Geotechnical Research Administrator

Members

Christophe Fillastre

Angela Murrell

Samuel Cooper, III

Xingwei Chen

Patrick Icenogle

Amar Raghavendra

Scott Nelson, FHWA

Directorate Implementation Sponsor

Chad Winchester, P.E.

DOTD Chief Engineer

Prediction of Road Condition and Smoothness for Flexible and Rigid Pavements in Louisiana Using Neural Networks

By

Zhong Wu, Ph.D., P.E.

Yilong Liu, Ph.D.

Louisiana Transportation Research Center
4101 Gourrier Avenue
Baton Rouge, LA 70808

LTRC Project No. 21-1P
SIO No. DOTLT1000376

conducted for

Louisiana Department of Transportation and Development
Louisiana Transportation Research Center

The contents of this report reflect the views of the author/principal investigator who is responsible for the facts and the accuracy of the data presented herein.

The contents do not necessarily reflect the views or policies of the Louisiana Department of Transportation and Development, the Federal Highway Administration or the Louisiana Transportation Research Center. This report does not constitute a standard, specification, or regulation.

March 2024

Abstract

The Louisiana Department of Transportation and Development (DOTD) currently utilizes pavement performance prediction models in treatment selection and budget planning. These models are solely based on the non-linear curve-fitting regression of existing pavement condition data available in its pavement management system (PMS) database. The objective of the research was to develop short-term and long-term pavement performance prediction models to estimate future pavement condition and smoothness for flexible and rigid pavements using artificial neural network (ANN) modeling. To achieve the objective, two different pavement condition datasets were prepared— one each for short-term and long-term pavement performance prediction. The datasets were assembled based on DOTD’s PMS and other pavement project management data sources. A feedforward neural network technique was used in the training, validation, and testing of the ANN modeling. Specifically, this study developed three groups of ANN pavement performance prediction models: 17 individual neural network models for short-term federal-designated cracking percent prediction, 8 incremental ANN models for long-term asphalt overlay pavement performance prediction, and 5 ANN-based regression models for asphalt pavement family curve generation. The developed short-term models will be used to support DOTD’s prediction of 2 and 4 year performance target values for federal pavement condition assessment. On the other hand, the incremental long-term performance models can be utilized to forecast pavement condition even with limited historical performance records, which are insufficient for developing site-specific curves. The developed ANN-based family curves, which incorporate additional factors such as climate and traffic, may replace the current family curves used in DOTD’s PMS with improved accuracy and flexibility.

Acknowledgments

This study was supported by the Louisiana Transportation Research Center (LTRC) and the Louisiana Department of Transportation and Development (DOTD) under LTRC Research Project Number 21-1P. The authors would like to express thanks to Christophe Fillastre, Christopher Cole, and other DOTD engineers who provided valuable help in this study.

Implementation Statement

The research methodology and findings provided in this study for ANN modeling and predicting short-term and long-term pavement performance can be implemented by DOTD in making a reliable and cost-effective project selection and budget allocation for pavement maintenance and rehabilitation. The developed short-term percent cracking models are recommended to implement directly into the FHWA-required pavement condition assessment analysis for DOTD's Interstate and NHS pavements. The incremental long-term performance models can be applied to forecast pavement conditions when historical performance records are not sufficient for developing site-specific curves. The developed ANN-based family curves can be used to replace current ones with better accuracy and flexibility, incorporating factors such as climate and traffic.

Table of Contents

Technical Report Standard Page	1
Project Review Committee	3
LTRC Administrator/Manager	3
Members	3
Directorate Implementation Sponsor	3
Prediction of Road Condition and Smoothness for Flexible and Rigid Pavements in Louisiana Using Neural Networks.....	4
Abstract	5
Acknowledgments.....	6
Implementation Statement	7
Table of Contents	8
List of Tables.....	9
List of Figures.....	10
Introduction.....	12
Literature Review.....	16
Pavement Performance Models	16
Review of Pavement Condition Datasets.....	32
Objective.....	39
Scope.....	40
Methodology.....	41
Project Selection and Data Collection	41
Pavement Performance Prediction Using Machine Learning.....	51
Discussion of Results.....	60
Short-Term Cracking Percent Prediction	60
Long-Term Performance Prediction for Asphalt Overlays	79
Conclusions.....	92
Acronyms, Abbreviations, and Symbols.....	94
References.....	96
Appendix A.....	106

List of Tables

Table 1. State pavement asset inventory [91]	35
Table 2. Average climate inputs by district	43
Table 3. Prepared HPMS data for modeling short-term performance	45
Table 4. PMS data extracted for long-term performance modeling.....	47
Table 5. Summary of overlay PMS database	50
Table 6. Membership functions in Matlab's Neuro-Fuzzy Designer.....	55
Table 7. Summary of optimal ANN models (ASP FUNCLAS=01)	63
Table 8. Federal goodness rating of predicted and measured cracking percent.....	66
Table 9. ANN ASP cracking models	67
Table 10. ANN COM cracking models.....	69
Table 11. ANN JCP cracking models.....	71
Table 12. ANFIS ASP cracking models	76
Table 13. ANFIS COM cracking models	76
Table 14. ANFIS JCP cracking models.....	77
Table 15. Comparison between ANN and ANFIS cracking percent perdition models.....	77
Table 16. Input parameters in long-term performance modeling	81
Table 17. Input parameters for distress family curves	83
Table 18. Correlations of input parameters for IRI family curves	85
Table 19. IRI model parameters.....	86
Table 20. Developed distress index family curves -ALCR.....	89
Table 21. Developed distress index family curves -RUFF	89
Table 22. Developed distress index family curves -RUT	90
Table 23. Developed distress index family curves -RNDM	90

List of Figures

Figure 1. Roughness index family curve for composite interstate pavements	13
Figure 2. Family of pavement performance models [17]	17
Figure 3. Sample of a 3-4-2 feed-forward neural network [42].....	27
Figure 4. Typical structure of ANFIS [82].....	30
Figure 5. Pavement condition criteria regulated by FHWA [91]	36
Figure 6. MERRA data in Pavement ME.....	37
Figure 7. The locations of selected overlay projects in Louisiana.....	48
Figure 8. Distribution of PMS records of selected projects among ADT ranges	49
Figure 9. Distribution of PMS records among functional classifications.....	49
Figure 10. Designed ANN structure in Matlab	52
Figure 11. Model performance and regression of trained ANN (JCP, Functional Class 14)	53
Figure 12. Neuro-Fuzzy Designer panel in Matlab	54
Figure 13. Flow chart of building short-term ANN pavement performance models.....	57
Figure 14. ANN model structure for IRI family curve	58
Figure 15. Relationships of RMSE values with neuron numbers (a) without cross validation (b) with five-fold cross validation	61
Figure 16. Neuron numbers vs. training/testing RMSE values with (a) Levenberg- Marquardt Algorithm, (b) Bayesian Regularization Algorithm and (c) Scaled Conjugate Gradient Algorithm.....	62
Figure 17. Comparison between measured and predicted cracking percent with (a) trainlm, (b) trainbr and (c) trainscg.....	65
Figure 18. Overall comparison between predicted and measured cracking percent on ASP	68
Figure 19. Goodness ranking between predicted and measured cracking percent on ASP	68
Figure 20. Overall comparison between predicted and measured cracking percent on COM	70
Figure 21. Goodness ranking between predicted and measured cracking percent on COM	70
Figure 22. Overall comparison between predicted and measured cracking percent on JCP	71
Figure 23. Goodness ranking between predicted and measured cracking percent on JCP	72

Figure 24. Overall cracking distress goodness levels predicted for three NHS pavement types	73
Figure 25. Overall cracking distress goodness levels predicted for interstate and non-interstate pavement sections	75
Figure 26. Structures and performances of incremental long-term performance models	82
Figure 27. Model performance of IRI family curve	85
Figure 28. IRI family curves for rural and urban roadways	87
Figure 29. Comparison between ANN and conventional family curves	88

Introduction

The accuracy of pavement performance models is crucial for local agencies in managing their transportation assets. Reliable models help determine the most cost-effective maintenance and rehabilitation (M&R) treatments based on specific traffic, climate and existing pavement conditions. The M&R project selection and priority can be determined and significantly improved for budget allocation and distribution with limited resources. An accurate pavement performance model can greatly enhance the selection and prioritization of M&R projects, leading to more effective budget allocation and distribution of limited resources. Louisiana has over 61,000 miles of roadways, with 18,359 miles (30%) being state-owned and maintained by DOTD [1]. Louisiana receives approximately \$677 million from FHWA along with the state matching funds, and the Governor raises nearly \$700 million annually for transportation funding. Considering the significant investment in transportation asset maintenance and rehabilitation, even a slight improvement in pavement performance modeling could result in substantial savings for taxpayers.

The Pavement Management System (PMS), supported and operated by the Pavement Management Unit (PMU) of Louisiana DOTD, monitors all state-maintained highway sections within the Louisiana roadway network. The PMU measures pavement conditions and optimizes repair strategies for pavement maintenance and rehabilitation based on pavement performance. The pavement condition data is collected through a consultant contract every two years and primarily consists of roughness, rutting, cracking, patching, and faulting. These pavement distresses are continuously measured and recorded by severity levels (high, medium, and low) and extents (number, length, or area). They are reported with average values for 0.1-mile sections. The extents and severities of a distress are combined as deduction points to obtain a single distress index, and a pavement condition index (PCI) is also calculated using multiple distress indices for overall evaluation, with a scale from 0 to 100. After processing and validation, these prepared PMS data can be accessed by all districts for their decision-making procedures to select treatment types and timing for specific pavement sections [2]. The iVision web-based application and dTIMS (Deighton Total Infrastructure Management System) are adopted for data visualization, analysis, and performance prediction. Based on the predicted overall condition of the entire roadway system, local agencies are able to determine the allocation of resources for maintenance and rehabilitation in the most cost-effective way.

To achieve this goal, the PMU predicts pavement performances with empirical models regressed from accumulated PMS data, which are presented as curves of distress index versus pavement age. These models have a similar format but different coefficients among pavement types (flexible, composite, jointed concrete, and continuously reinforced concrete) and functional classifications (interstate, principal and minor arterial, major and minor collector, local, and others), which are referred to as pavement family. The obtained pavement family and site-specific performance curves for each condition index are used for analysis with dTIMS, the pavement management software, to calculate condition indices and determine corresponding treatment for the coming years under the determined budget scenarios. The pavement performance models are core in this analysis, and their accuracy directly influences the distribution of the available resources, as well as the overall condition of the infrastructure system related to driving safety and comfort.

The distress models adopted for this task are based on at least four data points with 2-year intervals in between [1]. These models are functions of pavement age, with recommended transformations. For example, polynomial functions are used for the roughness index and exponential functions for rutting index.

Figure 1. Roughness index family curve for composite interstate pavements

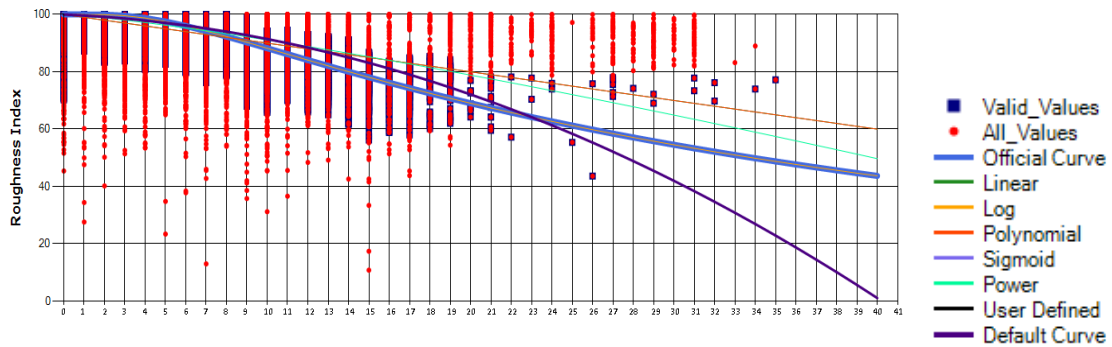


Figure 1 shows an example of the family curve for the roughness index of composite pavement on the interstate. The app in dTIMS offers various options, and the best-fit function can be selected based on correlation and judgement. The pavement family and site-specific performance curves provide relationships between pavement age and condition, which are directly obtained from data collected by Louisiana. The PMS team has full control over the input data. However, it is also evident that this model, based on pavement age, has significant variation and therefore cannot guarantee accuracy when used for predicting future performance. Considering the significant investment in the

maintenance and rehabilitation of the roadway system, a long-term performance model with better prediction power is necessary in preservation planning.

In order to improve and preserve the condition of the National Highway System (NHS), the State Department of Transportation is required to develop and implement an asset management plan mandated by the Moving Ahead for Progress in the 21st Century Act (MAP-21) [3]. One of the national goals of MAP-21 is “to maintain the highway infrastructure asset system in a state of good repair” for the NHS. The Federal Highway Administration (FHWA) defines the state of good repair as “a condition in which the existing physical assets, both individually and as a system, (a) are functioning as designed within their useful service life, and (b) are sustained through regular maintenance and replacement programs.”

This Transportation Asset Management Plan (TAMP) is a performance-based document [4] which focuses on replacing the historical “Worst First” practice of infrastructure improvement with a strategy of “Preservation First” of all interstate and NHS roadways and bridges. The traditional “Worst First” approach is not cost-effective. Instead of spending resources on replacing only a few of assets in very poor condition (“Worst First” Strategy), the “Preservation First” approach utilizes limited available funding on many more highway sections and bridges, reserving these structures in their current condition, and sustaining a desired “state of good repair” over the life cycle of the assets at minimum practicable cost.

To achieve these objectives, MAP-21 requires a data-driven and strategic method to improve driving safety, with a focus on highway performance [5]. Under the legislation of Title 23, Code of Federal Regulations (23 CFR Part 490 - National Performance Management Measures), guided by FHWA, performance measurements were established for assessing pavement and bridge conditions, which are percentages of interstate and non-interstate pavements in good and poor condition. Effective on May 2017 and started by January 2018, State Departments of Transportation (DOT) must collect data for interstate pavements including International Roughness Index (IRI), rutting, cracking percentage, and faulting. Based on these measurements and the availability of resources, State DOTs shall report baseline performance, 4-year performance targets for interstate pavements, and 2-year and 4-year targets for non-interstate NHS pavements. FHWA also requires State DOTs and Metropolitan Planning Organizations (MPOs) to establish performance targets, which will be tracked using the same measurements.

The 2-year and 4-year condition targets are identified based on historical trends, the latest funding projects, and future deterioration modeling [6]. However, the previous distress measurement for PMS for most of the State DOTs were different from the methods demanded in 23 CFR Part 490. The new data collected is insufficient to plot historical trends, and the deterioration models are also usually too simple to ensure the accuracy of predicting pavement performance. For example, Texas DOT used the moving-average method to set up the targets for the 2018–2021 Performance Period [7]. The New Hampshire DOT utilized condition data for five prior years (2013-2017), along with subject matter expertise, as the basis for establishing the 4-year target for the interstates, as well as the 2- and 4-year targets for non-interstate NHS pavement condition [8]. Other states, such as North Dakota [9], Arizona [10], California [11], and Arkansas [12], used commercial software to complete this task based on regression models derived from pavement conditions and ages. Therefore, there is a need for a more consistent and reliable approach in predicting the distresses for determining condition targets.

Literature Review

According to the needs for predicting long-term and short-term pavement conditions, the literature review of this research begins with a review of previous efforts in modeling pavement performance.

Pavement Performance Models

The primary goals of a network-level PMS include determining budget requirements for both short- and long-term periods and generating a list of possible projects based on budget limitations [13]. Performance models can be used to predict the need for maintenance, rehabilitation, or reconstruction of pavements. Pavements naturally degrade over time, but the pavement's lifespan can be extended by addressing damages to improve their condition [14]. Pavement performance prediction models can forecast the remaining service lives of pavements if they are developed based on past pavement performance data. This helps optimize the scheduling of rehabilitation activities and determine the necessary funding levels to achieve a predetermined level of performance [15]. To evaluate the quality of pavement in terms of its functional and structural aspects, various metrics are employed, such as its ability to support weight, the level of damage, the load carrying capacity of the pavement, and the roughness of its surface [16]. Performance models can be developed at either the network level or project level. Network-level models assess and model an entire state, while project-level models focus on localized needs. Both types of models typically take into consideration factors such as age, traffic, surface type, climate, materials, and types of distress as contributing factors for pavement performance.

Over the years, researchers have used mathematical tools to investigate and explore the impacts of these parameters on pavement conditions. With the rapid development of computer science in recent years, machine learning techniques have been applied to forecast pavement conditions. As a result, pavement performance models can be classified into two major groups: probabilistic reasoning and shallow machine learning models [17].

Figure 2. Family of pavement performance models [17]

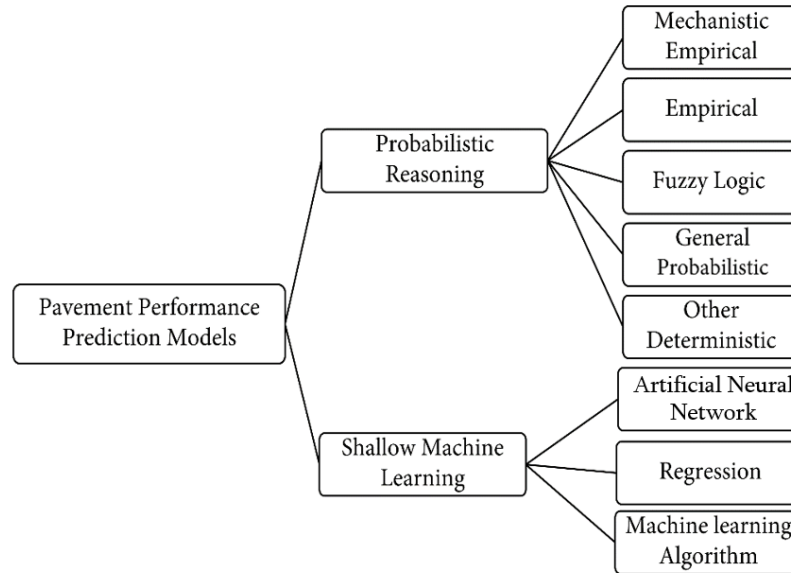


Figure 2 shows the categories of pavement performance models, in which the two main model categories could be further divided based on their inputs, model structures, and algorithms.

Probabilistic Reasoning Models

Empirical Models

Empirical models are mainly developed based on experimental data and field observation. These models have a long history and are widely accepted by State DOTs and local agencies due to the availability of accumulated project records and their feasibility in application.

As mentioned above, DOTD utilizes empirical models that have been regressed from more than 6 years of data collected at 2-year intervals. These models are equations of pavement age with recommended transformation functions [2]:

- Roughness index: polynomial function;
- All indices for continuously reinforced concrete pavement (CRCP): power function;
- Rutting index: exponential function; and
- All other indices: linear function.

For example, the longitudinal distress index for CRCP can be written as:

$$LongiCrack Index_{CRCP} = 100 - a(age)^b \quad (1)$$

Where, a and b are model coefficients equal to 0.0173 and 2.6 correspondingly.

For the newly constructed pavement, this index equals 100. The index equations for other pavement conditions also adopt this constant as the initial status of new pavement surfaces. The $a(age)^b$ deduct point represents the degradation of pavement performance with increased pavement age, in which the coefficients are obtained from the same category of pavements for family curve or average values on homogenous sections for site-specific curves.

To determine the appropriate maintenance strategy for existing pavements, other indicators such as PCI, Present Serviceability Rating (PSR), and roughness index have been widely utilized by other DOTs to prioritize maintenance and rehabilitation efforts [18]. The general form of the distress indices equation using deduct points, same as DOTD models in Equation 1, in which the distress index equals a constant of maximum pavement rating (e.g., 4, 5 or 100) minus the total deduct points. These deduct points are based on the type of distress, extent of the distress and severity level, and the policy of the transportation department [19]. The Washington State Department of Transportation (WSDOT) utilizes the pavement condition index based on this form to assess the condition of rigid pavements, reflecting the same trends observed in the field over time. The PCI is mainly related to pavement age:

$$PCI = 100 - c * Age^d \quad (2)$$

Where, c is the slope coefficient, Age is the time since the last maintenance or rehabilitation, and d is a constant that controls the degree of the performance curve (2). WSDOT also calculates pavement structural condition (PSC) in similar forms for both flexible and rigid pavements, where the deduct points are defined as equations of equivalent cracking (EC) numbers:

$$PSC_{flexible} = 100 - 15.8 * (EC)^{0.50} \quad (3)$$

$$PSC_{rigid} = 100 - 18.6 * (EC)^{0.43} \quad (4)$$

Where, $PSC_{flexible}$ and PSC_{rigid} are pavement structural conditions for flexible and rigid pavements. EC represents equivalent cracking numbers, which is the sum of all types of distress with their severities and extents. Equivalent cracking also has similar expression:

$$EC = \sum[T * (C * d)^P] \quad (5)$$

Where, T is the coefficient of distress type, and C and P are the coefficients of distress severity level (high, medium and low). This PSC evaluates the current condition of pavements based on the combination of various distress types, severity levels, and extents, but without considering pavement age. PSC is calculated separately for flexible and rigid pavements and described by four broad pavement condition categories: excellent (75-100), good (50-75), fair (25-50), and poor (0-25). In practice, a threshold value of $PSC = 50$ triggers pavement maintenance/rehabilitation.

The Arizona Department of Transportation (ADOT) uses a sigmoidal or S-shaped model to predict pavement performance, which allows for more flexibility in describing how a section deteriorates over time. The sigmoidal model used by Stantec's Highway Pavement Management Application (HPMA) for performance prediction modeling is showed below:

$$PSR = O - \exp[A - B * C^{\ln(1/age)}] \quad (6)$$

Where, the PSR and initial pavement condition (O) are used to predict pavement performance over time, measured in years since the last rehabilitation or construction activity. The model uses coefficients A, B, and C to shape the curve, which can be concave, convex, S-shaped, or almost linear, depending on the flexibility of the sigmoid. This flexibility helps the model fit the data and accurately describe performance trends [20].

The IRI has been utilized for evaluating road smoothness, estimating vehicle operating expenses, and assessing the environmental consequences of road conditions for network-level pavement management systems [21]. The IRI measures the total vertical movement of the axle relative to a reference point on a quarter-car per distance traveled along the pavement profile at a constant speed of 80.5 km/h (50 mph). The World Bank was the first organization to create the IRI [22]. The general form of the IRI prediction model is presented by the increment in IRI, initial IRI, and the time lapsed (in years) since the year of the initial IRI [23].

$$\ln\left(\frac{IRI_i}{IRI_n - IRI_i}\right) = \beta_1 + \beta_2 e^{Time\beta_3} \quad (7)$$

Where, IRI_i = initial IRI; IRI_n = IRI in year n; β_1 and β_3 = parameters controlling the IRI increment rate; β_2 = parameter controlling the year in which IRI begins to increase; and time = number of years since initial IRI.

Elhadidy et al. conducted research using the Long-Term Pavement Performance (LTPP) database to develop a simplified regression model that links PCI with IRI. They found that a sigmoid function best expresses the relationship between PCI and IRI, with a coefficient of determination (R^2) of 0.995. Their predicted IRI values had very low bias, and they also validated the model using a different dataset, obtaining highly accurate predictions ($R^2 = 0.992$). They proposed a pavement condition rating system based on IRI, which provides a rating equivalent to the widely used PCI rating method that is based on pavement condition [24].

Mechanistic-Empirical Models

While the introduced empirical models provide convenience in application for performance modeling, which usually consider pavement age or time span as the only or primary variable, they do not incorporate other factors that also have a significant influence on pavement deterioration. Researchers realized that considering parameters such as layer thickness, materials, traffic, and climate would provide more reliable prediction.

As early as the 1980's, George et al. [25] developed a mechanistic-empirical model based on PCI values collected from over 2000 miles in Mississippi, USA. Various parameters were studied, including traffic volume, pavement age, and structural number, to investigate their influences on maintenance strategies. The pavement condition rating (PCR) was defined as:

$$PCR = RR^{0.6} * DR^{0.4} \quad (8)$$

Where, RR is roughness rating and DR is distress rating.

The pavement condition rating at time t, PCR(t), for three pavement types (flexible pavement without overlay, with overlay, and the composite pavement), is obtained through Equation (9) to (11):

$$PCR(t) = 90 - a[\exp(Age^b) - 1]\log[ESAL/(SN^c)] \quad (9)$$

$$PCR(t) = 90 - a[\exp(Age^b) - 1]\log[ESAL/(SN^c * T)] \quad (10)$$

$$PCR(t) = 90 - a[\exp(Age/T)^b - 1]\log[ESAL] \quad (11)$$

Where, a, b, and c are regressed coefficients, ESAL is the equivalent single axle loads, SN refer to the structural number, and T represents the overlay thickness.

Sidess et al. [26] developed a model to predict IRI based on a combination of the empirical-mechanistic and regressive-empirical approach. The model coefficients consider the subgrade modulus, the pavement's structural number, the thickness of the asphalt layer, and climate zones. Their IRI deterioration model for pavements with a traffic loading history may be expressed as follows:

$$IRI(t \geq t_{ini}) = 1.10 + K * (W_0 + W_t)^y \quad (12)$$

Where, K and y are regressed coefficients, W_0 is the ESAL applied from IRI = 1.10 to IRI at time t_{ini} , and W_t is the ESAL accumulated until time t. This model demonstrates a strong correlation between prediction and measurement ($R^2 > 0.9$).

The most well-known application of mechanistic-empirical models is the Mechanistic-Empirical Pavement Design Guide (MEPDG). The MEPDG software serves as an advanced tool for designing flexible pavements and predicting future pavement performance [27]. The accuracy of the MEPDG performance models has been statistically evaluated, and the verification testing shows promising results in terms of its performance prediction accuracy [28]. While MEPDG software is relatively conservative for highway pavements with low traffic levels, the nationally averaged default parameters in MEPDG were not sensitive enough to account for variations in climates, traffic, and materials in Tennessee when predicting PSI [29]. Several modern regression techniques, including the generalized linear model and the generalized additive model, along with the assumption of Poisson distribution and the quasi-likelihood estimation method, were adopted to develop improved fatigue cracking models using the LTPP database. The proposed model showed significant improvements over existing models, although further enhancements were possible and recommended [30]. Auto-regression models can outperform other models in terms of accuracy, and the use of auto-regression models in pavement management systems by highway agencies is recommended for pavement performance models [23].

Probabilistic and Deterministic Models

Models used for predicting pavement performance can also be categorized into probabilistic and deterministic models. Probabilistic models use a probability function to estimate the likelihood of future pavement conditions with a certain degree of probability. The probability levels are determined by either expert opinion or an evaluation of past pavement performance [31]. An example of a probabilistic model is the Markov process, which is used to develop a probabilistic network-level PMS based on pavement performance prediction. The non-homogeneous Markov chains-based pavement performance prediction model can be successfully integrated into the MicroPAVER pavement deterioration process, effectively capturing the probabilistic search effort. By using the Markov process in conjunction with dynamic programming, the optimal budget requirements for the analysis period can be generated [32]. This approach has the potential to be utilized in pavement management to simulate the probabilistic nature of pavement deterioration and predict its serviceability level at different stages. This also helps to determine the appropriate time for rehabilitation and develop a priority program for pavement management at the network level [33]. However, Markov chain models are based on the assumption that the future state of the pavement depends only on its current state and not on its past states [34]. This is a major limitation of Markov chain model.

The other type of model used for predicting pavement performance is deterministic. The deterministic approach of the pavement performance prediction model is based on an incremental analysis of the American Association of State Highway and Transportation Officials (AASHTO) basic design equation developed for flexible pavement design. The AASHTO basic design equation is based on empirical data from the AASHTO Road Test and is derived using regression techniques. The model creates a specific performance curve for a particular pavement structure. It involves using a mathematical function to estimate the exact future condition of the pavement. The function is created based on observations or measurements of pavement deterioration using mechanistic, regression, or mechanistic-empirical methods [35]. Pavement deterioration prediction models play a crucial role in the pavement management systems at the network level. They are utilized to predict upcoming pavement conditions, create plans for maintenance and rehabilitation projects, and determine the financial requirements for the future [36]. To create performance prediction models for asphalt pavements on state highways and interstates, simple and multiple regression analysis methods were used. Regression techniques for predicting pavement performance are only applicable under specific circumstances such as certain climatic conditions, materials used, construction techniques employed, and

other relevant factors [31]. Implementing a multiple linear regression analysis-based model for predicting pavement performance in the Pavement Management System can significantly impact the decision-making process for managing asphalt pavements [37]. Johnson et al. categorized various pavement types and analyzed the data for any necessary adjustments. They initially attempted to use a linear regression model but found that the performance index would increase and then decrease due to road rehabilitation. To solve this problem, they removed records from the analytical pavement section database that were affected by rehabilitation. When they determined that the linear regression model was not providing satisfactory results, they used a non-linear regression modeling technique to create performance prediction models [37].

Shallow Machine Learning Models

Researchers have explained artificial intelligence (AI) as a system that either thinks or acts like a human or a system that thinks rationally or acts rationally [38]. IBM defines Machine Learning (ML) as a branch of AI and computer science that focuses on the use of data and algorithms to imitate the way that humans learn, gradually improving its accuracy. Deep learning, a more advanced and sophisticated branch of machine learning, requires more training data and greatly depends on the network's structure for performance [39]. Compared to traditional machine learning, deep learning involves more complex models that can solve more complex problems with greater accuracy and efficiency [40, 41]. On the other hand, shallow learning includes most ML models proposed before 2006, such as shallow neural networks with just one hidden layer of nodes. Despite its advantages, such as easy interpretation and computational efficiency, shallow learning models like logistic regression, decision trees, and support vector machines (SVM) have limitations like underfitting, overfitting, and struggling with large samples and missing data [39].

There are several types of machine learning. Supervised learning is a type of ML where the algorithms aim to predict and classify the predetermined attribute, and their performance measures such as accuracy and misclassification are determined by the correct prediction or classification of that attribute [42]. Conversely, unsupervised learning involves pattern recognition without the involvement of a target attribute [43]. Semi-supervised, as the name suggests, is when small amounts of labeled data are available. Reinforcement learning is a type of ML that involves using a scalar reward parameter to evaluate the input-output relationship in a trial-and-error manner. The

system, or "agent," uses information from its environment to determine the best way to optimize itself and adapt to its surroundings [44].

Pavement performance prediction using ML is not a new thing. As advancements in ML grow every year, they have been applied to make more accurate and comprehensive predictions by researchers.

ML has progressed dramatically over the past two decades, from laboratory curiosity to practical technology in widespread commercial use [45]. Researchers in the 1990's realized the advantages of ML, such as generalization, massive parallelism, and real-time solutions, over traditional methods [46]. ML algorithms are organized into a taxonomy based on the desired outcome of the algorithm [47]. There are several ML algorithms in use, including Artificial Neural Network (ANN), Recurrent Neural Network (RNN), Support Vector Regression (SVR), Convolutional Neural Network (CNN), Random Forest (RF), and Long Short-Term Memory (LSTM). The ML process follows a path, as shown in the figure below. It starts with gathering input data like ESAL, climate data, initial IRI, etc. Even before selecting the required data, one needs to make sure of the data they want to use. After data mining, the raw data needs to be cleaned using various techniques. The processed data is then used in the selected model, which is continuously refined based on the feedback. At the end, visual results are obtained, providing insight into the prediction. Before starting the steps of creating the model, knowledge of the platform on which the ML model is developed is necessary. A deep learning framework is a software tool that provides an infrastructure for building and training deep neural networks. Given the various machine learning algorithms discussed in the previous paragraph, it is essential to have the appropriate software tools to create and optimize models. In this context, deep learning frameworks Pytorch [47], NumPy, Keras [48], and Scikit-learn [49] of Python are commonly used. Researchers have also used R in determining calibration coefficients [50]. Software like Python, MATLAB, R, and NeuroSolutions 5 [51] can all be used to create models.

While most papers seem to use LTPP [51, 52-59], as their source of data, some papers have also used PMS [50, 60] for data collection. In some cases, data had to be generated so that the model could be trained for a full range of possibilities [61]. These data can be used in pavement performance prediction at both the network [50] and project level. After data collection, the next objective is to improve the quality of the data by detecting and removing errors and inconsistencies through data cleaning. These issues can stem from various sources, such as data entry errors, and the most effective approach to resolve

them depends on the specific context. In the case of pavement performance problems, performing sanity checks based on engineering judgment is a logical approach [54]. When using real data for modeling, one common challenge is the presence of "noise," which refers to random errors in the data. This term comes from the field of information theory and engineering, which was instrumental in early work on ANNs. While noise can be intentionally added to the training set to help the network learn a more general solution to the problem, it can also negatively impact model accuracy [62].

Most papers use traffic [49, 50, 54, 58, 63], climate [49, 50, 54], initial IRI [49], other distresses, material properties [49], age [53], rut depth [53], subgrade [50], layer thickness [58], structural number [63], and cracking as input parameters for models. Hossain et al. only used traffic and climate data in their model [64]. Kargah-Ostadi et al. used MATLAB stepwise regression and found that factors like age, traffic, annual average precipitation, subgrade moisture, and total post-overlay HMA thickness were not statistically significant [56]. The inclusion of too many parameters can cause overfitting, but excluding important predictors which influence pavement performance may limit the accuracy of the prediction [52]. Marcelino et al. used MissForest, which is a non-parametric imputation technique, when there were missing input data [54]. Hossain et al. developed and used synthetic data based on the statistical characteristics of the existing data when data were not available [64]. Damirchilo et al. employed XGBoost, which uses a sparsity-aware split finding approach to handle missing data [49].

Artificial Neural Networks

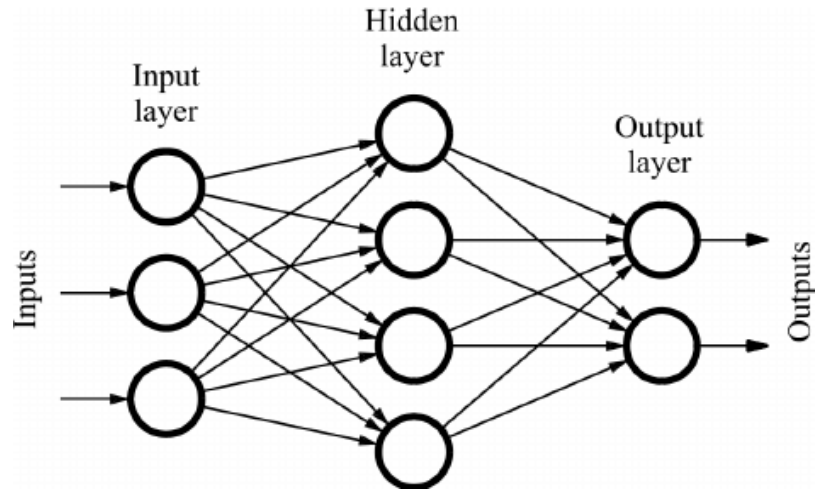
ANNs are computational models that process information through interconnected units with activation functions and weight optimization during training to learn and generalize from input data [47]. A key technique used in ANNs is backpropagation, which involves adjusting the weights between nodes based on the difference between the predicted and actual output during training. This process enables the network to continuously improve its performance over time, making ANNs a powerful tool in many applications. The use of ANNs [48, 53, 56] in building models is a widely used practice. ANNs can represent any non-linear function without the constraints of linearity. They can generalize relationships from limited data, remain robust in the presence of noise, and adapt to changing environments [62]. ANNs are generally good for fixed-length data. They are feedforward network algorithms, while RNNs have loops and are suitable for sequential data of variable length.

The feedforward neural network is a typical shallow artificial neural network, consisting of an input layer, one or more hidden layers, and an output layer. As one of the simplest forms of neural network, the data is processed only in one direction within a feedforward model. Figure 5 gives an example of ANN [42], consisting of an input layer, a hidden layer, and an output layer with 3, 4, and 2 neurons in each layer. The input layer contains neurons that receive input values and deliver these inputs to the following hidden layers. The number of an input layer's neurons is equal to the number of features in the dataset. There are also neurons in hidden layers, where the inputs are transformed when passing through them. The weights and bias are updated during the training procedure to provide an optimized value with prediction power. Weights refers to the connection between two neurons from adjacent layers. After being processed by hidden layer(s), the values will be passed to the output layer and generate predicted values.

As is shown in Figure 3, when the weights and bias values of this ANN are determined and the values are defined as input neurons, these values will pass through hidden layers with a certain algorithm and eventually generate output values. ANNs may have more than one hidden layer, but the data always moves in one direction, from input layer to output layer.

The predicted value of ANN is compared to the given output, and then an error is calculated and propagated back within the ANN. The weights are updated during this process based on their influence on the error. The algorithm applied in this procedure is called backpropagation.

Figure 3. Sample of a 3-4-2 feed-forward neural network [42]



RNN is another type of ANN that is specifically designed to analyze sequences of data, such as time-series data, speech, and text. Unlike traditional feedforward neural networks, RNNs can process input data of any length, and they use loops to retain information about the previous computations, making them well-suited for handling time-series data [48]. With the ability to classify, cluster, and make predictions about such data, RNNs are powerful tools for pattern recognition and analysis. When working with long sequences in an RNN, the gradients, which are essential for tuning the weight and bias, can become a problem during backpropagation. They can either vanish (due to multiplication of many small values less than 1) or explode (due to multiplication of many large values more than 1), leading to slow training of the model [65]. This is not the case in an ANN. An RNN is essentially a multi-layer perceptron (MLP) with added loops in its architecture, making it especially suitable for analyzing sequences of data like time-series data, speech, and text [65].

On the other hand, MLP neural networks consist of nodes organized into layers, with each layer consisting of nodes that connect to all nodes in the following layers. These networks are widely used for supervised learning tasks like image recognition and classification [66].

LSTMs are a unique form of RNNs that possess the ability to acquire long-term dependencies and retain information for extended periods [67]. RNNs typically use feedback loops to retain information over time, but they struggle to learn long-term temporal dependencies due to the vanishing gradient problem. LSTMs address this by introducing a memory cell that can hold information for extended periods. They use gates

to control when information enters and exits the memory cell, solving the vanishing or exploding gradient problem.

CNNs are a type of deep learning model designed for image and video processing. They extract and learn features from input data using specialized layers, which are then classified into different categories. Compared to traditional machine learning methods, which often rely on shallow learning techniques, CNNs use multilayer neural networks that can automatically learn increasingly complex features from the data [68].

Artificial Neural Networks has been applied to developing short-term pavement performance model. They can incorporate more factors and overcome the shortcomings of traditional regression methods by considering time series or identifying categories within the database. Even with the same input and output, the ANN models showed significantly better predicting performance than multiple linear regressions [69] on PMS database.

One application of the ANN in short-term pavement performance modeling is to predict or evaluate the effectiveness of preventive maintenance treatments in the coming years. Previous researchers have accumulated many outcomes with this topic based on ANN and pavement performance database. Luo et al. [70] evaluate the effectiveness of PM treatments in short-term asphalt pavement performance using the Specific Pavement Studies (SPS-3) data of the LTPP Program, including chip seal, crack seal, slurry seal, and thin overlay. The mixed-effects logistic regression was conducted to find the significant influential factors, and the influence of temperature, precipitation, cloud cover, subgrade material, truck traffic, and asphalt concrete layer thickness on the improvements of pavement performance was quantified. It was concluded that chip seal and thin overlay have the most significant effects on short-term cracking improvements, and thin overlay also showed the best effect on short-term roughness and rutting improvements. Amarasiri and Muhunthan [71] evaluated performance jump of thin asphalt overlay, slurry seal, crack seal, and chip seal under wet freeze climates based on LTPP database. The research concluded that thin overlay and chip seal were most effective in eliminating non-wheel-path longitudinal cracking, whereas the slurry seal and the crack seal were the least effective. Jia, Y. et al. [72] used LTPP SPS-3 database to evaluate the effectiveness of PM treatments on five typical pavement performances, including roughness, rutting, transverse cracking, longitudinal cracking, and alligator cracking. Similarly, thin overlay and chip seal provided the most effectiveness on most of these performance indicators. Researches were also conducted to investigate the short-

term performance on rutting, IRI reduction after treatment, and the deterioration rate of cracking [73-75].

ANN was also adopted to build short-term pavement performance models to support decision-making procedures in PMS. Ziari et al. [76] selected the group method of data handling (GMDH) and ANN to construct IRI prediction models based on the LTPP database. The models considered pavement structure information, climates, traffic, and pavement age. Kargah-Ostadi et al. [56] also used performance data after rehabilitation (LTPP SPS-5) to build IRI prediction models, in which the previous IRI was used as input, and overlay thickness, milling depth, and percentage of fine aggregate in the subgrade were included. The trained model was applied for recommending pavement rehabilitation treatments. Kaya et al. [77] used 35 flexible pavement projects and 60 composite pavement projects to build network-level resilient service life models with ANN. The performance data was extracted from the Iowa DOT pavement management information system (PMIS) database. These short-term models adopted previous pavement distresses, traffic (accumulated ESALs), age, and AC thickness to predict the distresses of the next year [77].

These research projects provided valuable reference and guidance in constructing ANN structures and selecting input parameters for model training. However, most of these models are based on LTPP data and IRI prediction only. Other distresses, such as faulting and cracking, were not involved, and some of the inputs (e.g. asphalt binder properties, pavement layer thickness, and subgrade soil information) are not available for most of the PMS, which is necessary for accomplishing the prediction of pavement condition targets required by TAMP.

Adaptive Neuro-Fuzzy Inference System (ANFIS)

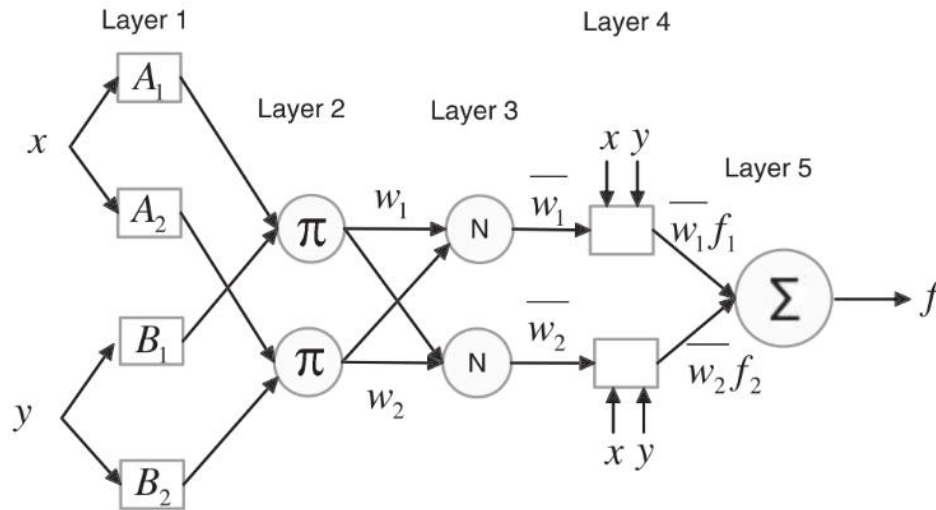
The Adaptive Neuro Fuzzy Inference System (ANFIS) is a combination of ANN and fuzzy inference system (FIS). It is well-known for its capacity to reduce noise and has many applications from identifying voice signals [78] [79] to diagnosing medical images [80] [81].

ANFIS is a data learning technique in which given input values are transformed with Fuzzy Logics into output by a highly interconnected neural network with weights and biases [82]. This structure adopts ANN to update the parameters of FIS and therefore benefits from both ANN and FIS techniques. ANFIS refines IF-THEN fuzzy rules to describe the behavior of a complex system, without requiring prior human expertise and

with simple implementation. ANFIS also provides various options of membership functions (MF) for explaining fuzzy rules, enabling learning efficiency and accuracy.

Figure 4 shows a typical example of ANFIS structure with two inputs (x and y) and one output (f). Assume that there are two IF-THEN rules based on the first order of the Sugeno model as shown:

Figure 4. Typical structure of ANFIS [82]



Rule 1: **IF** x is A_1 **AND** y is B_1 , **THEN** $f_1 = p_1x + q_1y + r_1$

Rule 2: **IF** x is A_2 **AND** y is B_2 , **THEN** $f_2 = p_2x + q_2y + r_2$

Where A_1 and B_1 are fuzzy sets, f_1 are the fuzzy region outputs obtained from fuzzy rules, and p_1 , q_1 and r_1 are design parameters determined by the training process.

The layer structure of ANFIS model in Figure 4 are explained as follows:

Layer 1: all the nodes in this layer are adaptive nodes with a fuzzy membership function:

$$O_{1,i} = \mu A_i(x), \quad i=1,2 \quad (13)$$

$$O_{1,j} = \mu B_j(y), \quad j=1,2 \quad (14)$$

Where, x and y are input values to nodes i or j , and A_1 and B_1 are the linguistic labels (such as high, low or medium, etc.) for membership functions of the nodes. These membership functions specify the degree to which the inputs are matched to the

quantifiers (fuzzy sets) A_1 or B_1 . An example of a bell-shaped function, denoted as $\mu A_i(x)$ with a maximum value of 1 and a minimum value of 0 can be written as:

$$\mu A_i(x) = \frac{1}{1 + \left[\left(\frac{x - c_i}{a_i} \right)^2 \right] b_i} \quad (15)$$

Similarly, a Gaussian membership function can be expressed as:

$$\mu A_i(x) = \exp \left[- \left(\frac{x - c_i}{a_i} \right)^2 \right] \quad (16)$$

Where, a_i , b_i , and c_i are parameters of the membership functions. The shape of the membership function varies as these parameters change.

Layer 2: The nodes in this layer are fixed and labeled as π , in which the outputs from the previous layer are multiplied as:

$$O_{2,i} = w_i = \mu A_i(x) * \mu B_j(y), \quad i, j = 1, 2 \quad (17)$$

The output $O_{2,i}$ of this layer is also called as firing strength.

Layer 3: The nodes in this layer are also fixed as well and labeled as N , in which the sum of all rules' firing strength is calculated as:

$$O_{3,i} = \bar{w}_i = \frac{w_i}{w_1 + w_2} \quad (18)$$

The outputs of this layer are called normalized firing strength.

Layer 4: The nodes in this layer are adaptive ones, with node function that is multiplied by normalized firing strength from the previous layer and first-order Sugeno model (IF-THEN Rules). The outputs of this layer are written as:

$$O_{4,i} = \bar{w}_i f_i = \bar{w}_i (p_i x_i + q_i y_i + r_i) \quad (19)$$

Where, p_i , q_i , and r_i are called as consequent parameters.

Layer 5: There is only one node in this layer that computes the overall output, which is the summation of all incoming signals:

$$O_{5,i} = \sum_i \bar{w}_i f_i = \frac{\sum_i w_i f_i}{\sum_i w_i} \quad (20)$$

The above five layers are the basic components of ANFIS structure.

ANFIS is famous for its capacity of noise reduction and has many applications from identifying voice signals [78][79] to medical image diagnosing [80][81]. ANFIS has also been utilized in predicting pavement roughness [83][84] and PCI [85], especially for short-term pavement roughness prediction [86]. This advantage would be very useful in dealing with the noise of the network-level database, such as error and variation due to device and operators.

Regression Models

Random Forest is another popular algorithm that creates an ensemble of decision trees using a modified bagging technique to improve predictive accuracy. Each tree in the ensemble is constructed using a randomly selected training subset, which is replaced as many times as the number of trees. The bootstrap aggregation technique is typically used in the construction of the trees, where scenarios from the training subset are replaced by the constructed populations during analysis [87-89]. The Random Forest algorithm builds multiple decision trees and combines them to make more accurate predictions. The underlying idea is that several independent models (the individual decision trees) perform better as a team than they do individually.

Other Machine Learning Techniques

Support Vector Regression (SVR) is a technique used to develop a regression function that can map input predictor variables to observed output response values. One of the key benefits of SVR is its ability to strike a balance between the complexity of the model and the prediction error, making it a useful tool for analyzing high-dimensional data [90]. SVR was chosen for pavement performance modeling due to its flexibility in finding the best hyperplane to fit the data in higher dimensions and customize control errors within an acceptable range [60].

Review of Pavement Condition Datasets

DOTD's Pavement Management System (PMS)

DOTD has been collecting pavement data on various distress types using Automatic Road Analyzer (ARAN) vehicles for over 20 years. Louisiana has been a national leader in Quality Assurance and Quality Control (QA/QC) for pavement distress data collection. In

the “Practical Guide for Quality Management of Pavement Condition Data Collection” issued by the FHWA in 2013, DOTD was one of the three agencies provided as a “Case Study” example of proper Quality Management.

DOTD has continually signed contracts with Fugro Roadware to collect roadway data, including the state-maintained highways (State Highway System, SHS), interstate highways (Interstate Highway System, IHS), regional roadways (Regional Highway System, RHS), and other off-system NHS routes. Currently, the entire pavement network of Louisiana is surveyed once every two years. The full spectrum of pavement information is collected in a single pass at highway speeds. This includes data on alligator, longitudinal, transverse cracking, rutting, faulting, patching, sealed cracks, horizontal and vertical curves and degrees, right-of-way records, and pavement images. Other data, such as surface texture, ground penetration radar (GPR), pavement types, number of lanes, functional classifications, date of data collection, and coordinates of global positioning system (GPS), are also added to describe the properties of the roadway sections. The measured data is utilized to build up Louisiana’s PMS to monitor current and future pavement conditions. Each pavement condition data point is analyzed and summarized for every 0.1 miles, and the performance data is rated with low, medium and high severity levels. Various distress data collected from each 0.1-mile segment are then transferred as pavement distress indices scaled from 0 to 100. For any given 0.1-mile flexible pavement section, the alligator index is obtained by reducing the deduction points for all three severity levels from 100.

DOTD adopts these distress indices as a reference for evaluating pavement conditions, including alligator cracking index (ALCR), random cracking index (RNDM), rutting index (RUT), patching index (PTCH) and roughness index (RUFF) for flexible pavements [91]. The pavement performance index for flexible pavement is calculated based on these indices using the following equation:

$$\text{Pavement Performance Index} = \frac{\text{MAX}(\text{MIN}(\text{RNDM}, \text{ALCR}, \text{PTCH}, \text{RUFF}, \text{RUT}), [\text{AVG}(\text{RNDM}, \text{ALCR}, \text{PTCH}, \text{RUFF}, \text{RUT}) - 0.85 \text{STD}(\text{RNDM}, \text{ALCR}, \text{PTCH}, \text{RUFF}, \text{RUT})])}{100} \quad (21)$$

Where, RNDM, ALCR, PTCH, RUFF, and RUT are distress indices.

For composite pavement, the performance index equation is similar but without ALCR. For jointed plain concrete pavement (JPCP), longitudinal and transverse cracking indices

are considered separately, while CRCP only considers the longitudinal cracking index, PTCH, and RUFF.

The overall condition is analyzed on homogenous sections to determine optimum pavement treatment based on all these pavement condition indices. DOTD also uses the trigger value system to recommend maintenance and rehabilitation treatments based on the combination of the distress indices. The trigger values vary for different pavement types and functional classifications.

The PMS database available for this study ranges from 2003 to 2021. The pavement performance data is stored in 10 sub datasets, with each sub dataset containing PMS data collected from a 2-year cycle. Typically, each PMS dataset contains 191,000 to 197,000 rows, collected from more than 18,000 miles of state owned highways.

DOTD's Highway Performance Monitoring System (HPMS)

Federal legislation (23 CFR Part 490 - National Performance Management Measures) requires each state DOT to develop a risk-based TAMP to improve and preserve the condition of assets on the federal NHS. As part of TAMP structure, the asset condition measurements and collected data are used to build the HPMS database. This database serves as the foundation for setting performance targets required by the FHWA and for conducting life cycle planning and risk management analysis within TAMP.

Although PMS and HPMS use similar equipment for data collection, there is a key difference between the two. PMS is collected from all state-maintained roadways, whereas HPMS is only surveyed from interstate highways and non-interstate national highway systems. HPMS does not cover roadways within SHS or RHS. The mileage distribution of PMS and HPMS for these asset classes is listed in Table 1.

Table 1. State pavement asset inventory [91]

Asset Class	*Center Line Miles			**PMS Analysis Lane Miles			~Federal Analysis Lane Miles		
	Pavements	Bridges	Total	Pavements	Bridges	Total	Pavements	Bridges	Total
Interstate	675	268	943	1,350	533	1,883	2,846	1,195	4,041
Non-Interstate NHS	1,804	291	2,095	2,801	479	3,280	6,230	1,026	7,256
Local NHS	65	26	91	n/a	n/a	n/a	260	105	365
SHS	6,419	486	6,905	6,562	505	7,067	n/a	n/a	n/a
RHS	6033	523	6,556	6,159	535	6,694	n/a	n/a	n/a
Totals	16,590			18,924			11,662		

* = Center Line mileage includes bridge decks, gravel and brick surfaces; however, this mileage is excluded for both PMS & Federal Analysis

** = PMS mileage represents the primary direction of travel for all undivided roadways and both directions for multi-lane divided roadways

~ = Federal mileage represents the primary direction of travel times the number of through lanes for both directions

The survey for PMS is conducted every two years, while HMPS collects data annually. There are also several differences between PMS and HPMS, which are listed as follows:

- **Purpose of database:** As mentioned above, the major tasks of PMS are to supervise and forecast pavement conditions as well as select the optimal treatment and timing. HPMS monitors the network-level conditions of interstate and other NHS pavements, and accesses the overall performance of pavements for these asset classes.
- **Data measurement:** The IRI and rutting measurements are same for both DOTD PMS and federal data. However, there are differences in cracking and faulting measurements between these two datasets.

Cracking: DOTD determines treatment selection using PMS; therefore, cracking width is added to support this procedure. PMS also evaluates cracks in both the inside and outside wheel path area, while HPMS only focused on cracks within the wheel path area. In addition, there is also a difference in the definitions of “wheel path,” in which HPMS uses 39-inch wide wheel path while DOTD PMS uses a 36-inch path. Although it is possible to convert the historical 2D PMS data into new 3D federal measures, it would be very complicated and costly to transfer the previous cracking measures on the 36-inch wheel path into the 39-inch results required by the FHWA. Additionally, with the new federal asphalt protocols, the results of composite pavement needs to be reanalyzed. Furthermore, the current condition of the interstate pavement is much better than the 5% poor threshold. Therefore, the previous PMS data was not adjusted to be consistent with the federal assessment.

Faulting: The current PMS only records faulting over 0.20 inches, and the average faulting values for 0.1-mile sections are calculated only from all faulting values over 0.20 inches because the criteria for joint repair treatment projects is 0.40 inches. The measured faulting values below 0.20 inches were not kept. However, the range of faulting from 0 to 0.20 inches covers all three rating levels in the federal assessment: good, fair and poor.

Because the HPMS and DOTD PMS use the same IRI and rutting measurements, these data have been available since 2003, and the PMU is satisfied with the prediction using this previous data. However, for cracking percent and faulting, when the PMU was preparing the TAMP report, only 2017 to 2020 datasets were available. This was due to the different new measurements required by FHWA.

Figure 5. Pavement condition criteria regulated by FHWA [91]

Federal Pavement Condition Criteria 23 CFR Part 490.313(b)			
Metric	Good	Fair	Poor
IRI (inches/mile)	<95	95 - 170	>170
Cracking (%)			
- Asphalt	<5	5 - 20	>20
- Jointed Concrete	<5	5 - 15	>15
- Continuously Reinforced Concrete	<5	5 - 10	>10
Rutting Asphalt (inches)	<0.20	0.20-0.40	>0.40
Faulting Jointed Concrete (inches)	<0.10	0.10-0.15	>0.15

With the measured IRI, rutting, cracking percent, and faulting, the conditions of these distress types can be rated. The criteria of the goodness rating is listed in Figure 5. In this figure, IRI and rutting have same criteria for all pavement types: asphalt pavement (ASP), composite pavement (COM), and jointed concrete pavement (JCP). However, the cracking percent rating depends on pavement type. The overall condition of a 0.1-mile section is rated by considering the combination of all these metrics' rating:

- If all the distress ratings are GOOD, then the overall rating is GOOD.
- If one or more distress ratings are POOR, then the overall rating is POOR.

- Any other conditions are rated as FAIR.

Currently, the analysis of interstate pavements is based on 521 homogeneous sections. The overall condition of the interstate highway system is therefore calculated by summing the average conditions and section lengths.

The Modern Era Retrospective-Analysis for Research and Applications (MERRA)

The Modern Era Retrospective-Analysis for Research and Applications (MERRA) was undertaken by NASA’s Global Modeling and Assimilation Office and was released in 2009. It is based on a version of the GEOS-5 atmospheric data assimilation system and collected data from 1979 through 2016. The data after 2016 was measured by an upgraded MERRA-2 system. MERRA is also incorporated in pavement research and design, such as LTPP database and pavement ME. Therefore, this database is selected as the source of climate input in this study.

Five climate parameters were provided in the Pavement ME system for Louisiana, including average annual air temperature, average annual precipitation, average annual freeze index, average annual wet days, and annual freeze/thaw cycles. These five parameters are widely accepted as factors influencing pavement performance.

Figure 6. MERRA data in Pavement ME

Date/Hour	Temperature (deg F)	Wind Speed (mph)	Sunshine (%)	Precipitation (in.)	Humidity (%)	Water Table (ft)
1/1/1985 12:00	68.7	8.4	2.3	0.139	95	20
1/1/1985 1:00	68	6.2	2.3	0.136	95.3	20
1/1/1985 2:00	65.9	5.6	8	0.119	94.8	20
1/1/1985 3:00	62.6	5.6	4.3	0.089	94.3	20
1/1/1985 4:00	58.6	6.2	3.5	0.047	94	20
1/1/1985 5:00	54.8	5.6	4.8	0.018	93.5	20
1/1/1985 6:00	51.8	6.7	7	0.004	93	20
1/1/1985 7:00	50	6.7	6.8	0	92.5	20
1/1/1985 8:00	49.6	6.7	9.8	0	89	20
1/1/1985 9:00	50.8	7.3	11.5	0	83.3	20
1/1/1985 10:00	53.1	7.3	11	0	76.8	20
1/1/1985 11:00	55.2	7.8	13.3	0	71.8	20
1/1/1985 12:00	56.8	7.3	16	0	69	20

These datasets are stored as weather stations within Louisiana, with hourly climate data available from 1985 to 2017 (Figure 6). Such a large dataset would be difficult to apply for analysis. Therefore, the average values of these five climate inputs were calculated for each district.

Project/Highway Information and Highway Needs Files

The DOTD Construction Project database provides a query tool for users to search all types of highway project records from DOTD TOPS (old projects, mainframe), LaGov PS (Project Systems), AASHTO Projects, and SiteManager Applications. The obtained project information includes project number, control section information (control section number and start/end point of log miles), final inspection dates, and work types (i.e., asphalt new pavement, asphalt widen and overlay, etc.). The main application of this database is to determine the pavement age using the final inspection date and the start-end log mile of the control section. To achieve this goal, all maintenance and rehabilitation project records are extracted, along with their control section and final inspection information. For every 0.1-mile section in HPMS or PMS, the project history can be obtained by comparing the control section information and final inspection date. A program in Matlab is compiled to assign the latest three project records on every 0.1-mile sections. This allows the pavement age in each year to be obtained.

The Highway Needs files provide additional network-level information, such as homogenous section data, including pavement type, average daily traffic (ADT), number of lanes, and functional classification.

In addition to the network-level information obtained from the DOTD Construction Project database, more detailed project-level data such as treatment type (thin-overlay, medium overlay, chip seal, etc.), design traffic information (ADT and truck percent), pavement structural information (overlay thickness and milling depth) can be obtained by verifying them with their design documents in FileNet and Plans Room.

Objective

The main objective of the research project was to develop both short-term and long-term pavement performance prediction models that can be used to estimate future pavement condition and smoothness for Louisiana's flexible and rigid pavements based on DOTD's PMS and other related pavement data using the soft computing technique— ANN modeling.

Specifically, the following objectives were accomplished in this study:

1. Develop an accurate short-term pavement cracking forecasting model (ANN modeling) to predict the 2- and 4-year future cracking percentage for all asphalt surfaced pavement (ASP and COM) and jointed concrete pavement (JCP) segments currently included in Louisiana's interstate and NHS pavement network, based on DOTD's 2017-2020 pavement performance condition database.
2. First, establish a historical pavement condition database for all asphalt overlay projects constructed after 2009, including various thicknesses and pavement types of ultra-thin, thin, medium, and structure overlays. The developed overlay pavement database was then used to develop the long-term pavement performance models (ANN modeling) using two different approaches:
 - a. Incremental performance models: Use two previous cycles' PMS pavement condition data, mill/overlay thickness, and accumulative traffic information to predict the future pavement performance (up to 15 years) for three flexible pavement performance indicators (IRI, rutting, and percent cracking) and five distress indices (ALCR, RNDM, PTCH, RUT, and RUFF).
 - b. Family-curve prediction models: Use project-based information of pavement age, functional class, thickness, and five weather-related project data to develop IRI and distress indices' family-curve performance models for different functional class ASP pavements in Louisiana.

Scope

To achieve the objectives, pavement condition data was collected from the PMS database and from the DOTD and HPMS databases for federal analysis. Other parameters such as pavement age, traffic, structural information, and climate were also extracted from the DOTD system and combined with pavement condition data. Short-term pavement performance models for various pavement types and functional classes were developed based on the HPMS database. ANN and ANFIS were applied for model training, and different algorithms and model structures were examined to obtain optimal short-term performance models to forecast 2-year and 4-year cracking conditions. Similarly, the long-term models were built with PMS data extracted for 255 ASP overlay projects to predict network-level pavement performance for IRI, rutting, percent cracking, and five distress indices (ALCR, RNDM, PTCH, RUT, and RUFF). Based on long-term prediction, a set of family curves was also generated for various functional classes.

Methodology

The methodology of this research was divided into two parts. First, the procedures for short-term and long-term pavement performance modeling are presented. The objective of these performance models was to support network-level decision-making procedures within maintenance strategy and supervise the overall condition of the roadway system. The data used for the modeling was collected from Louisiana PMS and HPMS databases. Considering the differences in purposes and applications between long-term and short-term models, the methods for their project selections were also different, as presented in this chapter. Other factors influencing pavement performance, such as treatment types, layer thicknesses, pavement age, traffic, and climate, were also incorporated within the models developed in this study. Therefore, the procedures for collecting these parameters from PMS and HPMS data were developed in this section correspondingly. The first part of this methodology chapter aims to provide a comprehensive procedure for project selection and data preparation, which can be immediately extracted from the current DOTD system and conveniently updated with newly surveyed data in the future, without major revision. To achieve this goal, the following databases were investigated:

- Louisiana PMS and HPMS
- Louisiana Highway Needs File
- DOTD Construction Projects and FileNet
- MERRA dataset

Second, based on a literature review, several shallow machine learning techniques were selected for training long-term and short-term performance models. The collected data is organized according to the structure design of the models, serving the purpose of performance modeling. The following artificial neural networks were investigated to explore optimal methods for forecasting pavement conditions.

Project Selection and Data Collection

Louisiana DOTD has been working on collecting and maintaining various of databases of pavement performance and treatment history records for decades. These databases provide a wealth of valuable information for modeling pavement performance and supporting decision-making procedures.

According to the previous research focused on pavement performance modeling, the model inputs can be generally categorized as (1) pavement performance data, (2) traffic data, (3) climate data, and (4) treatment and structural information. Considering the availability of these categories of databases in Louisiana DOTD, pavement performance datasets were obtained from PMS and HPMS. The traffic data was extracted from the Highway Needs Database. The climate data used in this project was provided by the MERRA, and the detailed records of pavement maintenance and rehabilitation were collected from the Highway Project Information database and FileNet. The details of these databases are as follows.

Dataset for Short-term Performance Modeling

The database for short-term pavement performance modeling is prepared based on the purpose of this research, the availability of datasets from DOTD, and the future implementation for local agencies.

The HPMS database used in this study contains 0.1-mile record of pavement condition for the entire NHS system of Louisiana roadways collected from 2017 to 2020. The database includes measures such as roughness, rutting, cracking (alligator, transverse, and longitudinal cracks), faulting, patching, roadway geometry (number of lanes, route, district, direction and GPS coordinates), and operating information (date, driving speed of data collection). Due to the treatment projects applied during this period, the pavement conditions of the roadways under construction could not be measured. Thus, the records of some specific sections were not consecutive.

The first step in processing the HPMS database was to filter the data by ElementID to obtain the sections with all 4 years' performance. ElementID is the description of each 0.1-mile section of HPMS data, consisting of pavement control section, the starting log-mile, and traffic direction of the section, which is unique for each 0.1-mile section. It was found that 35,913 0.1-mile sections, equaling 3,591 miles of NHS pavements, have integrated records for further analysis.

The HPMS database only contains pavement performance conditions. In order to incorporate other factors recommended by previous research, such as climate, traffic, and age information, the following databases were utilized to combine with the filtered HPMS data:

Climate: The MERRA dataset was adopted, considering its wide application in pavement analysis such as MEPDG. The average climate factors, including annual air temperature, annual precipitation, freezing index, annual number of freeze-thaw cycles, and annual number of wet days for all districts in Louisiana, were extracted. The average climate inputs by district were calculated and listed in Table 2:

Table 2. Average climate inputs by district

District	Mean annual air temp (F)	Mean annual precipitation (in)	Freezing Index (deg F - days)	Average annual number of freeze/thaw cycles	Number of wet days
2	69.7	49.3	1.2	3.3	305.2
3	67.9	48.7	4.0	11.3	307.2
4	65.5	52.0	13.3	28.9	293.2
5	65.3	53.0	18.3	31.2	287.6
7	67.7	50.9	3.5	12.9	308.7
8	66.2	52.2	8.1	23.4	302.0
58	66.0	51.8	13.0	26.2	297.0
61	67.6	50.7	4.2	14.0	308.6
62	67.7	52.5	3.4	12.9	308.4

Traffic: The most recent 2019 Highway Needs file available contains homogenous section performance and traffic information, including annual average daily traffic (AADT) and truck percent. Matlab code was compiled to extract ADT and truck percent for each 0.1-mile HPMS section.

Pavement age: The pavement construction and preservation projects recorded in the DOTD Construction Projects database was used for calculating pavement ages. A total of 7,751 projects records from 1990 to 2021 were obtained from this system, including new construction, structural overlay, maintenance overlay, or surface treatment projects on all state-maintained roadways. The information in these records consisted of project number, control section, project cost, final inspection date, begin and end log mile, and work types. For each HPMS section, its beginning and ending log mile were examined with the 1990-2021 project records to obtain all construction and preservation history on this 0.1-mile section. This information was used to determine the pavement ages for 2017-2020.

With this information combined, the updated HPMS database included traffic data, existing pavement condition, age, and climate. For each year's data, the accumulated truck numbers on 0.1-mile sections were calculated based on its pavement age, ADT, and truck percent. The data was cleaned by removing records such as no construction and preservation records (pavement age larger than 32) or changes in pavement types.

The data collection device for faulting of JCP surfaces was updated from 2D to 3D in 2020. Therefore, it is not appropriate to train an ANN model with 2018 and 2020 performance as input and output. Although the faulting data from 2017 to 2019 was consistent, the trained models based on these 2D collected specimens would not be suitable for predicting the 2022 performance prediction, since the 2020 data was measured with different methods. Therefore, the faulting model in this study was not determined by machine learning methods.

Each year, HPMS has a varying number of rows due to the interference caused by project construction on roadway surface condition survey. The rows in Louisiana HPMS during 2017 to 2020 were 41,679, 38,464, 42,731, and 42,651, respectively.

The inputs for training this model included the initial pavement condition (cracking percent), ADT, accumulated trucks, and climate. The output of the model was the pavement condition after a 2-year time interval. The updated HMPS database was then reformatted based on this proposal by using the pavement conditions of 2017 and 2018 to predict the conditions of 2019 and 2020, respectively. For each 0.1-mile section, the 4-year record was transferred as two specimen for model training. If there was a significant distress reduction (e.g., cracking percent reduction > 5%) without any project information in between, these samples were also removed.

FHWA requires State DOTs to separately report the conditions of interstate highways. The traffic conditions of interstate highways vary from rural to urban areas, and the traffic conditions also vary among interstate, arterial, collectors, and local roadways. Therefore, multiple models were for these functional classifications. For the other non-interstate NHS roadway sections, there were five functional classifications. Note that not all non-interstate NHS functional classifications had enough samples for training ANN models. The CRCP data has less than 20 miles for each group, which is also not sufficient for ANN training and was therefore removed from this study.

Table 3 presents a final list of short-term performance modeling datasets prepared using the 4 years of pavement condition data (2017-2020) available in HPMS. As shown in

Table 3, those datasets were categorized based on three pavement types (i.e., ASP, COM and JCP) and six functional classifications. In addition, the numbers in the table represent the quantity of 0.1-mile sections of each considered modeling dataset in this study.

Table 3. Prepared HPMS data for modeling short-term performance

UN	Roadway Functional Classification	ASP	COM	JCP
01	Interstate Rural	3879	4317	4641
02	Principal Arterial Rural	9469	9825	4566
06	Minor Arterial Rural	2	4	-
11	Interstate Urban	1728	1840	2738
12	Freeway Urban	469	183	561
14	Principal Arterial Urban	1840	4982	3656
16	Minor Arterial Urban	486	104	17

Dataset for Long-term Performance Modeling

Long-term performance models play a vital role in the decision-making procedure, serving as the foundation for comparing and analyzing optimal pavement treatment scenarios. In order to build the long-term performance models, the first step was to locate and verify the records of these treatments. PMS treatment history records were adopted since they contain the information of both treatment types and project numbers on 0.1-mile sections distributed across all functional classifications of state maintained roads in Louisiana. Additionally, after the verification of these projects, their ElementIDs would be very convenient for extracting and combining information from other databases from DOTD.

The ElementIDs of these 0.1-mile sections with various maintenance and rehabilitation types were extracted from PMS treatment history records. An ElementID is a nine-digit unique identifier describing the control section, lane direction, and starting log mile of the 0.1-mile section, which is unique within every PMS sub datasets (collected within one cycle). For each treatment type, its ElementID list and project name was obtained, and the final inspection dates of these projects are verified with Highway Project Information database to determine the ages for each PMS record of every specific 0.1-mile section. For example, for a 0.1-mile section with previous project final inspection data of September 2010, the age of the pavement performance collected on this section on December 2013 was 3.25 years (36 months).

The design files for these projects were searched in the FileNet system and DOTD's Plans and Proposals system to investigate the project-level information of the involved pavement structures. Details of the roadway sections, such as design AADT, truck percentage, overlay thicknesses, and milling depth, were recorded to confirm the maintenance or rehabilitation information from the PMS treatment history. The number, beginning, and end of the control section were checked with the range of the selected project's ElementIDs, and the design ADT and truck percent were extracted from the project plan. The structural information, including layer thickness, cold plane thickness, number of lanes, and width of lanes, was checked on the page of the typical section.

For every ElementID, their related project information was verified based on the procedure above, and a table summarizing the project number and the information (final inspection date, ADT, and structure) was generated. Then, for each pavement treatment type, their 0.1-mile sections with ElementID lists and corresponding project information, age, and climate was obtained.

The next step was to obtain and organize the pavement performance data of these pavement treatment types on their 0.1-mile sections. The obtained ElementID was used to extract 10 records of this 0.1-mile section from all sub datasets from 2003 to 2021. Access database was applied for this record extraction by importing and combining both ElementID lists and PMS sub dataset, and the ElementID was used as the key for record searching and exporting. For each pavement treatment type, every individual of its 0.1-mile sections has 10 rows of performance records (some of them have less than 10 rows of records due to the construction activities on related roadway segments). Climate parameters in Louisiana obtained from MERRA (the average climate factors including annual air temperature, annual precipitation, freezing index, annual number of freeze-thaw cycles, and annual number of wet days) were added by district in this step, same as the procedure in short-term performance modeling. The pavement age values corresponding to the surface condition data were calculated with the final inspection date of the project and the date of data collection in PMS.

The contents of these data rows are listed in Table 4.

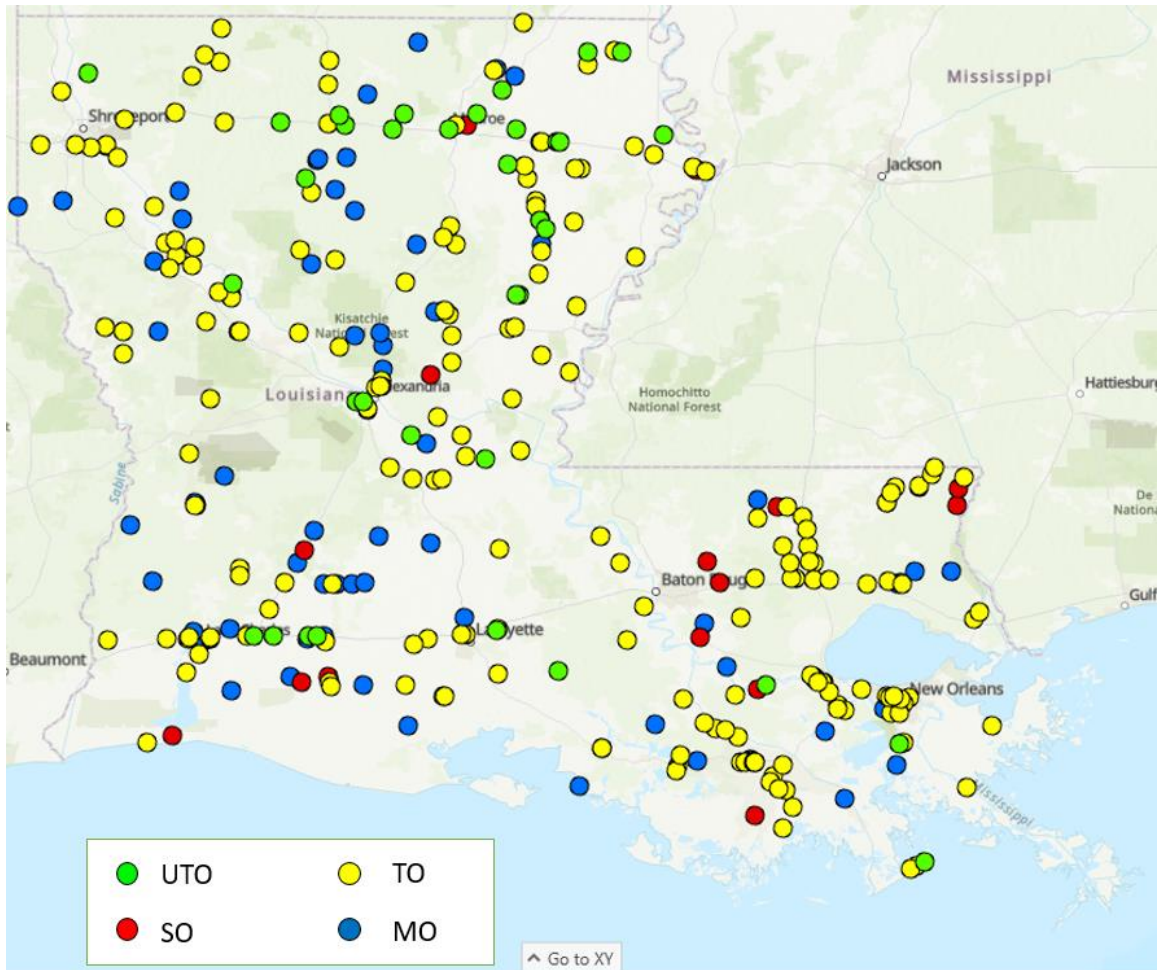
Table 4. PMS data extracted for long-term performance modeling

Categories	Items
Description	Control section, Roadway name, Direction, ElementID, District, Parish, Log mile from, Log mile to, Functional Class, Pavement type, Date of data collection
Pavement Performance	ALCR, RNDM, PTCH, RUT, RUFF, Average IRI, Average rut depth, Alligator cracking extents (High, Low, and Medium), Longitudinal cracking extents (High, Low, and Medium), Transverse cracking extents (High, Low, and Medium)
Project Info	Project name, Design ADT, Truck %, Final inspection date, Overlay thickness, Milling depth
Climate	Annual air temperature, Annual precipitation, Freezing index, Annual number of freeze-thaw cycles, Annual number of wet days

Due to the variations of in these 0.1-mile section pavement performance data, it is usually difficult to obtain a smooth performance curve with a clear trend, and thus not immediately adopted for long-term pavement performance modeling. In addition, local agencies do not determine maintenance strategies or select pavement treatments based on a 0.1-mile section. Therefore, the average value of pavement performance was obtained for modeling long-term pavement condition.

There were a total 112,487 PMS records collected for thin overlay (TO), ultra-thin overlay (UTO), medium overlay (MO), and structural overlay (SO) projects. Out of these records, 46,895 records have a negative value of age, indicating that these pavement conditions were measured before the construction of these overlay projects and were therefore removed from the database. The remaining 65,592 records belong to 1,348.5 lane-miles of roadways on 12 functional classifications. There are a total of 363 overlay projects verified with design documents, and they are located in all the districts within Louisiana (Figure 7). These projects cover all four major overlay treatment types on all highway functional classifications, with the ADT ranging from low volume local routes (less than 300) to high volume interstate highways (larger than 60,000).

Figure 7. The locations of selected overlay projects in Louisiana



The distribution of collected PMS records in various ADT ranges is plotted in Figure 8. 36% of the data samples of the selected projects have an ADT of less than 3000. Another 30% of the samples have a medium traffic volume (ADT 5000~15000). The data distribution in various functional classifications is shown in Figure 9.

Figure 8. Distribution of PMS records of selected projects among ADT ranges

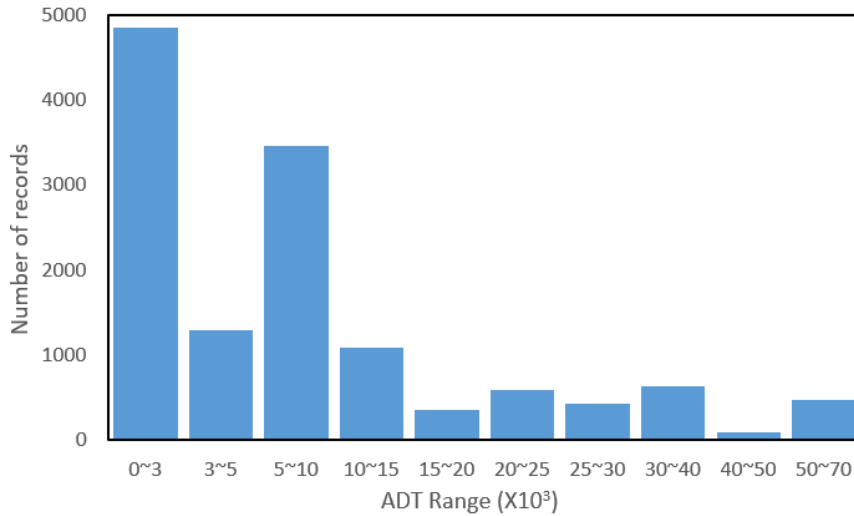


Figure 9. Distribution of PMS records among functional classifications

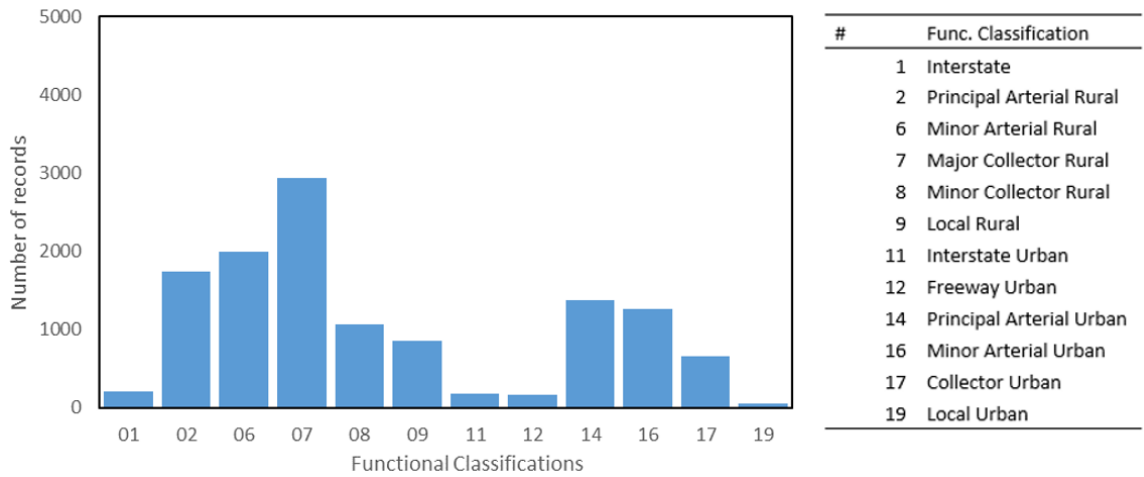


Figure 7 through Figure 9 show that the investigated PMS data represents most of the conditions in Louisiana. However, the noises and errors present in these single 0.1-mile PMS performance data were introduced due to variations of field measurements, changes in equipment for data collection, and the shifting of the start and end point of the sections. Additionally, the decision-making procedures performed by local agencies for selecting maintenance and rehabilitation treatments are not determined by a single 0.1-mile section. Therefore, the condition data of these 0.1-mile sections were processed to obtain the average performance values of the roadway sections of the overlay projects.

The averaged performance data showed a more consistent trend, and therefore has more reliability in performance modeling, especially for long-term performance. The 0.1-mile PMS condition data was averaged by overlay project and roadway directions (some of the roadway projects are constructed on both directions), and these 1,794 average data are summarized in Table 7.

The description of this overlay PMS database is listed in Table 5.

Table 5. Summary of overlay PMS database

Type	Projects	mileage	Age	ADT range	Truck%	Milling depth	Overlay thickness	Number of data
UTO	37	171.2	0-12.6	400-37,300	5-34	0-2	0.75-1.0	147
TO	230	746.6	0-14.8	75-66,700	3-34	0-4	1.5-2	1,236
MO	79	374.3	0-15.1	100-28,600	7-25	0-4	2.5-4	340
SO	17	56.4	0.4-11.1	650-23,600	5-40	0-2	2-8	71
Total	363	1348.5		75-66,700	3-40			1,794

Difference in Long-term and Short-term datasets

The differences between the datasets prepared for long-term and short-term pavement performance models are summarized here:

- **Pavement surface condition data:** the surface condition data for long-term performance was extracted from the PMS and represents the average values of a series of connected 0.1-mile sections of a treatment project or a homogenous section/control section within a project. These data were collected from pavement treatment projects spread all over the Louisiana area from 2003 to 2021. These data were collected every two years for most of the roadway functional classifications. On the other hand, the data used for short-term performance was obtained from the HPMS database, specifically from the interstate highways and NHS within Louisiana for the years 2017, 2018, 2019, and 2020. More details about the difference between roadway condition survey methods of PMS and HPMS can be found in previous sections.
- **Pavement structural information:** The structural information for long-term performance condition data was collected and verified from design files. However, no structural data was available for short-term performance prediction.
- **Traffic data:** The traffic information for long-term performance models, including ADT and truck percentage, was extracted from design documents,

which represent the traffic condition at the year of design. For short-term data, these parameters were obtained by matching the log mile and control section with Highway Needs files, in which the ADT and truck percent of 2009 are used.

Pavement Performance Prediction Using Machine Learning

Artificial Neural Network (ANN)

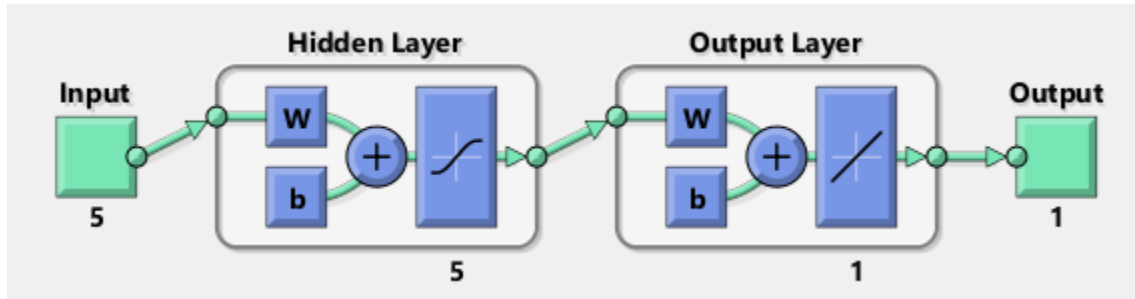
In this research, the Matlab Deep Learning Toolbox was adopted for the training procedure of ANN models for predicting pavement performance [92]. The ANN can be built using both Deep Learning Applications and coding.

The dataset was randomly divided into training, validation, and testing sub datasets before training with designed ratios. During the training procedure, the training samples were presented to the ANN and used for computing the gradient, updating the network weights and biases. Additionally, the ANN was adjusted according to its error. Validation samples were used to measure the network's generalization and to halt the training procedure when generalization stops improving [92]. The error on the validation set was monitored during the training process, which typically decreases during the initial phase of training, similar to the training set error. However, when the network began to over-fit the data, the error on the validation set typically began to rise. The network weights and biases were saved at the minimum of the validation set error.

The testing dataset did not have an effect on training; instead, it provided an independent measure of network performance during and after the training procedure. If the error on the test set reached a minimum at a significantly different iteration number than the validation set error, this might indicate a poor division of the dataset. The default ratio among these three datasets was 70%, 15%, and 15%.

The number of hidden layers and the numbers of neurons in each layer were designed. The numbers of neurons in hidden layers directly affected the model performance. Having too many or too few neurons resulted in overcomplicated or oversimplified models. Therefore, it was necessary to determine the optimized numbers of neurons through a trial-and-error process. Figure 10 shows an example of designed ANN structure with 5 input neurons, a hidden layer with 5 neurons, and 1 output neuron in Matlab.

Figure 10. Designed ANN structure in Matlab



The training algorithm should be defined before training the designed ANN. The Neural Net Fitting (nftool) Application of the Matlab Deep Learning Toolbox offers three of the most commonly used training algorithms: Levenberg-Marquardt, Bayesian Regularization, and Scaled Conjugate Gradient:

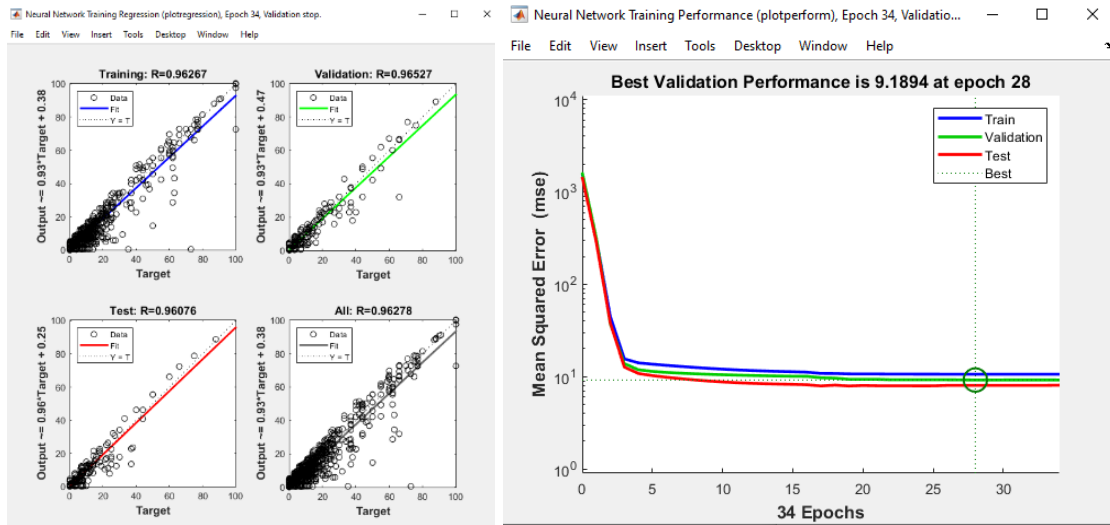
Levenberg-Marquardt Algorithm typically requires more memory but less time. With this algorithm, the training procedure stops when generalization is not improving anymore. This can be dragonized by increasing the mean square error (MSE) of the validation sample dataset.

Bayesian Regularization Algorithm requires more computing time, but its algorithm is suitable for datasets with a smaller sample population and noise. With this algorithm, the training procedure stops according to adaptive weight minimization (regularization).

Scaled Conjugate Gradient Algorithm has the benefit of requiring less memory. Similar to the Levenberg-Marquardt Algorithm, the training procedure using this algorithm stops when generalization is not improving.

The prediction power of trained ANN models was evaluated by the mean squared error (MSE) and regression R values. Figure 11 shows an example of ANN training based on data of the cracking percentage of JCP pavement collected on functional class 14 (Minor Arterial Urban). The training used the Levenberg-Marquardt algorithm and stopped at epoch 28, where the validation dataset had the best performance with an MSE of 9.2. The R values for all 3 datasets and the overall dataset were all above 0.96 ($R^2 > 0.92$), indicating a strong correlation between the outputs (predicted cracking percentage with trained ANN) and the targets (measured cracking percentage).

Figure 11. Model performance and regression of trained ANN (JCP, Functional Class 14)



In this study, the ANN was applied to obtain short-term performance models based on the PMS and HPMS databases. For each dataset from a specific pavement category (pavement distress, pavement type, and functional class), various combinations of input values were tested to examine the most suitable parameters for predicting future pavement performance. Trail-and-error procedures were also applied to obtain the optimized ANN structures (number of neurons) and training functions. Due to the fact that various MSE and R values were generated from random training, validation and testing dataset sample selection within the same database, the same model was trained for multiple times, and the average MSE and R were used for model evaluation.

Neuro-Fuzzy Designer

The Matlab Fuzzy Logic Toolbox software provides a command-line function and an interactive app (Neuro-Fuzzy Designer) for Sugeno fuzzy inference systems using neuro-adaptive learning techniques, similar to the techniques used for training ANN models. The panel of the Neuro-Fuzzy Designer is shown in Figure 12.

Figure 12. Neuro-Fuzzy Designer panel in Matlab

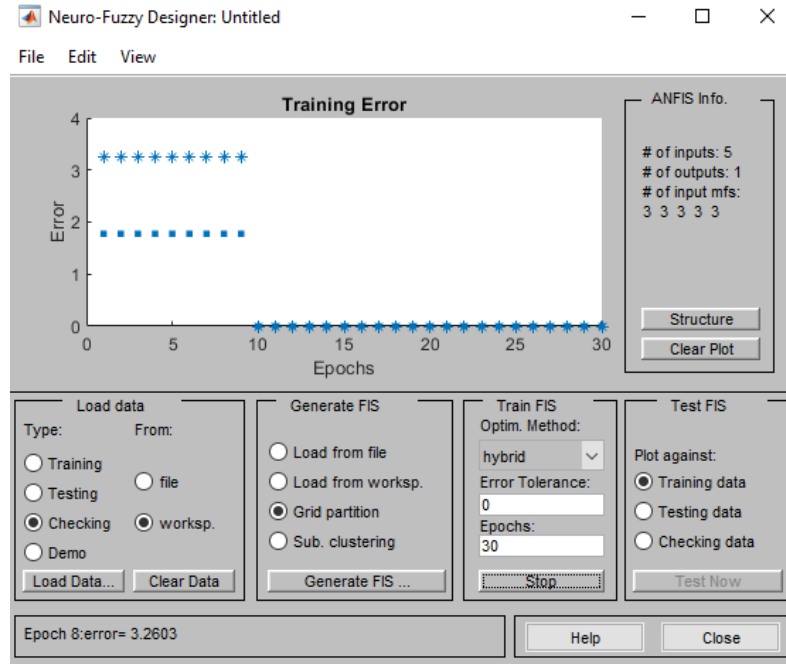
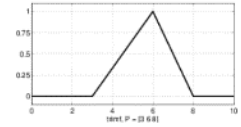
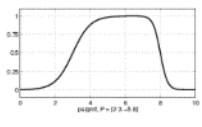
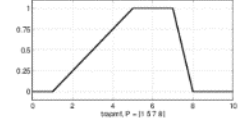
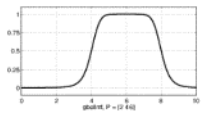
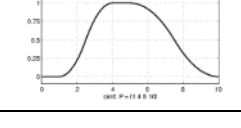
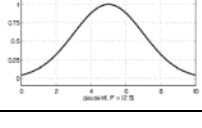
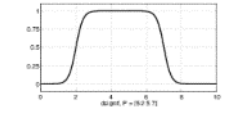
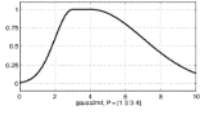


Figure 12 presents the main panel of ANFIS Panel in Matlab, where the training, testing, and checking datasets were loaded using this graphical user interface (GUI) either through a file or workspace. The FIS was created using either the grid partition method or the subtractive clustering method. The grid partition is the default method of the FIS generation in Matlab. It generates rules by enumerating all possible combinations of membership functions for all inputs. However, this resulted in a large number of rules when more than 4 or 5 inputs are defined for the FIS, with 3 to 5 MFs for each input. Having too many inputs or MFs significantly increased computing time. To reduce the performance deterioration due to large number of rules, Matlab also provided an alternative by generating rules through the subtractive clustering method. The subtractive clustering method categorized the input data into clusters and generated an FIS with the minimum number of rules required to distinguish the fuzzy qualities associated with each cluster. However, this simplification may have resulted in a loss of accuracy in the built prediction models.

Neuro-Fuzzy Designer also provided various options for membership functions to build FIS models. In addition to the bell-shaped and Gaussian membership functions introduced above, MFs with other shapes and equations were also available for users to perform trial-and-error to locate suitable MFs and determine their corresponding

parameters through training procedures. The MFs and their details available in Neuro-Fuzzy Designer are listed in Table 6.

Table 6. Membership functions in Matlab’s Neuro-Fuzzy Designer

MF	Name	Plot	MF	Name	Plot
trimf	triangular		psigmf	product sigmoidal	
trapmf	trapezoidal		gbellmf	generalized bell-shaped	
pimf	π shaped		gaussmf	Gaussian	
dsigmf	difference sigmoidal		gauss2mf	two-sided composite of different Gaussian	

The parameters of these MFs are also shown in the panels, and the main task of the training procedure was to update and obtain these MF parameters to fit the given input data.

With the designed structure of membership function numbers and types, the ANFIS can be trained with a given error tolerance and number of epochs. The training was stopped when either of these two criteria is achieved. The training procedure was monitored, as shown in Figure 10, where the error values (RMSE) of both the training and checking datasets for each completed epochs are plotted in the window.

K-Fold Cross Validation in Machine Learning

During the developing of ANN models, the training, validation, and testing datasets were usually randomly selected from original database. To evaluate the performance of the trained models, R^2 values and root mean square errors (RMSE) of both the training and testing datasets were observed, and the optimal model structures were determined. However, the RMSE values could greatly vary due to the bias of the randomly divided datasets, which introduced difficulty in model optimization. The R^2 and RMSE were calculated as follows:

$$R^2 = 1 - \frac{\sum(y_i - y_{ip})^2}{\sum(y_i - y_{ave})^2} \quad (22)$$

$$RMSE = \left[\left(\frac{1}{N} \right) \sum(y_i - y_{ip})^2 \right]^{1/2} \quad (23)$$

Where, y_i is the i -th measurement, y_{ip} is its corresponding prediction, N is the number of data points, and y_{ave} is the average value of all y_i .

One method for avoiding this drawback was to train the model (with the same model configuration) multiple times, with different training and testing sets each time (these sets came from same dataset), then evaluate the average RMSE and R^2 . K-Fold cross validation provided a standard procedure for this methodology.

- The first step was to divide the original dataset into K equally-sized folds.
- Then the No. K fold of data was assigned as the testing dataset, the No.1 through $K-1$ sets were applied as training set, and the R^2 and RMSE were recorded after model development.
- Next, use No. $(K-1)$ fold as the testing set and all the remaining folds as training set, and record R^2 and RMSE.
- Repeat this procedure until every individual fold has been used as the testing sets, then take the average R^2 and RMSE as a reference for model evaluation.

In order to further optimize this method, the original dataset was shuffled before dividing it into K folds. This K-fold cross-validation was implemented as a loop for ANN modeling to detect the optimal model structures.

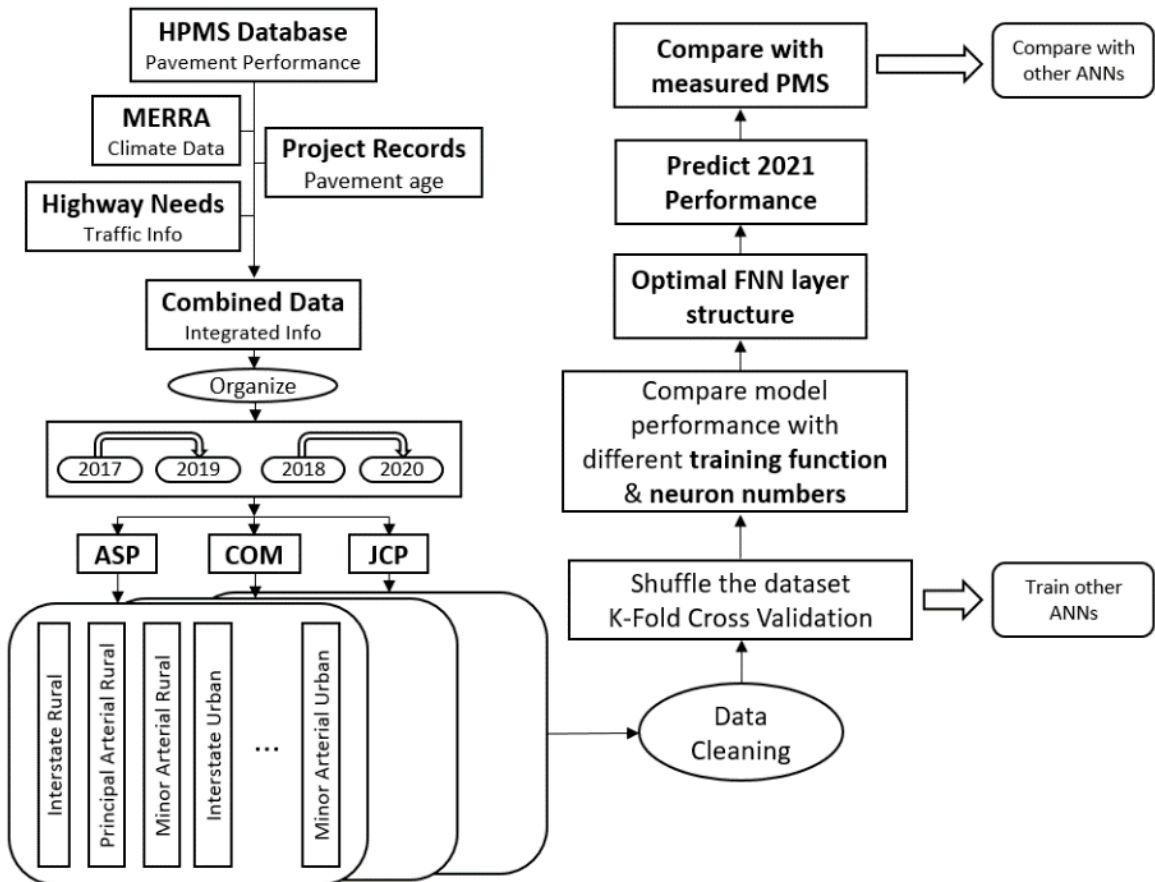
Development of Short-Term Prediction Models

For every individual model, a correlation matrix was constructed to determine the optimal climate factor out of the five MREEA parameters for model training. Using the selected climate factor, existing cracking percent, ADT per lane, and accumulated trucks as input, and cracking percent after two years as output, the dataset for each model was loaded into an ANN for model training.

The performance of various ANN structures (hidden layer size) and training algorithms were examined based on correlation coefficients and RMSE. K-Fold validation was applied within this procedure to minimize the variation introduced by random selection of datasets (training, testing, and validation) and provide a stable trend for RMSE values.

For each algorithm, the optimal model considering R^2 and the least RMSE was obtained. These candidate models were further validated with a newly measured dataset in HPMS (i.e., pavement condition data collected in 2021). Since the pavement age is missing in the dataset of the HPMS 2021, the 0.1-mile sections with a significant decrease in cracking percent from 2019 to 2021 were considered as sections where treatments were applied during this period, and therefore removed. The remaining 2021 measured data was used to test the prediction power of the candidate models, and the final optimal model was determined for future implementation. Two machine learning techniques, ANN and ANFIS, were selected in this short-term performance modeling, and their prediction power was compared. The procedure is shown in the flow chart in Figure 13.

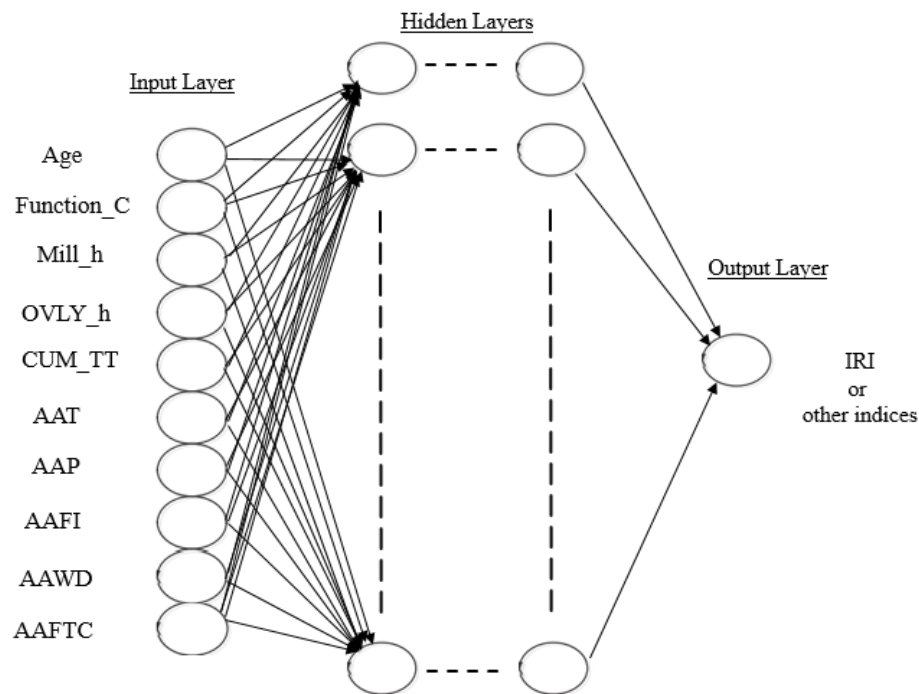
Figure 13. Flow chart of building short-term ANN pavement performance models



Development of Long-term Prediction Models

Different machine learning and neural network methods, such as including the SVM model, tree-shaped models, and artificial neural network (ANN) models, have been successfully used to forecast short-term pavement conditions at either the project level or network level [56, 92]. However, existing models still face challenges in accurately predicting long-term pavement conditions under real-world conditions. These conditions include different types of sequential and non-sequential variables that affect the development of pavement performance, and the variables have varying levels of values. One of the purposes of this study was to develop long-term pavement condition prediction models at the network level for DOTD's asset management implementation. To achieve this, the following neural network modeling approaches were considered (Figure 14).

Figure 14. ANN model structure for IRI family curve



Similar to the optimizing procedure for short-term performance models, the model structures of both hidden layer sizes and number of layers was investigated. Their R^2 and RMSE values were used as references for model evaluation. In addition, the predicted long-term performance curves was also considered when selecting models with better

prediction power. For example, performance curves with significant variation after 13 years were not rated as desired models, even though they may have had excellent R^2 and RMSE during training.

Discussion of Results

Short-Term Cracking Percent Prediction

Based on the methodology mentioned above, in order to predict 2- and 4-year future cracking percentages for all interstate and NHS pavement segments in Louisiana, a group of short-term performance modeling datasets were assembled, as shown in Table 3. The modeling datasets were prepared through data mining from all 2017-2020 HPMS 0.1-mile sections together with associated traffic loading and site-specific climate data. Two machine learning techniques, ANN and ANFIS, were considered to build each individual short-term cracking percent prediction model. Specifically, all prediction models were developed using the MATLAB® computer programming platform. Each individual prediction model was specifically coded, trained, validated, and tested. The model development and results are presented in the following sections.

ANN Model Training and Performance

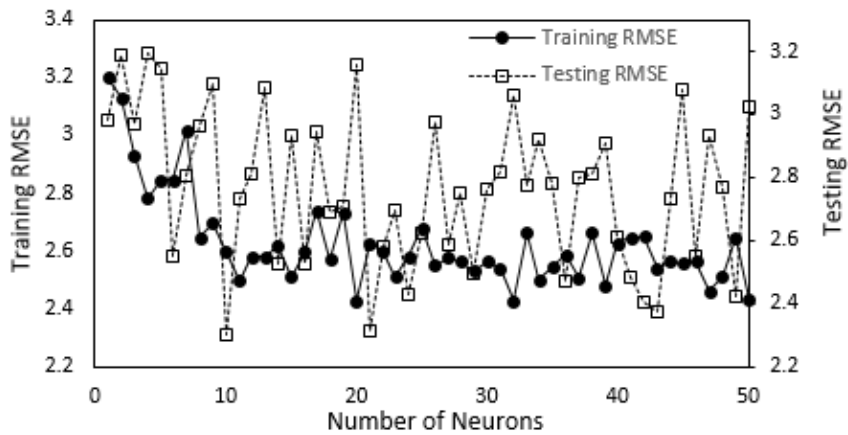
Selection of Neuron Numbers and Backpropagation Algorithms

In this study, a single layer feedforward ANN model structure was adopted for training short-term pavement cracking percent prediction datasets. However, due to the variation in the quality and quantity of data samples among different pavement categories, it was difficult to obtain a single model suitable for all pavement types and functional classifications. In addition, each backpropagation algorithm also had pros and cons when working with different types of datasets. Therefore, for every individual pavement family, various single hidden layer ANN models were built with different neuron numbers and training algorithms. The training and testing RMSE values were compared to evaluate model performance and determine the optimal ANN.

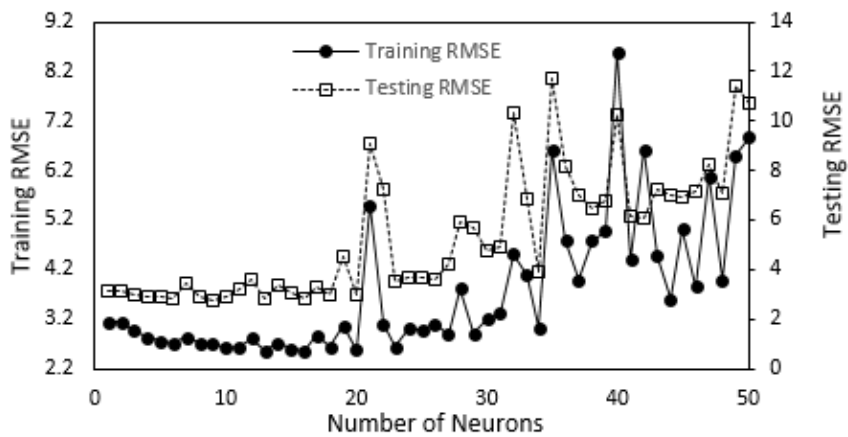
This procedure is explained here based on an example of selecting neuron numbers and training algorithms for asphalt pavement sections on Interstate Rural (ASP, Functional Classification 01). There were total 3,869 rows of data prepared in this category, with five inputs, including current cracking percent, freezing index, pavement age, and ADT per lane. Freezing index was selected as the climate feature because this parameter has the most relevance to the output, future cracking percent (measured two years later than the input cracking percent), out of the five MERRA climate data. These 3,869 samples were shuffled with randomly generated series numbers and were evenly divided into five data

folds for a five-fold cross validation. The benefits of the K-fold cross validation can be seen in Figure 15, where the noise in both training and testing RMSE curves was too significant to determine the extremum points for capturing the optimal hidden layer size (Figure 15 (a)). However, when a five-fold cross validation was applied, it became obvious that when the number of neurons was larger than 20, the ANN model lost the stability in performance and showed significant oscillation in RMSEs. This indicates that the model is overfitting the data (Figure 15 (b)). Therefore, the ANNs with a number of neurons over 20 were not investigated in the following steps.

Figure 15. Relationships of RMSE values with neuron numbers (a) without cross validation (b) with five-fold cross validation



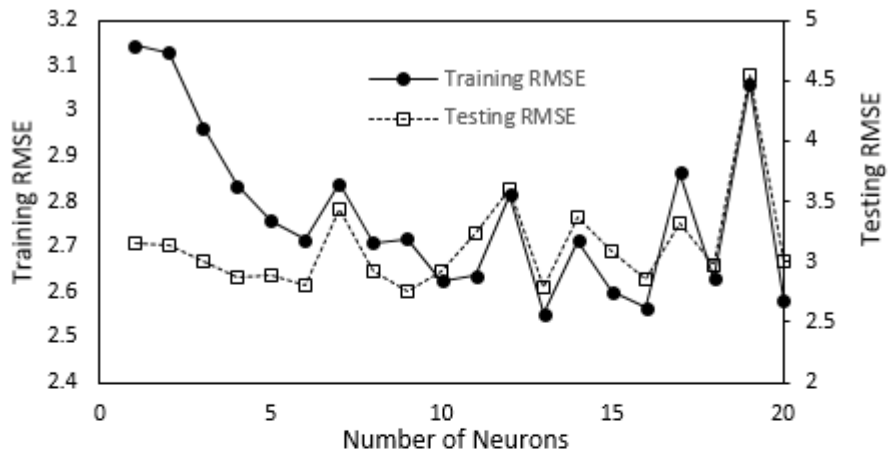
(a)



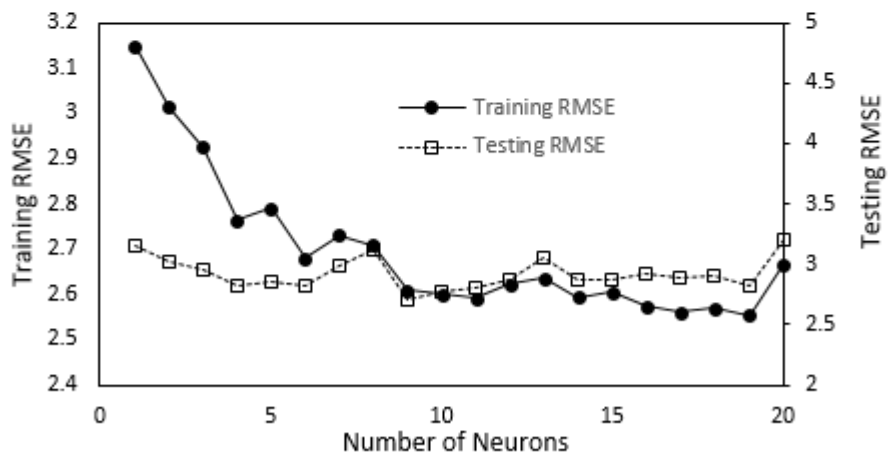
(b)

Three training algorithms commonly adopted by other researchers were also examined: Levenberg-Marquardt (trainlm), Bayesian Regularization (trainbr), and Scaled Conjugate Gradient (trainscg). For each training algorithm and a specific number of neurons, K-fold validation was added to obtain the average RMSE for both training and validation as well as testing datasets. The relationships between RMSE and the number of neurons for the three algorithms are plotted in Figure 16.

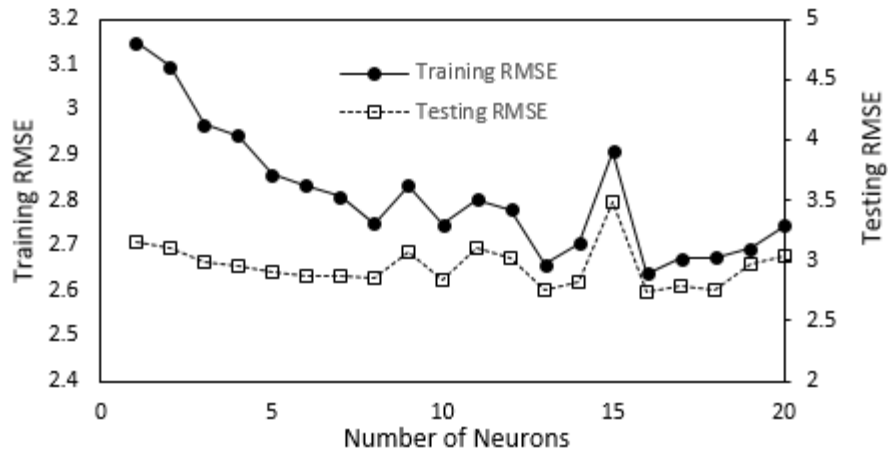
Figure 16. Neuron numbers vs. training/testing RMSE values with (a) Levenberg-Marquardt Algorithm, (b) Bayesian Regularization Algorithm and (c) Scaled Conjugate Gradient Algorithm



(a)



(b)



(c)

The curves in Figure 16 were used to evaluate the performance of models and algorithm for the dataset of the selected pavement category. The optimal ANN model, including model structure (hidden layer size) and suitable algorithm, could be determined as well. (1) The ANN models using Levenberg-Marquardt Algorithm (trainlm) with a hidden layer size from 1 to 6 showed consistently decreasing trends in both training and testing RMSEs. The RMSE curves began to fluctuate starting from 7. Therefore, neuron number 6 was selected as optimal structure for the ASP Interstate Rural ANN with trainlm. (2) The Bayesian Regularization Algorithm (trainbr) was similar to trainlm and also showed 6 as the optimal number of neurons. However, this algorithm showed a smoother curve, indicating a better stability than trainlm. (3) Scaled Conjugate Gradient Algorithm took more neurons to reach the optimal RMSEs at 8. The fluctuations after this point were better than trainlm, but not as good as trainbr. The summary of the optimal ANN models with three algorithms is listed in Table 7.

Table 7. Summary of optimal ANN models (ASP FUNCLAS=01)

Training Algorithm	Optimal Neurons	R ²	RMSE	
			Training	Testing
'trainlm'	6	0.875	2.71	2.80
'trainbr'	6	0.883	2.68	2.82
'trainscg'	8	0.851	2.75	2.85

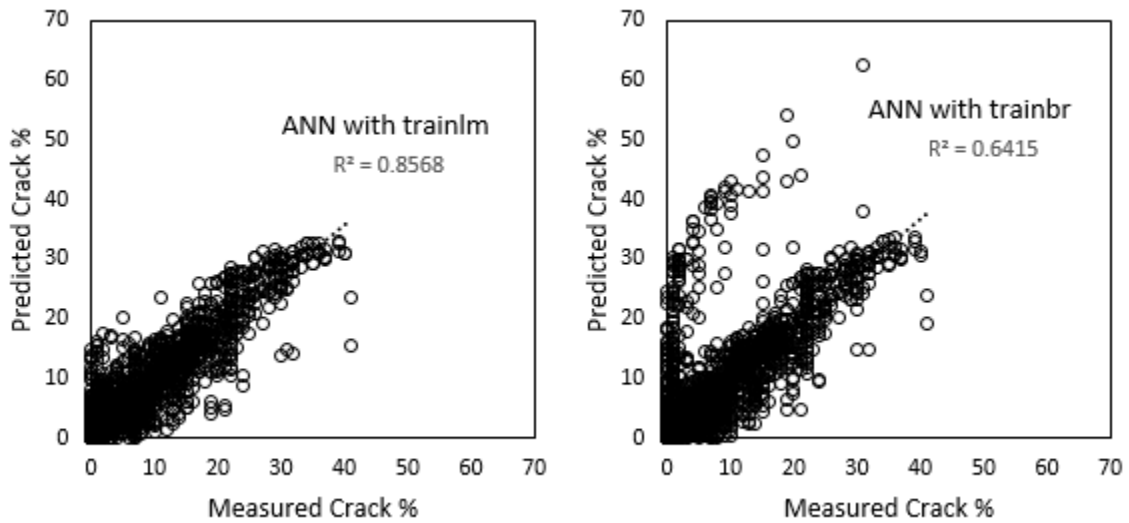
From the comparison in Table 7, it can be seen that `trainlm` and `trainbr` have better R^2 in prediction, however the RMSEs of all three models were at the same level; therefore, more evaluation is needed to determine the best model for this pavement group.

The developed ANN models in Table 7 were then applied to predict the future pavement performance. Although the HPMS data for year 2021 was delivered, its project records during 2020-2021 were not yet prepared. Therefore, this year's performance was not used for model training. However, it would still be valuable for testing the model's performance and evaluating its capability in assisting DOTs in determining their condition targets.

The cracking percent of 2019 and its corresponding age were used as input, while ADT/lane, climate (freezing index in this model), and truck percent were the same. The output was 2021's cracking percent. The difference in the cracking percent values between 2019 and 2021 was reviewed. If the reduction in the cracking percent from 2019 to 2021 was larger than 5%, it was assumed that a project constructed on this pavement section, and this row of data was therefore deleted. There were a total 3,553 rows of 2019-2021 data remaining for testing the models.

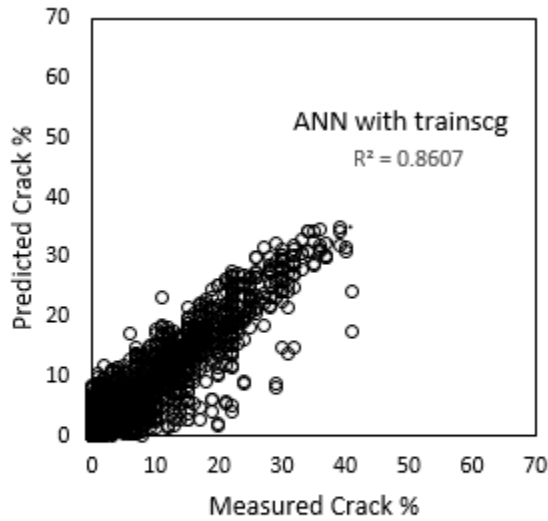
The five inputs of these datasets were fed into the trained ANN models, and the outputs, which were the predicted 2021 cracking percent values, were compared with the field-measured HPMS data. The comparisons are plotted in Figure 17.

Figure 17. Comparison between measured and predicted cracking percent with (a) trainlm, (b) trainbr and (c) trainscg



(a)

(b)



(c)

It is observed that there was a group of data points that could not be predicted well with the model developed using training function trainbr (Figure 17b), which significantly reduced the overall prediction power of this model. On the other hand, the other two models showed a sound correlation with an R^2 value greater than 0.85 (Figure 17a & 17c).

Instead of using cracking percent values, FHWA has regulations for rating pavement cracking condition goodness as good, fair and poor. The goodness of the predicted cracking percent and measured cracking percent were rated according to FHWA criteria and summarized in Table 8.

Table 8. Federal goodness rating of predicted and measured cracking percent

Models	Rating	Crack%	Number of 0.1-miles			% of this category		
			Measured	Predicted	Δ	Measured	Predicted	Δ
trainlm	GOOD	<5	2522	2486	36	71.0	70.0	1.0
	FAIR	5 – 20	828	885	-57	23.3	24.9	-1.6
	POOR	>20	203	182	21	5.7	5.1	0.6
trainbr	GOOD	<5	2522	2454	68	71.0	69.1	1.9
	FAIR	5 – 20	828	845	-17	23.3	23.8	-0.5
	POOR	>20	203	254	-51	5.7	7.1	-1.4
trainscg	GOOD	<5	2522	2556	-34	71.0	71.9	-1.0
	FAIR	5 – 20	828	826	2	23.3	23.2	0.1
	POOR	>20	203	171	32	5.7	4.8	0.9

Table 8 indicates that the ANN model with the training function “trainscg” has the least difference in both the number of 0.1-mile sections and the percent of total pavement mile length. Based on the overall performance shown in Table 8 and Figure 17, an ANN model with 8 neurons and the Scaled Conjugate Gradient Algorithm is considered the optimal one for predicting the short-term pavement performance of asphalt pavement on interstate highways in rural area.

Developed ANN Models for Predicting Short-Term Cracking Percent of NHS Pavements

A similar ANN modeling procedure was followed to generate various ANN cracking percent prediction models for three pavement types (ASP, COM and JCP) and various roadway function classes, as listed in Table 3. Note that each model has the same four inputs (Age, ADT, T% and Current Cracking Percent), along with a unique weather input selected from the five MERRA average climate parameters by district. Additionally, all three training functions (trainlm, trainbr and trainscg) were tested with various neuron numbers. For each training function, the optimal model was determined by disregarding the testing RMSE, which began to rise, indicating that overfitting occurred when more neurons were assigned. These three optimal models, obtained using various training functions, were used to predict the cracking percent for 2021 based on 2019 values. The

predicted cracking percent was then compared with the measured 2021 performance. The best model was selected by considering both the training performance (R^2 , RMSE) and its prediction power in simulating the 2021 performance. In general, models with better prediction accuracy (compared to 2021 measured crack percent) and fewer neuron numbers are preferred.

ANN Models in ASP Pavements. The developed ANN models of 7 functional classes for ASP pavements are listed in Table 9. Functional Classification 06 (Minor Arterial Rural) was excluded because there were only 4 data records in this category, which was not sufficient to build up ANN models. It can be concluded that all these models have sound prediction power with R^2 values larger than 0.85 and RMSE values less than 3.1. This can be seen in the overall comparison between measured and predicted cracking percent of these 16,965 0.1-mile ASP sections plotted in Figure 18.

Table 9. ANN ASP cracking models

FUN	Rows	Weather Input*	Trained Models				Pred. 2021
			TrainFcn	Neurons	R^2	RMSE (test)	R^2
01	3879	AAFI	trainscg	8	0.88	2.85	0.86
02	9469	AAFI	trainbr	7	0.94	3.04	0.91
06	2	-	-	-	-	-	-
11	1728	AAFTC	trainbr	2	0.95	1.75	0.92
12	469	AAWD	trainlm	3	0.95	2.52	0.86
14	1840	AAP	trainbr	4	0.94	2.92	0.94
16	486	AAFTC	trainbr	2	0.95	2.72	0.91

*AAT - Average annual air temperature
 AAP - Average annual precipitation
 AAFI - Average annual freeze index
 AAWD - Average annual wet days
 AAFTC - Average annual freeze/thaw cycles

Figure 18. Overall comparison between predicted and measured cracking percent on ASP

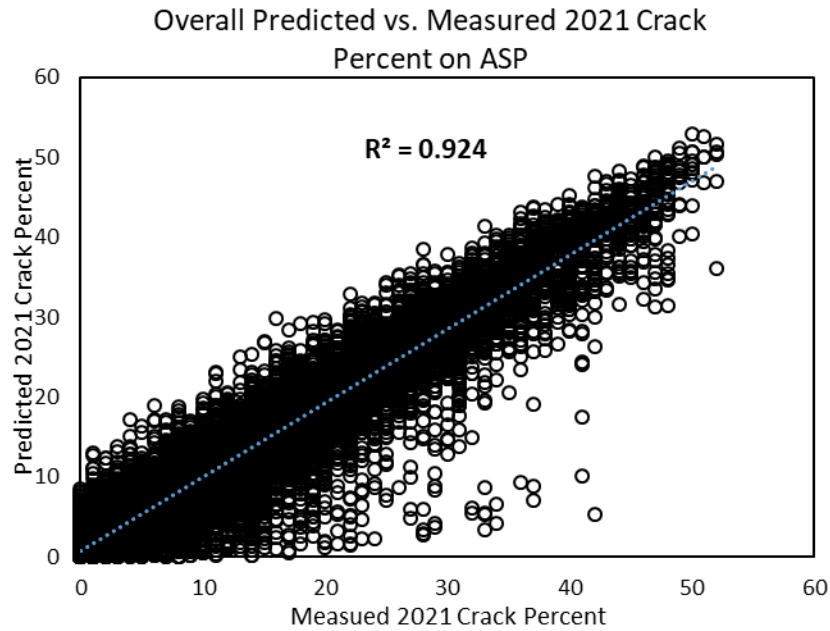


Figure 19. Goodness ranking between predicted and measured cracking percent on ASP

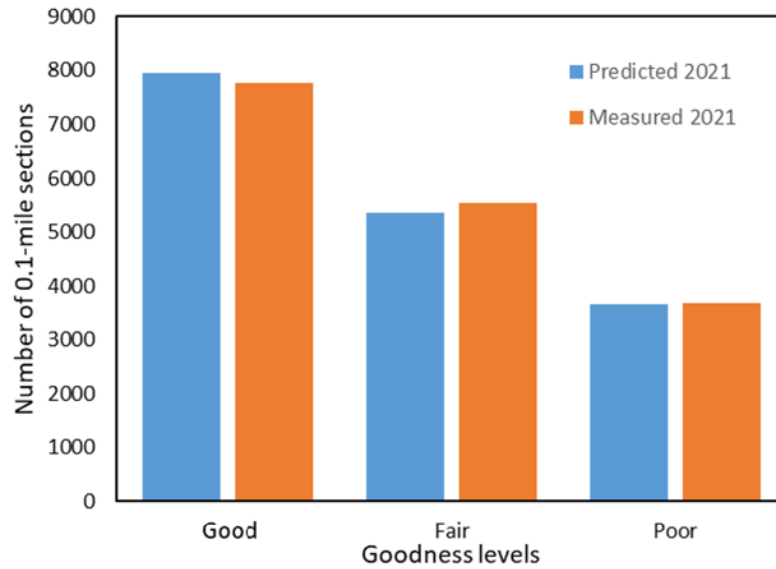


Figure 19 also compared the goodness levels of predicted and measured crack percentage on overall ASP 0.1-mile sections. Only 190 out of 16,965 (1.1%) 0.1-mile sections were different, indicating the soundness of this short-term performance model.

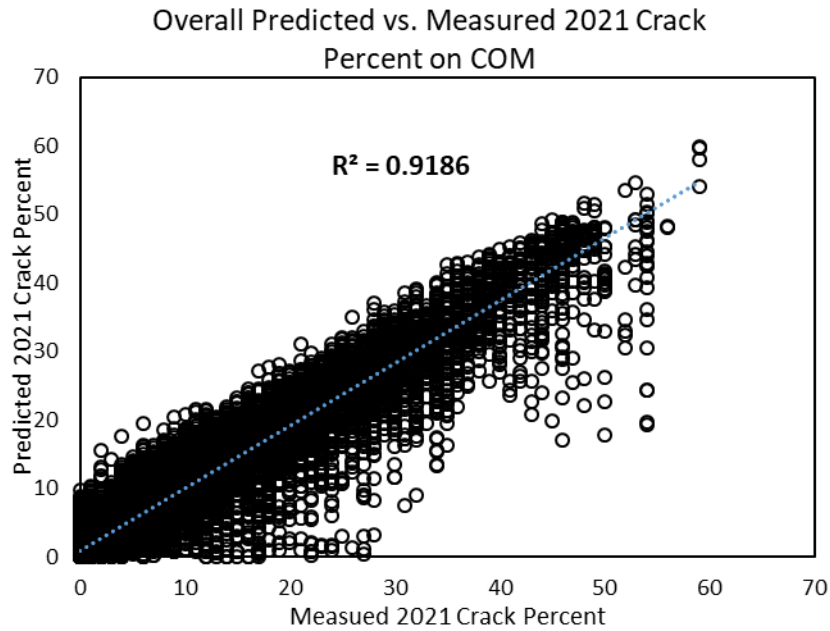
ANN Models in COM Pavements. The developed ANN models of 6 functional classes in COM pavements are listed in Table 10. Note that the R^2 value of the ANN model for functional class 16 (Minor Arterial Urban) was relatively low. This is because the available data for this group were insufficient for model training (the same category for ASP had 400 data and sound model performance).

Table 10. ANN COM cracking models

FUN	Rows	Weather Input	Trained Models				Pred. 2021 R^2
			TrainFcn	Neurons	R^2	RMSE (test)	
01	4317	AAP	trainbr	7	0.89	2.40	0.88
02	9825	AAFI	trainlm	5	0.91	3.30	0.91
06	4	-	-	-	-	-	-
11	1840	AAWD	trainlm	5	0.94	1.84	0.93
12	183	AAP	trainbr	2	0.99	1.85	0.94
14	4982	AAWD	trainlm	3	0.92	2.93	0.93
16	104	AAT	trainscg	1	0.43	1.54	0.74

In general, the overall performance of ANN models developed for COM pavements showed very promising potential in predicting 2-year future cracking percent conditions, as is shown in Figure 20. This overall performance would be improved if the Functional Class 16 data were removed.

Figure 20. Overall comparison between predicted and measured cracking percent on COM



Regarding the goodness rating of 2021 cracking prediction for COM pavements, there was only a difference of less than 1% (0.89%, 151 out of 19,564 0.1-mile sections) when compared with the measured values.

Figure 21. Goodness ranking between predicted and measured cracking percent on COM

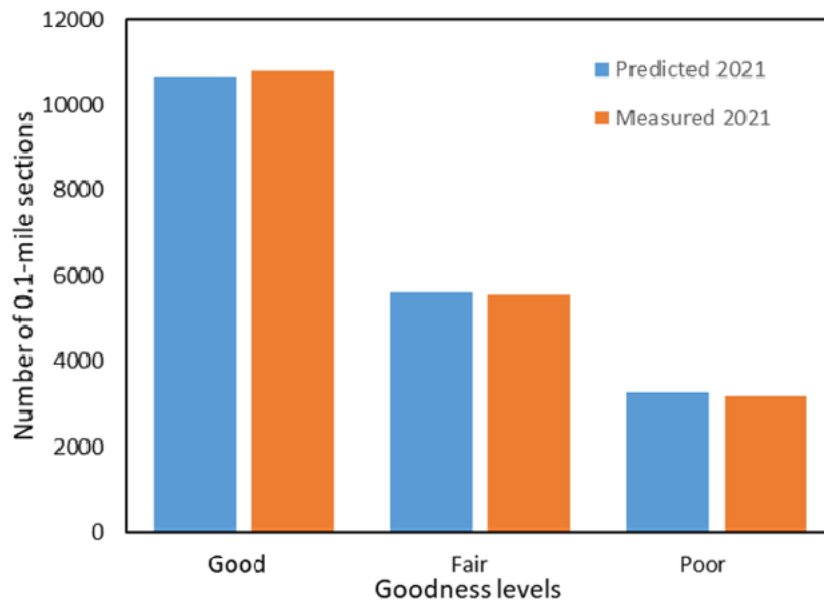


Figure 21 shows the predicted and measured 2021 goodness rating of cracking percent, in which the two overall rating percent values are very close.

ANN Models in JCP Pavements. Functional Class 06 and 16 were not available for JCP models. Furthermore, Functional Class 01 did not show a very high R^2 value, although the RMSE was less than 1.5. However, the rest four models were still suitable for implementation, as the model training results showed in Table 11.

Table 11. ANN JCP cracking models

FUN	Rows	Weather Input	Trained Models				Pred. 2021 R^2
			TrainFcn	Neurons	R^2	RMSE (test)	
01	4641	AAP	trainbr	4	0.67	1.46	0.76
02	4566	AAFTC	trainlm	5	0.92	4.68	0.95
06	-	-	-	-	-	-	-
11	2738	AAT	trainlm	5	0.95	3.23	0.96
12	561	AAT	trainlm	1	0.94	7.27	0.90
14	3656	AAWD	trainbr	1	0.93	3.14	0.93
16	17	-	-	-	-	-	-

The combined 5 JCP models in Table 11 showed good prediction power in both cracking percent values and goodness rating (Figure 22 and 23).

Figure 22. Overall comparison between predicted and measured cracking percent on JCP

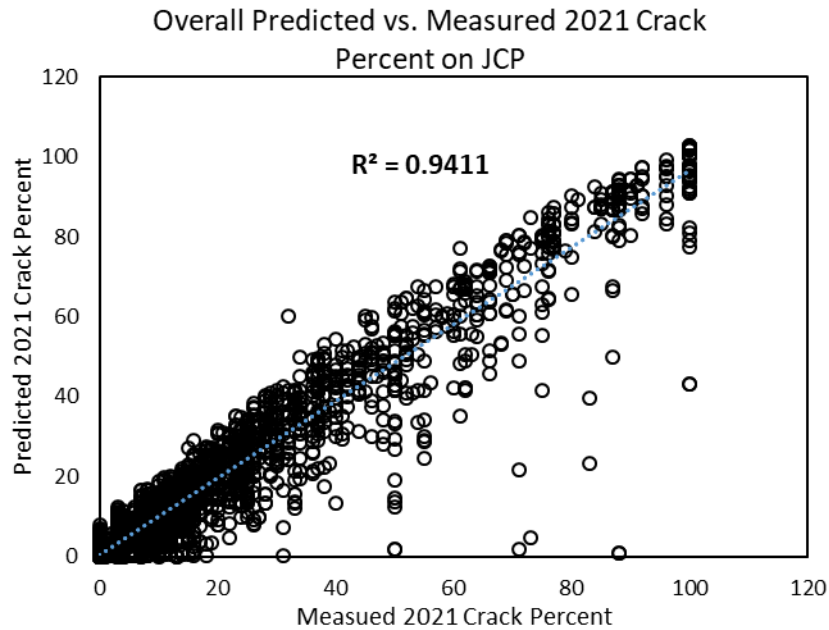
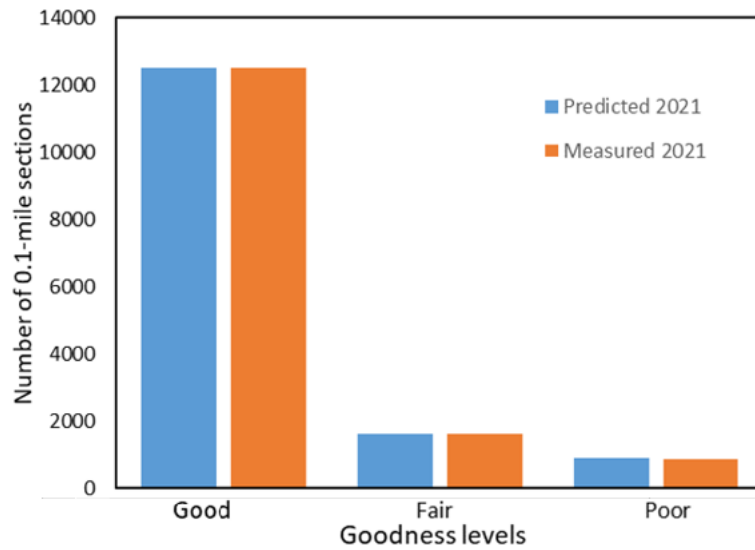


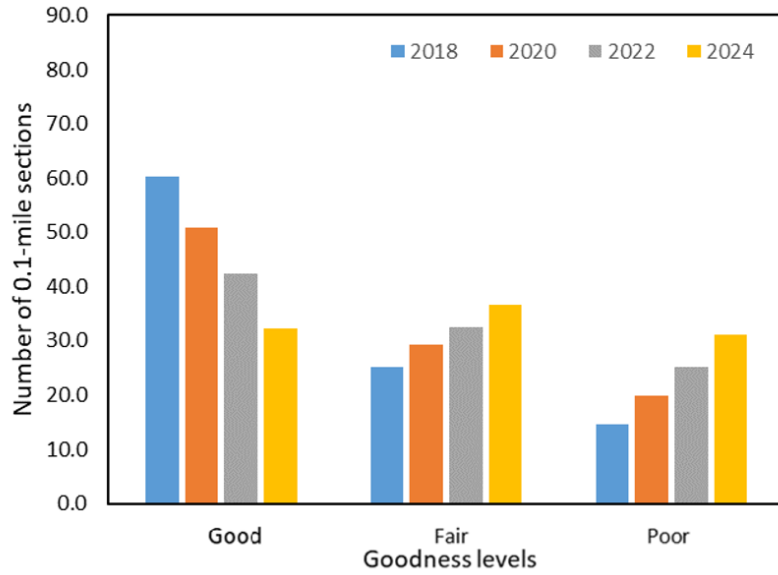
Figure 23. Goodness ranking between predicted and measured cracking percent on JCP



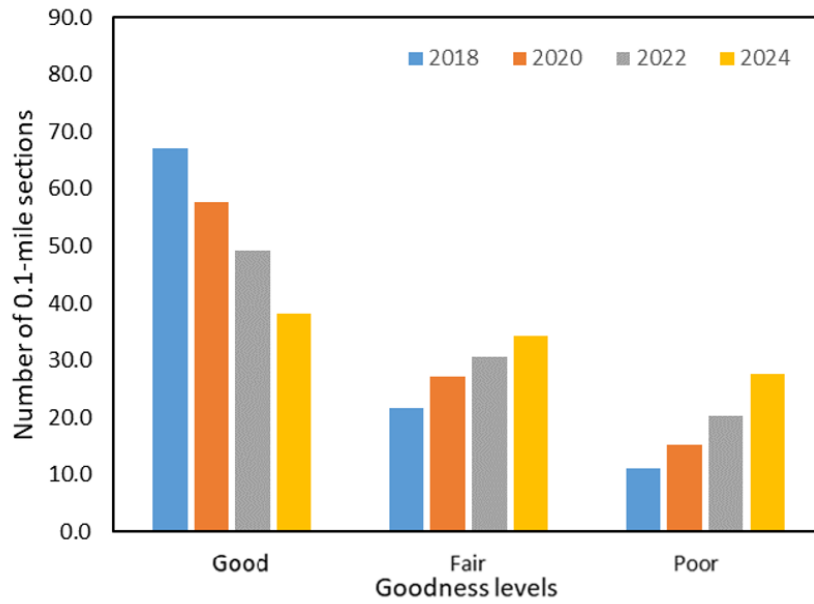
Prediction of 2022 and 2024 Cracking Percent Goodness Levels and Targets

The above comparison and validation indicate that the developed short-term models have the capability to predict 2-year performance with high accuracy. Therefore, they could be adopted in forecasting the 2-year and 4-year cracking percent and determining the condition targets required by FHWA. With the developed models for each pavement types and functional classification, their 2020 cracking percentages and pavement ages were used as inputs, along with other constant parameters (climate, truck percentage, and ADT), to predict 2022 cracking percents on these 0.1-mile sections. Then, the predicted 2022 cracking percentages were used as inputs for predicting 2024 performances (age values were +2 from 2022 inputs) following the same procedure. The predicted 2022 and 2024 cracking percentages of the three pavement types were transferred as goodness condition rating and plotted in Figure 24.

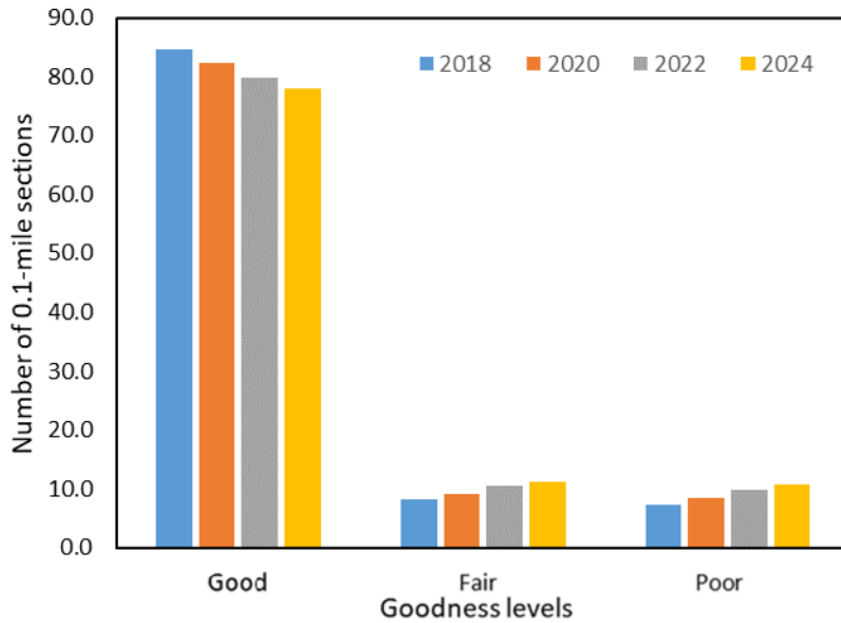
Figure 24. Overall cracking distress goodness levels predicted for three NHS pavement types



(a) ASP sections



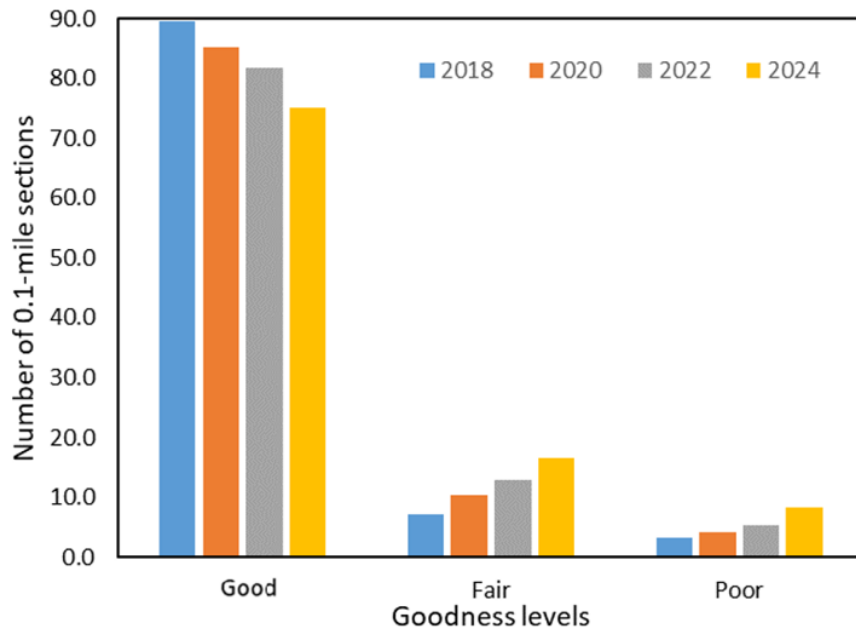
(b) COM sections



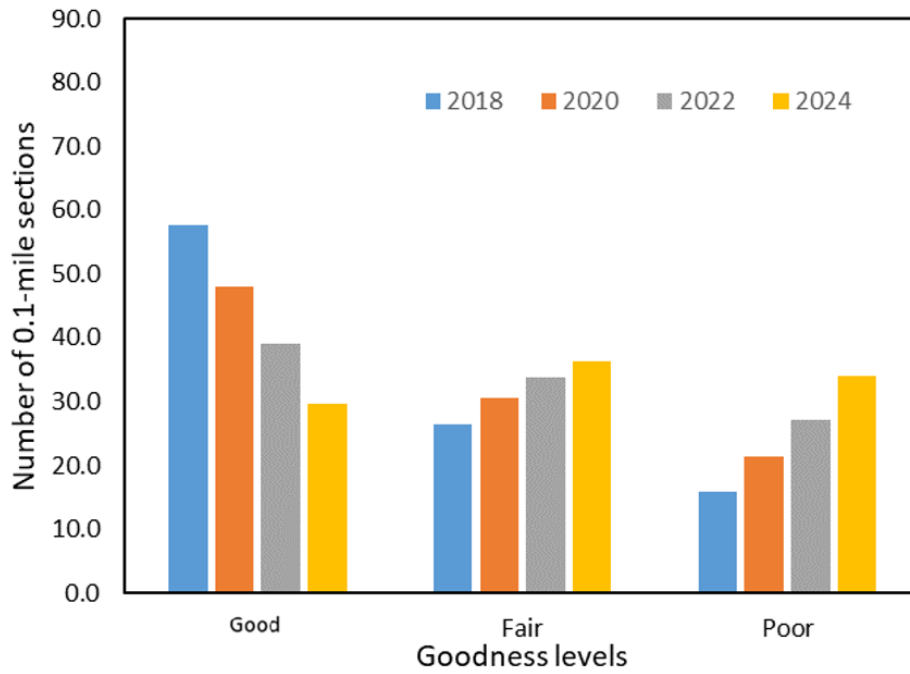
(c) JCP sections

In order to validate the trend of the predicted cracking percents for 2022 and 2024, the corresponding measured values of 2018 and 2020 were also plotted in Figure 24. Within these four years of cracking performances, the differences between the simulated results (from 2020 to 2022 and from 2022 to 2024) and the measured ones (from 2018 to 2020) showed consistent trends for three pavement categories. This indicates that the simulated results were able to accurately reflect the changes in conditions on these roadway networks. It should be noted that the 0.1-mile sections used for model training, condition prediction and verification were those with increasing cracking percentages, assuming no treatment was applied in between (any difference larger than -5% was accepted due to variation in PMS data). Therefore, the effects of maintenance and rehabilitation on the roadway network were not included. This is the reason why the trends of the simulation results were larger than the actual conditions of the overall roadway system. In Figure 25, the plots only show the deterioration rate over a 6-year span. To obtain the actual conditions, the rest percentages of pavement treatments should be added.

Figure 25. Overall cracking distress goodness levels predicted for interstate and non-interstate pavement sections



(a) interstate sections



(b) non-interstate sections

The short-term models were developed based on pavement types and functional classification. Therefore, the overall performance of interstate highways and NHS can be easily summarized by grouping 0.1-mile sections from all three pavement types by functional classifications.

ANFIS Training and Model Performance

ANFIS is another neural network training technique often used in engineering prediction models. One potential benefit is that ANFIS can handle incomplete or noisy data by using fuzzy logic to transform given inputs into a desired output through highly interconnected neural network processing elements and information connections. In this study, the Neuro-Fuzzy Designer in Matlab [92] was used to train ANFIS cracking percent prediction models based on the same datasets used in the aforementioned ANN model training, as listed in Table 3.

Specifically, three typical ANFIS membership functions were examined to obtain candidate models: triangular (trimf), Gaussian (gaussmf), and difference sigmoidal (dsigmf) membership functions. The candidate models were then used to predict cracking percentages for the year 2021, using data from 2019. The predicted 2021 conditions were compared to the HPMS measurements to determine the optimal models for their function classes. The obtained models are listed below in Table 12 through Table 14.

Table 12. ANFIS ASP cracking models

FUN	Rows	Weather Input	Trained Models			Pred. 2021 R ²
			MF	R ²	RMSE (test)	
01	3879	AAFI	trimf	0.89	2.61	0.41
02	9469	AAFI	trimf	0.93	3.20	0.88
06	2	-	-	-	-	-
11	1728	AAFTC	trimf	0.96	1.64	0.92
12	469	AAWD	-	-	-	-
14	1840	AAP	trimf	0.94	2.86	0.86
16	486	AAFTC	-	-	-	-

Table 13. ANFIS COM cracking models

FUN	Rows	Weather Input	Trained models			Pred. 2021 R ²
			MF	R ²	RMSE (test)	
01	4317	AAP	gaussmf	0.87	2.61	0.88

FUN	Rows	Weather Input	Trained models			Pred. 2021 R ²
			MF	R ²	RMSE (test)	
02	9825	AAFI	gaussmf	0.90	3.66	0.91
06	4	-	-	-	-	-
11	1840	AAWD	trimf	0.94	1.79	0.83
12	183	AAP	gaussmf	0.99	1.56	0.92
14	4982	AAWD	trimf	0.9	3.28	0.93
16	104	AAT	trimf	0.74	1.20	0.21

Table 14. ANFIS JCP cracking models

FUN	Rows	Weather Input	Trained models			Pred. 2021 R ²
			MF	R ²	RMSE (test)	
01	4641	AAP	trimf	0.66	1.45	0.78
02	4566	AAFTC	trimf	0.92	4.52	0.93
06	-	-	-	-	-	-
11	2738	AAT	trimf	0.96	3.04	0.95
12	561	AAT	-	-	-	-
14	3656	AAWD	trimf	0.93	3.09	0.93
16	17	-	-	-	-	-

It can be observed in the tables above that ANFIS also demonstrated sound prediction performance for the short-term cracking percent modeling. Out of the 14 obtained ANFIS models, 10 of them had R² values over 0.85. On the other hand, some of the ANN trainable datasets could not be trained using ANFIS (i.e., ASP FUN 12 and 16, and JCP FUN 12) due to constant parameters in the input arrays. For example, all training data for JCP FUN 12 were within the same district, resulting in the climate inputs.

A direct performance comparison between the ANN and ANFIS models are listed in Table 15. In general, ANN demonstrated better performance in 9 out of 17 models, while ANN and ANFIS showed very similar performance in the remaining models.

Table 15. Comparison between ANN and ANFIS cracking percent perdition models

Pavement	FUN	ANN			ANFIS			Select
		R ²	RMSE	2021 R ²	R ²	RMSE	2021 R ²	
ASP	01	0.88	2.85	0.86	0.89	2.61	0.41	ANN
	02	0.94	3.04	0.91	0.93	3.20	0.88	ANN
	06	-	-	-	-	-	-	
	11	0.95	1.75	0.92	0.96	1.64	0.92	Both

	12	0.95	2.52	0.86	-	-	-	ANN
	14	0.94	2.92	0.94	0.94	2.86	0.86	ANN
	16	0.95	2.72	0.91	-	-	-	ANN
COM	01	0.89	2.40	0.88	0.87	2.61	0.88	Both
	02	0.91	3.30	0.91	0.90	3.66	0.91	Both
	06	-	-	-	-	-	-	
	11	0.94	1.84	0.93	0.94	1.79	0.83	ANN
	12	0.99	1.85	0.94	0.99	1.56	0.92	Both
	14	0.92	2.93	0.93	0.9	3.28	0.93	Both
	16	0.43	1.54	0.74	0.74	1.20	0.21	ANN
JCP	01	0.67	1.46	0.76	0.66	1.45	0.78	Both
	02	0.92	4.68	0.95	0.92	4.52	0.93	ANN
	06	-	-	-	-	-	-	
	11	0.95	3.23	0.96	0.96	3.04	0.95	Both
	12	0.94	7.27	0.90	-	-	-	ANN
	14	0.93	3.14	0.93	0.93	3.09	0.93	Both
	16	-	-	-	-	-	-	

Guidance for Implementation of Short-Term Cracking Models

Based on the results of this section, it is recommended to implement the trained ANN models for predicting the future performance of the corresponding pavement family. The models should be used with collected pavement conditions and related parameters as inputs.

The trained neural networks listed in Table 9 through 11 have been saved. Users can directly copy the trained models into their own folders and load them into Matlab. The inputs, including current cracking percent, truck percent, the selected average climate parameter by district, pavement age, and ADT per lane, should be loaded as a matrix following this specific order, and the predicted crack percent to years later is calculated by the command line:

$$\text{Pred} = \text{sim}(\text{net}, \text{input});$$

Where, input is the n by 5 array, n is the number of data rows, and the input parameters are sorted into 5 columns as order. The 'net' represents the trained ANN for the inputs' pavement family.

An Excel spreadsheet has also been prepared for users who do not have access to Matlab software. The weight and bias values of the trained neural networks are extracted in Matlab and copied into the Excel sheet as an array. These arrays include the bias array $b1$ and the weight array iw of the hidden layer (there is only one weight array for the shallow neural network trained in this section with a single hidden layer), and the weight array lw and bias array $b2$ of the output layer.

The predicted crack percent array can be calculated with input array, weight arrays, and bias arrays as follows:

$$output = lw \cdot \left\{ \frac{2}{[1+EXP(-2*(iw \cdot input + b1))] - 1} \right\} + b2 \quad (24)$$

Where, $output$ is the array of predicted crack percent, and $input$ is the array of 5 input parameters.

The detailed weights and bias values (i.e., iw , lw , $b1$ and $b2$) of the developed ANN cracking models are presented in Appendix A. Using an Excel spreadsheet, the future crack percent of HPMS pavements can be predicted, taking into account the traffic condition, climate, and pavement age, in addition to the saved Matlab ANN networks, which can also be directly implemented.

In the future, the above procedures can be repeated with more collected data to update the neural networks with better prediction power, especially for functional classes and pavement types that currently have insufficient data.

Long-Term Performance Prediction for Asphalt Overlays

According to the current state of practice, DOTD uses five distress indices to model pavement deterioration for its flexible pavement performance: three cracking and patching indices (ALCR, RNDM, and PTCH), RUFF (roughness), and RUT (rutting) indices. When all the values are loaded into a pavement management software called dTIMS, it generates pavement age-based deterioration curves for each distress index based on a simple curve-fitting method. For each homogenous segment, five performance curves are generated for each of the distress indices based on historic-collected PMS performance data. These performance curves are referred to as the site-specific curves. Additionally, DOTD uses another type of performance curve called pavement family. DOTD uses the following criteria to define the family curve: pavement type (ASP,

Composite, JCP, and CRCP), roadway functional class (i.e., Interstate, Principal Arterial, Minor Arterial, Collector, Local, and Others) and pavement type-related distress indices. These categories allow for 126 pavement family curves to be generated for DOTD, including 70 related to flexible pavements and 56 for rigid pavements. While the most desirable of these pavement deterioration models (or curves) are the site-specific curves, when site-specific curves are not available, family curves must be used as a replacement.

As reported in the literature [57, 66, 76, 77], ANN-based models are very useful tools for modeling pavement deterioration at the network level when taking into account multiple pavement sections with various traffic, thickness (network level), or deterioration trends. They are also very fast tools that can solve thousands of pavement scenarios with various traffic scenarios, thickness, and conditions in seconds.

Development of Incremental Performance Prediction Models Using ANN

In this study, an ANN-based pavement performance model was developed for each of the three flexible pavement performance indicators (i.e., IRI, rutting and percent cracking) and five performance indices (ALCR, RNDM, PTCH, RUT, and RUFF) for the considered flexible pavement sections. The Neural Network toolbox in the MATLAB software was used for the ANN simulation analysis. A total of 255 ASP overlay pavement projects with 484 biennially-PMS data points for each pavement performance indicator were used in the model development and testing. Specifically, 70%, 15%, and 15% of the 484 data points in each model development were used as training, testing, and validation datasets, respectively.

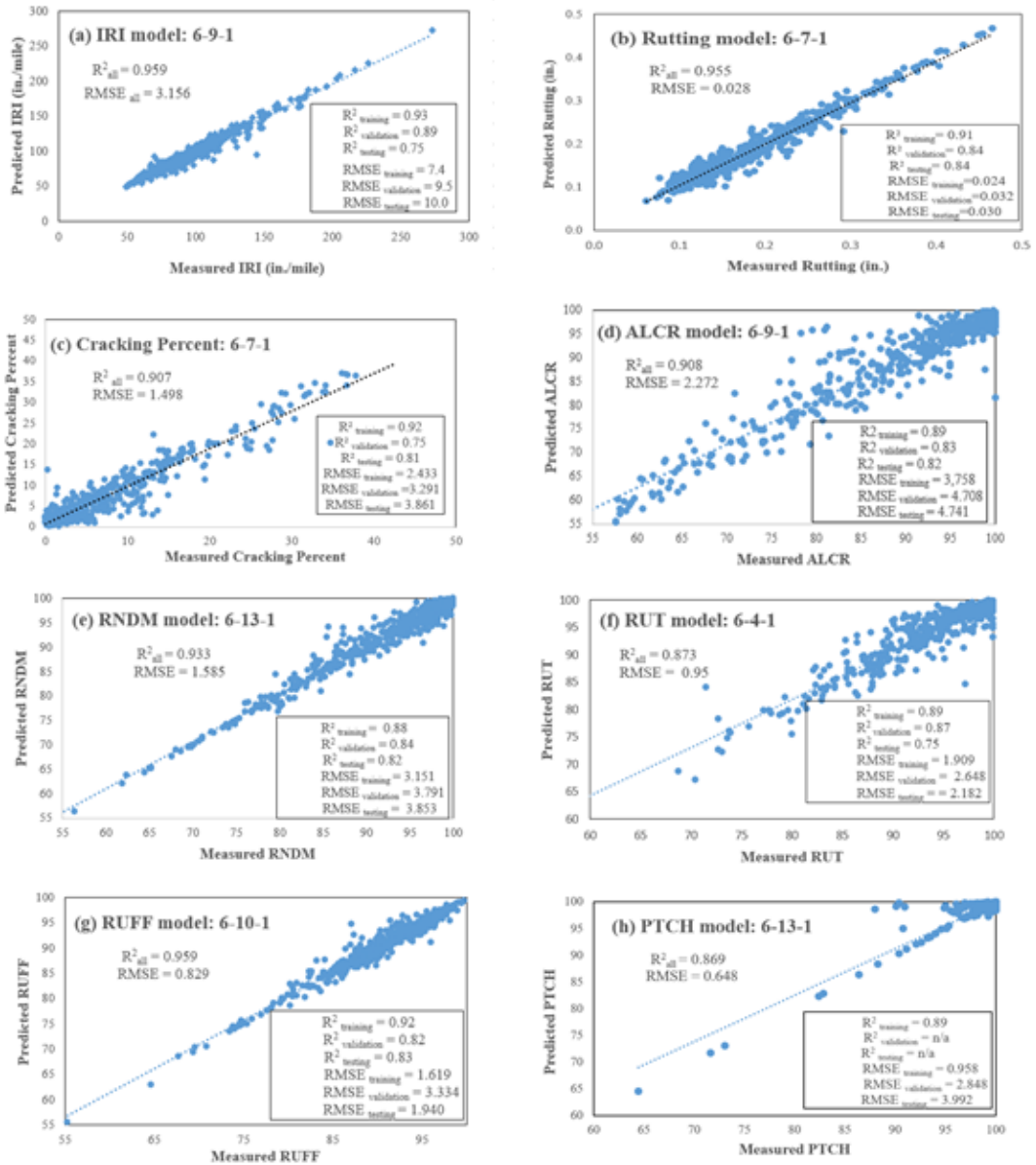
Table 16 summarizes input and output parameters used in the eight ANN models developed for flexible pavement. Those developed pavement deterioration models may be implemented by DOTD as an alternative method for developing the site-specific curves using the simple regression method. The eight ANN models used incremental methods, where the previous two pavement conditions (collected in year $i-2$ and $i-4$) were adopted to predict the same pavement condition in year i . With the trained ANN model, the time-series pavement condition in the future could be predicted incrementally (e.g., predict performance at year $i+2$ using year i and $i-2$, then predict $i+4$ based on predicted $i+2$ and i , etc.). This method combines the advantages from both machine learning and site-specific curves incorporating the previous performance trends and characteristics of the pavement section (treatment, weather, traffic and climate).

Table 16. Input parameters in long-term performance modeling

Model name	Input Parameters	Output
IRI	IRI _(i-4) , IRI _(i-2) , age _(i) , accumulative truck, overlay_h, mill_h	IRI _{(i) year}
Rutting	RD _(i-4) , RD _(i-2) , age _(i) , accumulative truck, overlay_h, mill_h	RD _{(i) year}
Percent of Alligator Cracking	CK _(i-4) , CK _(i-2) , age _(i) , accumulative truck, overlay_h, mill_h	CK _{(i) year}
ALCR	ALCR _(i-4) , ALCR _(i-2) , age _(i) , accumulative truck, overlay_h, mill_h	ALCR _{(i) year}
RNDM	RNDM _(i-4) , RNDM _(i-2) , age _(i) , accumulative truck, overlay_h, mill_h	RNDM _{(i) year}
PTCH	PTCH _(i-4) , PTCH _(i-2) , age _(i) , accumulative truck, overlay_h, mill_h	PTCH _{(i) year}
RUT	RUT _(i-4) , RUT _(i-2) , age _(i) , accumulative truck, overlay_h, mill_h	RUT _{(i) year}
RUFF	RUFF _(i-4) , RUFF _(i-2) , age _(i) , accumulative truck, overlay_h, mill_h	RUFF _{(i) year}

Figure 26 presents the structures and prediction performances of the developed incremental ANN models (predicted vs. measured performance). Overall, all the developed ANN models showed high R^2 and low RMSE, indicating their high accuracy in producing results that are very similar to the measured distresses. These models also provided physically meaningful future distress based on two previous distress data points and information regarding traffic and pavement thickness.

Figure 26. Structures and performances of incremental long-term performance models



As described above, at least 6 years of PMS data was required to build site-specific curves for a homogenous section or project. If there was insufficient data for the section, or if the precious time-series performance records did not show a consistent trend, family curves were recommended for forecasting the performance. However, it is important to note that the family curves, which are regressed from a large group of roadways, may not reflect the specific condition of a particular section. This can introduce a significant

difference. To address this issue, the developed incremental models effectively combined the performance trend of the pavement family together with existing site specific conditions (e.g., traffic, overlay thickness). This helped mitigate the problems caused by using the family curves alone. The predicted performance curves are useful for the analysis of remaining life, cost-benefit and pavement preservation at a project-level using limited PMS data.

Development of Family-Curve Prediction Models Using ANN

A suite of ANN models was developed for distress family curves of ASP pavements. These individual family curves were predicted based on weather factors (i.e., temperature, precipitation, and freeze-thaw cycles), traffic loading, pavement age, overlay thicknesses, and pavement functional classes.

In the analysis, the climate and weather data, including annual average air temperature (AAT), annual average precipitation (AAP), annual average freezing index (AAFI), annual number of wet days (AAWD), and average annual number of freeze/thaw cycles (AAFTC), were obtained from the PavementME weather MERRA database for the nine districts of DOTD. IRI, annual ADT, truck percentage, and treatment age were collected from the DOTD’s PMS and other databases. To confirm the treatment history and further validate the collected PMS condition data, any projects without an as-built plan were not considered in this study. An overview of the selected overlay pavement sections and the duration for which data has been collected is included in Table 17. According to Table 5, the service lives for the selected flexible pavements are generally around 11 to 16 years. The pavements were chosen in such a way that maintenance operations had not been conducted to improve IRI during the listed service life. Pavements that have undergone maintenance operations can be identified by the sudden improvement in IRI or a lower value of IRI compared to the previous year. The parameters adopted in this ANN modeling is listed in Table 17.

Table 17. Input parameters for distress family curves

VARIABLES	DESCRIPTION	DATA RANGE	SEQUENTIAL
PROJECT NO.	DOTD project number	n/a	No
DISTRICT	02,03,04,05,61,62,07,08,58	n/a	No
FUNCTION_C	1,2,4,6,7,8,11,14,16,17,19	n/a	No
MILL_H	Milling thickness		No

VARIABLES	DESCRIPTION	DATA RANGE	SEQUENTIAL
OVLY_H	Overlay thickness		No
AGE	Pavement age		Yes
ADT	Two-way average daily traffic		No
T%	Truck percentage		No
IRI_{AVE}	Average IRI		Yes
IRI_{INIT}	Initial IRI		No
RD_{AVE}	Average rut depth		Yes
ALCR	Alligator cracking index		Yes
RNDM	Random cracking index		Yes
PICH	Patching index		Yes
RUT	Rutting index		Yes
RUFF	Roughness index		Yes
AAT	Average annual air temperature		No
AAP	Average annual precipitation		No
AAFI	Average annual freeze index		No
AAWD	Average annual wet days		No
AAFTC	Average annual freeze/thaw cycles		No

Table 17 provides the pavement overlay dataset constructed for the long-term performance prediction analysis in this study. As shown in Table 17, pavement condition data (e.g., pavement age, IRI, rutting) and pavement indices (e.g., ALCR, RNDM, ROUGH) are sequential variables that change over time. On the other hand, the pavement functional class, districts, ADT, truck percentage, and five average climate/weather parameters are non-sequential variables, meaning that one value is received for each variable over the entire life of a selected pavement project.

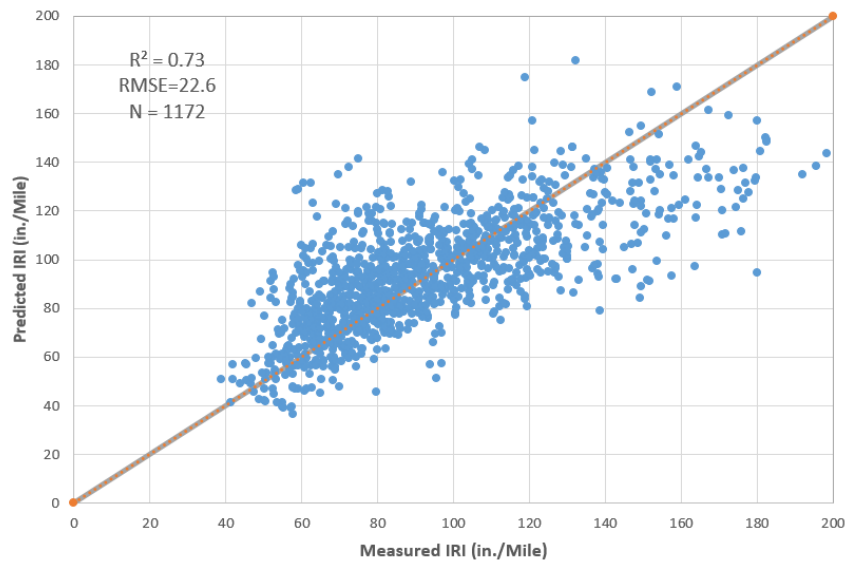
To develop a long-term pavement performance model for ASP pavements in DOTD, an ASP dataset consisting of 1172 rows was prepared. This dataset includes the average IRI and all five distress indices, along with different pavement functional classes, pavement ages, cumulative trucks, mill and overlay thicknesses, and five climate factors. In addition, the dataset contains a total of 257 homogeneous sections and 899 miles. Table 18 presents the correlations between the average IRI and different influencing variables. As seen in Table 18, the main contributing variables include age, ADT and truck, function class, and overlay thickness. The five climate factors were also included in the IRI prediction model development because the pavement condition performance is known to be influenced by local climate and weather.

Table 18. Correlations of input parameters for IRI family curves

Input	R ²
Age	0.30
ADT*Truck%	-0.23
Function	0.17
Mill	-0.07
Overlay	-0.29
AAFTC	-0.02
AAT	0.05
AAP	-0.07
AAFI	0.02
AAWD	-0.07

It can be observed from Table 18 that pavement age, trucks (ADT*Truck%), functional classification, and overlay thickness have the highest correlations with the output. However, the correlations of these parameters were not strong enough to build a model with conventional regression methods. Nevertheless, the ANN model demonstrated significant improvement, as indicated by an improved R² value of over 0.73, as shown in Figure 27.

Figure 27. Model performance of IRI family curve



The finalization of the number of layers and neurons in an ANN was achieved through a trial-and-error process. Different number of neurons were used during the training of ANN model. It was observed that increasing the number of neurons and hidden layers generally led to an improvement in the overall training R-value. However, the prediction results fluctuated due to the limited data size of the data (1172 rows) and the presence of 10 input variables, indicating the occurrence of overfitting. Similar to the procedures used in short-term performance modeling, the optimal ANN structures were determined considering both training and testing performance. Furthermore, a correlation equation that takes into account the initial IRI value was obtained for each of the model-predicted IRI curves for future implementation. The general expression of IRI vs. age may be expressed as:

$$\ln\left(\frac{IRI_{init}}{IRI-IRI_{init}}\right) = A * \text{EXP}(-B * \text{Age}) \quad (25)$$

Where, A and B are regression parameters.

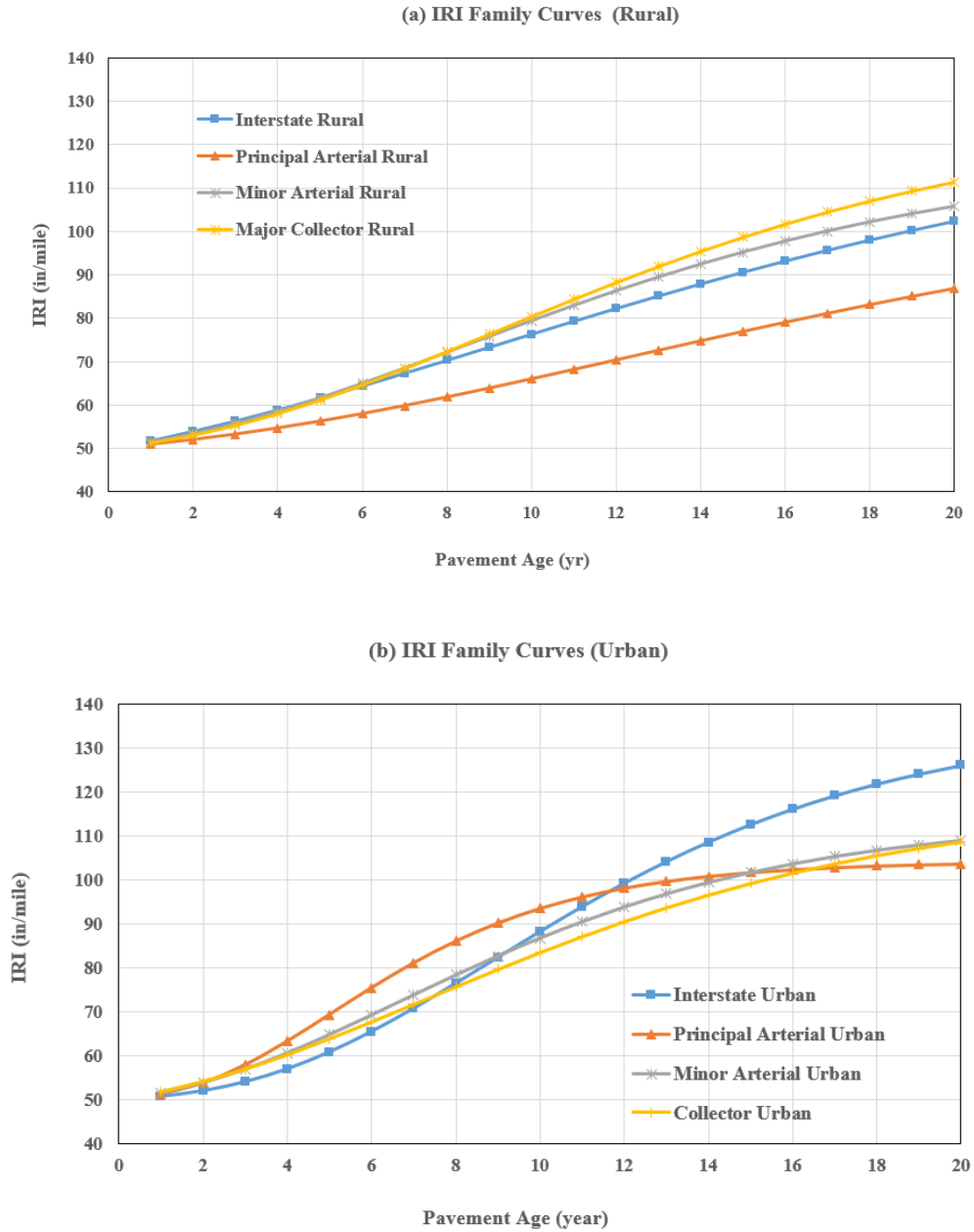
Table 19 lists the obtained correlation model parameters of A and B for each function class of ASP pavement considered.

Table 19. IRI model parameters

Functional Class No.	Roadway Category	A	B	R ²
01	Interstate Rural	2.3433	0.094	0.92
11	Interstate Urban	5.1427	0.185	0.99
02	Principal Arterial Rural	3.1261	0.093	0.97
14	Principal Arterial Urban	4.7372	0.308	0.84
06	Minor Arterial Rural	3.1799	0.139	0.99
16	Minor Arterial Urban	3.4975	0.188	0.99
07	Major Collector Rural	3.541	0.138	0.98
17	Collector Urban	3.0566	0.152	0.99

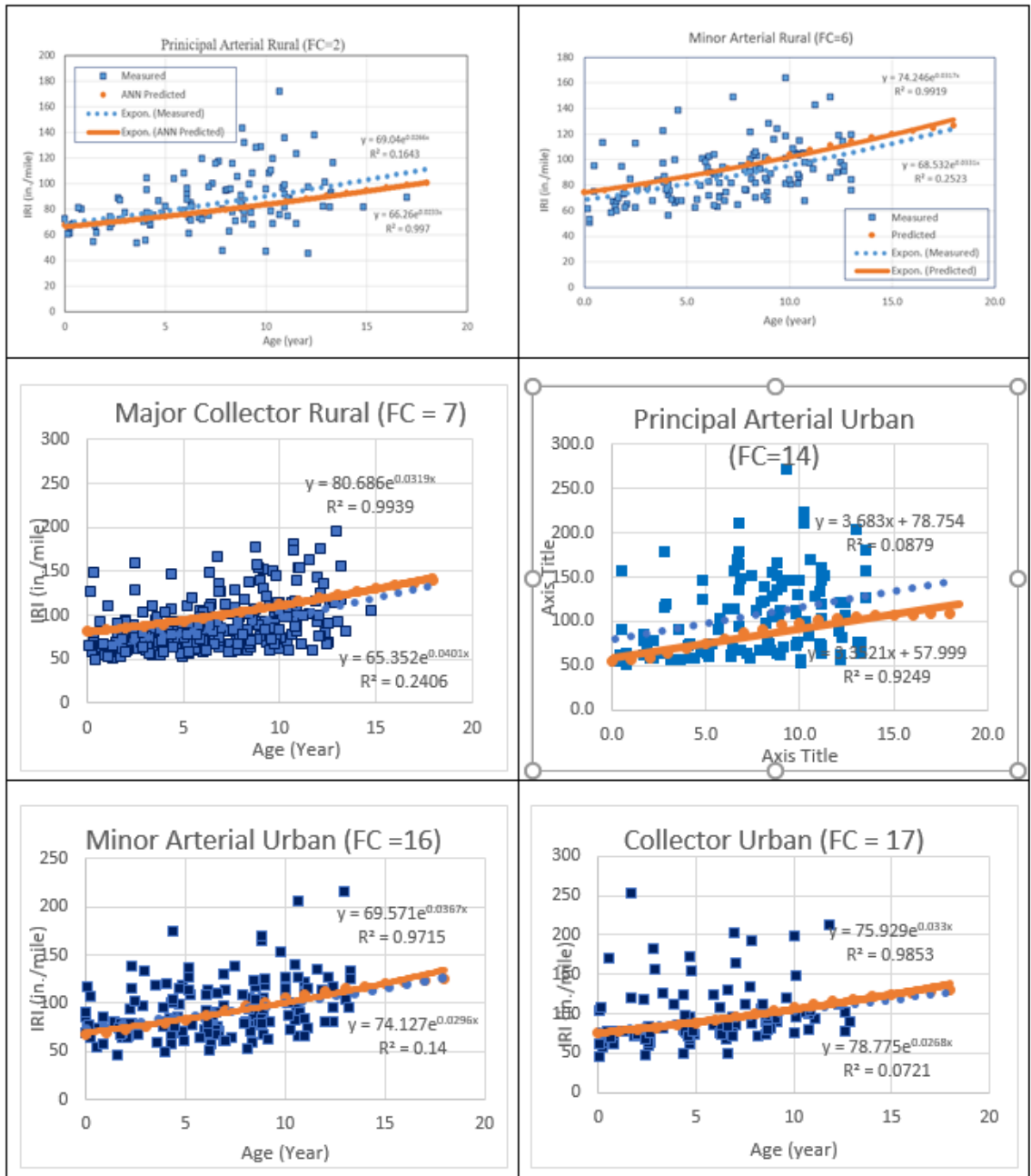
Using the developed ANN IRI model, the predicted IRI curves for various function class of ASP pavement were obtained. The average values of the input parameters were applied as new inputs to calculate the average performance. When normalizing the developed IRI family curves based on initialized IRI of 50 in./mile, Figure 28 below shows a comparison between urban and rural IRI family curves of different functional classes. In general, urban pavements had higher IRI development rates than rural pavements.

Figure 28. IRI family curves for rural and urban roadways



To compare with the current DOTD application, the pavement age and IRI values were also extracted from training datasets for building ANN models. Thus, a conventional family curve can be regressed. The comparison between these two family curves is plotted in Figure 29.

Figure 29. Comparison between ANN and conventional family curves



As is shown in Figure 29, the family curves derived from ANN predicted results were consistent with the traditional ones in all functional classifications. This indicates that the family curve obtained from the average condition and ANN models can replace the traditional ones. The traditional family curves only considered pavement age, resulting in low correlations with measured values, as seen in Figure 29. However, the ANN-predicted family curves have high correlations with measured values and incorporates

many factors. This allowed them to simulate more detailed conditions within a pavement family, such as overlay thickness and traffic volume. These advantages make the ANN-predicted family curves more suitable for planning specific pavement projects with better accuracy.

Similarly, family curves were developed for four distress indices (ALCR, RNDM, RUT and RUFF) based on the developed ANN model. The developed family curves for each distress index are presented in Tables 20-23.

Table 20. Developed distress index family curves -ALCR

Functional Class No.	Roadway Category	ANN-Model Based Family Curves	R ²
02	Principal Arterial Rural	$ALCR_{02} = -0.1748(\text{Age})^2 + 0.5965\text{Age} + 99.731$	0.997
14	Principal Arterial Urban	$ALCR_{14} = -0.1269(\text{Age})^2 + 0.4957\text{Age} + 98.736$	0.992
06	Minor Arterial Rural	$ALCR_{06} = -0.1389(\text{Age})^2 + 0.3237\text{Age} + 98.969$	0.992
16	Minor Arterial Urban	$ALCR_{16} = -0.0678(\text{Age})^2 - 0.3781\text{Age} + 100.76$	0.995
07	Major Collector Rural	$ALCR_{07} = -0.0571(\text{Age})^2 - 0.5717\text{Age} + 100.14$	0.998
17	All Collector Urban	$ALCR_{17} = -0.0314(\text{Age})^2 - 0.7684\text{Age} + 101.23$	0.995

Table 21. Developed distress index family curves -RUFF

Functional Class No.	Roadway Category	ANN-Model Based Family Curves	R ²
02	Principal Arterial Rural	$RUFF_{02} = 102.58 e^{-0.013\text{Age}}$	0.970
14	Principal Arterial Urban	$RUFF_{14} = 99.59 e^{-0.011\text{Age}}$	0.977
06	Minor Arterial Rural	$RUFF_{06} = 97.404 e^{-0.008\text{Age}}$	0.995
16	Minor Arterial Urban	$RUFF_{16} = 95.726 e^{-0.013\text{Age}}$	0.995
07	Major Collector Rural	$RUFF_{07} = 96.088 e^{-0.007\text{Age}}$	0.999

Functional Class No.	Roadway Category	ANN-Model Based Family Curves	R ²
17	All Collector Urban	$RUFF_{17} = 94.478 e^{-0.006Age}$	0.999

Table 22. Developed distress index family curves -RUT

Functional Class No.	Roadway Category	ANN-Model Based Family Curves	R ²
02	Principal Arterial Rural	$RUT_{02} = 0.038(Age)^2 - 1.4178Age + 99.293$	0.970
14	Principal Arterial Urban	$RUT_{14} = 0.0594(Age)^2 - 1.7905Age + 100.07$	0.981
06	Minor Arterial Rural	$RUT_{06} = -0.0187(Age)^2 - 0.6599Age + 100.02$	0.988
16	Minor Arterial Urban	$RUT_{16} = 0.0009(Age)^2 - 1.1822Age + 100.61$	0.995
07	Major Collector Rural	$RUT_{07} = -0.0203(Age)^2 - 0.4969Age + 100.94$	0.999
17	All Collector Urban	$RUT_{17} = -0.0296(Age)^2 - 0.4371Age + 99.661$	0.999

Table 23. Developed distress index family curves -RNDM

Functional Class No.	Roadway Category	ANN-Model Based Family Curves	R ²
02	Principal Arterial Rural	$RNDM_{02} = 99.259 e^{-0.018Age}$	0.995
14	Principal Arterial Urban	$RNDM_{14} = 100.61 e^{-0.014Age}$	0.995
06	Minor Arterial Rural	$RNDM_{06} = 101.47 e^{-0.016Age}$	0.996
16	Minor Arterial Urban	$RNDM_{16} = 102.64 e^{-0.015Age}$	0.990
07	Major Collector Rural	$RNDM_{07} = 101.78 e^{-0.015Age}$	0.971
17	All Collector Urban	$RNDM_{17} = 104.49 e^{-0.014Age}$	0.961

Due to the limitation of the used database (i.e., all ages <14 years) in the model training, when more IRI data is collected, the developed ANN model was retrained, and a set of

new prediction results was obtained. The significance lies in the approach used for ANN model development. The above approach for developing the long-term IRI prediction model not only utilized the ANN approach, but also incorporated regression methods and some engineering judgements.

Conclusions

In this study, a detailed step-by-step methodology was established and explained for development of both short-term and long-term ANN-based pavement performance prediction models. Real pavement performance data obtained from various DOTD databases were used for this purpose. To achieve the research objectives, two different network-level pavement condition datasets were prepared. One dataset was used for short-term cracking percent prediction, while the other was used for long-term smoothness and load-induced distress condition predictions. As a result, three types of ANN pavement performance prediction models were developed. This included seventeen individual neural network models for short-term prediction, eight for incremental long-term prediction, and five for family curve generation. Although the ANN approach has been successfully used by many researchers in developing pavement deterioration models based on a project-level pavement condition dataset (e.g., LTTP), only a few reported using network-level PMS data with many variations in pavement structure and materials, as well as distress data with various traffic, thickness, and climate conditions. The following observations were drawn from this research:

- In general, the developed ANN-based pavement performance models showed greater accuracy to statistical regression models for the network level pavement performance prediction. They exhibited higher R^2 and lower RMSE values. Additionally, these models were also efficient and easily implemented for predicting pavement performance indicators of multiple pavement sections with varying traffic, thickness, and climate conditions.
- The feedforward neural network technique was used for training, validation, and testing of the ANN model in this study. It was found that increasing the number of neurons and/or hidden layers resulted in very high R^2 (near to 1.0) with very low RMSE values. However, adding more neurons and/or hidden layers could potentially lead to overfitting of the ANN model, making future pavement performance prediction unstable and inaccurate.
- In the development of the short-term cracking percent prediction model, several modeling approaches were studied. It was found that both the feedforward ANN and ANFIS approaches were suitable for this prediction. However, determining an optimum ANFIS prediction model would require more computing time and be more difficult to implement by DOTD than a feedforward ANN model. In addition, the developed ANN-based cracking percent prediction models, which

were based on the 2017-2020 HPMS dataset, were validated using the newly collected 2021 PMS data. The validation results showed that the ANN modeling approach developed has the potential to be implemented in developing short-term prediction models for other pavement distress and condition indicators, such as IRI and rutting.

- A similar ANN modeling approach was used in developing long-term pavement performance models. The developed ANN incremental pavement performance models were found to be capable of making network-level long-term pavement performance predictions for IRI, rutting, percent cracking, and five distress indices (ALCR, RNDM, PTCH, RUT, and RUFF) for all DOTD asphalt pavements. Those ANN-based models can make future pavement performance calculations for any pavement sections using only milling and overlay thickness, traffic, age, and two previous cycles of PMS pavement condition records. Therefore, the developed ANN-based incremental pavement performance models can be a good alternative when a site-specific performance curve cannot be generated in PMS due to insufficient historic pavement condition data for a homogeneous pavement section. On the other hand, because the overlay pavement database considered in the ANN model training of this study was all constructed after the year 2009, the developed incremental pavement performance models are only recommended to be used for long-term pavement performance prediction up to 15 years of pavement life.
- This study also developed a long-term pavement performance prediction model using only pavement age, traffic, climate, and overlay information as ANN model training inputs. The results were used to generate a set of family curve models for various functional classes of ASP pavements of DOTD. The developed family curve models are deemed more accurate than those generated in the current PMS system, which are only pavement-aged based regression models.

Acronyms, Abbreviations, and Symbols

Term	Description
AASHTO	American Association of State Highway and Transportation Officials
ADT	Average daily traffic
ALCR	Alligator cracking index
ASP	Asphalt pavement
ANN	Artificial Neural Network
ANFIS	Adaptive Neuro-Fuzzy Inference System
COM	Composite Pavement
CRCP	Continuously Reinforced Concrete Pavement
dTIMS	Deighton Total Infrastructure Management System
EC	Equivalent cracking
FHWA	Federal Highway Administration
CNN	Convolutional Neural Network
DOT	Department of Transportation
DOTD	Louisiana Department of Transportation and Development
ESAL	Equivalent single axle load
FIS	fuzzy inference system
GPR	Ground Penetration Radar
GPS	Global Positioning System
IRI	International Roughness Index
JCP	Jointed Concrete Pavement
JPCP	Jointed Plain Concrete Pavement
LSTM	Long Short-Term Memory
LTPP	Long-term pavement performance
LTRC	Louisiana Transportation Research Center
MAP-21	Moving Ahead for Progress in the 21st Century Act
MEPDG	Mechanistic-Empirical Pavement Design Guide
MERRA	The Modern Era Retrospective-Analysis for Research and Applications
MLP	Multi-layer Perceptron

MPO	Metropolitan Planning Organizations
M&R	Maintenance and Rehabilitation
NHS	National Highway System
PCI	Pavement Condition Index
PCR	Pavement Condition Rating
PMS	Pavement Management System
PMU	Pavement Management Unit
PSC	Pavement Structural Condition
PSR	Present Serviceability Rating
PTCH	Patching Index
RNDM	Random Cracking Index
RUFF	Roughness Index
RUT	Rutting Index
RHS	Regional Highway System
RNN	Recurrent Neural Network
SHS	State Highway System
SVM	Support Vector Machine
SVR	Support Vector Regression
TAMP	Transportation Asset Management Plan

References

- [1] ASCE Report Card 2021: Louisiana, Available:
<https://infrastructurereportcard.org/wp-content/uploads/2021/09/Louisiana.pdf>.
[Accessed 8 May 2022]
- [2] J. Khattak, G. Baladi, Z. Zhang and S. Ismail, “Review of Louisiana’s Pavement Management System: Phase I,” *Transportation Research Record 2084*(1), p.18-27, 2008.
- [3] Federal Highway Administration, “Transportation Asset Management Plan Development Processes Certification and Recertification Guidance,” FHWA [Online]. Available: <https://www.fhwa.dot.gov/asset/guidance/certification.pdf>.
[Accessed 8 December 2022].
- [4] Louisiana Department of Transportation and Development, “2019 Federal NHS Transportation Asset Management Plan,” Available:
http://www.dotd.la.gov/Inside_LaDOTD/Divisions/Multimodal/Data_Collection/Asset%20Management/LADOTD%20TAMP%202019%20Final%20Issued.pdf. 2019.
- [5] E. Finkel, C. McCormick, M. Mitman, S. Abel, J. Clark. “Integrating the Safe System Approach with the Highway Safety Improvement Program: An Informational Report.” No. FHWA-SA-20-018. United States. Federal Highway Administration. Office of Safety, 2020.
- [6] Oregon Department of Transportation, “Oregon Transportation Asset Management Plan.” 2019.
- [7] Texas Department of Transportation, “2019 Texas Transportation Asset Management Plan.” 2019.
- [8] New Hampshire Department of Transportation, “Asset Management Plan for Pavements & Bridges on the National Highway System.” June 2019.
- [9] North Dakota Department of Transportation, “Transportation Asset Management Plan.” June 2019.

- [10] T. Anderson, "Transportation Asset Management Plan." Arizona Department of Transportation Arizona, 2019.
- [11] California Department of Transportation, "California Transportation Asset Management Plan." 2019.
- [12] Arkansas Department of Transportation, "2019 Transportation Asset Management Plan." August 2019.
- [13] A.A. Butt, M.Y. Shahin, S.H. Carpenter, J.V. Carnahan, "Application of Markov Process to Pavement Management Systems at Network Level." 3rd International Conference on Managing Pavements, Citeseer, 1994.
- [14] W.K. Smeaton, S.S. Sengupta, R.C. Haas, "Interactive Pavement Behavior Modeling: A Clue to the Distress-Performance-Problem." *Transportation Research Record*, 766, 1980.
- [15] S. Kim and N. Kim, "Development of Performance Prediction Models in Flexible Pavement Using Regression Analysis Method." *KSCE Journal of Civil Engineering*, 10, p. 91-96, 2006.
- [16] A. Mosa, "Neural Network for Flexible Pavements Maintenance and Rehabilitation." *Applied Research Journal*, Vol. 3, Issue, 4, pp.114-129, April, 2017.
- [17] A. Shtayat, S. Moridpour, B. Best, and S. Rumi, "An Overview of Pavement Degradation Prediction Models." *Journal of Advanced Transportation*, Vol. 2022, p. 7783588, 2022.
- [18] Y. Shah, S. S. Jain, D. Tiwari, and M. K. Jain, "Development of Overall Pavement Condition Index for Urban Road Network," *Procedia - Social and Behavioral Sciences*, Vol. 104, p. 332-341, Doi: 10.1016/J.Sbspro.2013.11.126, 2013.
- [19] N. Jackson, "Development of Revised Pavement Condition Indices for Portland Cement Concrete Pavement for the WSDOT Pavement Management System." Washington State Transportation Center, November 2008.
- [20] Stantec Consulting Inc., "Development and Implementation of Arizona Department of Transportation (ADOT) Pavement Management System," April 2006.

- [21] S. Islam and W. Buttlar, “Effect of Pavement Roughness on User Costs.” *Transportation Research Record*, Journal of Transportation Research Board, 2285: 47-55, 2022.
- [22] M. Sayers, “The International Road Roughness Experiment: Establishing Correlation and a Calibration Standard for Measurements,” University of Michigan, Ann Arbor, Transportation Research Institute, 1986.
- [23] Z. Luo, “Pavement Performance Modelling with an Auto-Regression Approach.” *International Journal of Pavement Engineering*, 14(1): p. 85-94, 2013.
- [24] A. A. Elhadidy, S. M. El-Badawy, and E. E. Elbeltagi, “A Simplified Pavement Condition Index Regression Model for Pavement Evaluation,” *International Journal of Pavement Engineering*, Vol. 22, No. 5, p. 643-652, 2021, Doi: 10.1080/10298436.2019.1633579.
- [25] K. P. George, A. S. Rajagopal, and L. K. Lim, “Models for Predicting Pavement Deterioration,” *Transportation Research Record*, No. 1215, 1989.
- [26] A. Sidess, A. Ravina, and E. Oged, “A Model for Predicting the Deterioration of the International Roughness Index,” *International Journal of Pavement Engineering*, p. 1–11, 2020.
- [27] J. Li, L. Pierce, and J. Uhlmeyer, “Calibration of Flexible Pavement in Mechanistic–Empirical Pavement Design Guide for Washington State.” *Transportation Research Record*, 2095(1): 73-83, 2009.
- [28] S. Kim, H. Ceylan, K. Gopalakrishnan and O. Smadi, “Use of Pavement Management Information System for Verification of Mechanistic–Empirical Pavement Design Guide Performance Predictions.” *Transportation Research Record*, 2153(1): p. 30-39, 2010.
- [29] C. Zhou, B. Huang, X. Shu, and Q. Dong, “Validating MEPDG with Tennessee Pavement Performance Data.” *Journal of Transportation Engineering*, 139(3): p. 306-312, 2013.
- [30] H. Ker, Y. Lee, and P. Wu, “Development of Fatigue Cracking Prediction Models Using Long-Term Pavement Performance Database.” *Journal of Transportation Engineering*, Vol. 134, No. 11, p. 477-482, 2008.

- [31] A. Butt, M. Shahin, K. Feighan and S. Carpenter, "Pavement Performance Prediction Model Using the Markov Process." *Transportation Research Record*, 1123, 1987.
- [32] A. A. Butt, M. Shahin, S. H. Carpenter, and J. V. Carnahan, "Application of Markov Process to Pavement Management Systems at Network Level," In 3rd International Conference on Managing Pavements, Vol. 2: Citeseer, p. 159-172, 1994.
- [33] N. Li, W. Xie, and R. Haas, "Reliability-Based Processing of Markov Chains for Modeling Pavement Network Deterioration." *Transportation Research Record*, 1524(1), 203-213, 1996.
- [34] Yang, J., M. Gunaratne, J. J. Lu, and B. Dietrich, "Use of Recurrent Markov Chains for Modeling the Crack Performance of Flexible Pavements." *Journal of Transportation Engineering*, 131(11): 861-872, 2005.
- [35] Abaza, K., "Deterministic Performance Prediction Model for Rehabilitation and Management of Flexible Pavement." *International Journal of Pavement Engineering*, p. 111-121, 2004.
- [36] Rosa, F. D., L. Liu, and N. G. Gharaibeh, "IRI Prediction Model for Use in Network-Level Pavement Management Systems." *Journal of Transportation Engineering*, 143(1), 2017.
- [37] K. D. Johnson and K. A. Cation, "Performance Prediction Development Using Three Indexes for North Dakota Pavement Management System," *Transportation Research Record*, No. 1344, 1992.
- [38] S. J. Russell and P. Norvig, "Artificial Intelligence: A Modern Approach," 2010.
- [39] Y. Xu, Y. Zhou, P. Sekula, and L. Ding, "Machine Learning in Construction: From Shallow to Deep Learning," *Developments in the Built Environment*, Vol. 6, p. 100045, 2021.
- [40] E. Alpaydin, "Introduction to Machine Learning." MIT Press, 2020.
- [41] Y. Bengio, I. Goodfellow, and A. Courville, "Deep Learning." MIT Press Cambridge, MA, USA, 2017.
- [42] S. B. Kotsiantis, "Supervised Machine Learning: A Review of Classification Techniques," *Informatica* 31, 2007.

- [43] M. Alloghani, D. Al-Jumeily, J. Mustafina, A. Hussain, and A. J. Aljaaf, "A Systematic Review on Supervised and Unsupervised Machine Learning Algorithms for Data Science," *Supervised and Unsupervised Learning for Data Science*, p. 3-21, 2020.
- [44] Richard S. Sutton and Andrew G. Barto, "Reinforcement Learning: An Introduction." MIT Press (Bradford Book), Cambridge, Mass., 1998.
- [45] M. I. Jordan and T. M. Mitchell, "Machine Learning: Trends, Perspectives, and Prospects," *Science*, Vol. 349, No. 6245, p. 255-260, 2015.
- [46] N. O. Attoh-Okine, "Analysis of Learning Rate and Momentum Term in Backpropagation Neural Network Algorithm Trained to Predict Pavement Performance," *Advances in Engineering Software*, Vol. 30, No. 4, p. 291-302, 1999.
- [47] F. Osisanwo, J. Akinsola, O. Awodele, J. Hinmikaiye, O. Olakanmi, and J. Akinjobi, "Supervised Machine Learning Algorithms: Classification and Comparison," *International Journal of Computer Trends and Technology (IJCTT)*, Vol. 48, No. 3, p. 128-138, 2017.
- [48] Q. Zhou, E. Okte, and I. L. Al-Qadi, "Predicting Pavement Roughness Using Deep Learning Algorithms," *Transportation Research Record*, Vol. 2675, No. 11, p. 1062-1072, 2021.
- [49] F. Damirchilo, A. Hosseini, M. Mellat Parast, and E. H. Fini, "Machine Learning Approach to Predict International Roughness Index Using Long-Term Pavement Performance Data," *Journal of Transportation Engineering, Part B: Pavements*, Vol. 147, No. 4, p. 04021058, 2021.
- [50] F. Dalla Rosa, L. Liu, and N. G. Gharaibeh, "IRI Prediction Model for Use in Network-Level Pavement Management Systems," *Journal of Transportation Engineering, Part B: Pavements*, Vol. 143, No. 1, p. 04017001, 2017.
- [51] R. Abd El-Hakim and S. El-Badawy, "International Roughness Index Prediction for Rigid Pavements: An Artificial Neural Network Application," *Advanced Materials Research*, Vol. 723, p. 854-860, 2013.

- [52] W. Li, J. Huyan, L. Xiao, S. Tighe, and L. Pei, "International Roughness Index Prediction Based on Multigranularity Fuzzy Time Series and Particle Swarm Optimization," *Expert Systems with Applications: X*, Vol. 2, p. 100006, 2019.
- [53] N. Abdelaziz, R. T. Abd El-Hakim, S. M. El-Badawy, and H. A. Afify, "International Roughness Index Prediction Model for Flexible Pavements," *International Journal of Pavement Engineering*, Vol. 21, No. 1, p. 88-99, 2020.
- [54] P. Marcelino, M. De Lurdes Antunes, E. Fortunato, and M. C. Gomes, "Machine Learning Approach for Pavement Performance Prediction," *International Journal of Pavement Engineering*, Vol. 22, No. 3, p. 341-354, 2021.
- [55] H. Gong, Y. Sun, X. Shu, and B. Huang, "Use of Random Forests Regression for Predicting IRI of Asphalt Pavements," *Construction and Building Materials*, Vol. 189, p. 890-897, 2018.
- [56] N. Kargah-Ostadi, S. M. Stoffels, and N. Tabatabaee, "Network-Level Pavement Roughness Prediction Model for Rehabilitation Recommendations," *Transportation Research Record*, Vol. 2155, No. 1, p. 124-133, 2010.
- [57] M. R. Kaloop, S. M. El-Badawy, J. Ahn, H.-B. Sim, J. W. Hu, and R. T. Abd El-Hakim, "A Hybrid Wavelet-Optimally-Pruned Extreme Learning Machine Model for the Estimation of International Roughness Index of Rigid Pavements," *International Journal of Pavement Engineering*, Vol. 23, No. 3, p. 862-876, 2022.
- [58] H. Ziari, J. Sobhani, J. Ayoubinejad, and T. Hartmann, "Prediction of IRI in Short and Long Terms for Flexible Pavements: ANN and GMDH Methods," *International Journal of Pavement Engineering*, Vol. 17, No. 9, p. 776-788, 2016.
- [59] A. Fathi, M. Mazari, M. Saghafi, A. Hosseini, And S. Kumar, "Parametric Study of Pavement Deterioration Using Machine Learning Algorithms," In *Airfield and Highway Pavements 2019: Innovation and Sustainability in Highway and Airfield Pavement Technology*: American Society of Civil Engineers Reston, VA, p. 31-41, 2019.
- [60] J. Zhao, H. Wang, and P. Lu, "Impact Analysis of Traffic Loading on Pavement Performance Using Support Vector Regression Model," *International Journal of Pavement Engineering*, Vol. 23, No. 11, p. 3716-3728, 2022.

- [61] B. J. Lee and H. D. Lee, "Position-Invariant Neural Network for Digital Pavement Crack Analysis," *Computer-Aided Civil and Infrastructure Engineering*, Vol. 19, No. 2, p. 105-118, 2004.
- [62] C. A. Roberts and N. O. Attoh-Okine, "A Comparative Analysis Of Two Artificial Neural Networks Using Pavement Performance Prediction," *Computer-Aided Civil and Infrastructure Engineering*, Vol. 13, No. 5, p. 339-348, 1998.
- [63] S. Terzi, "Modeling for Pavement Roughness Using the ANFIS Approach," *Advances in Engineering Software*, Vol. 57, p. 59-64, 2013.
- [64] M. Hossain, L. Gopiseti, and M. Miah, "International Roughness Index Prediction of Flexible Pavements Using Neural Networks," *Journal of Transportation Engineering, Part B: Pavements*, Vol. 145, No. 1, p. 04018058, 2019.
- [65] N. K. Manaswi, "Deep Learning with Applications Using Python: Chatbots and Face, Object, and Speech Recognition with Tensorflow and Keras," Publisher: Apress, 1st edition, 2018.
- [66] W. H. Delashmit and M. T. Manry, "Recent Developments in Multilayer Perceptron Neural Networks," In Proceedings of the Seventh Annual Memphis Area Engineering and Science Conference, MAESC, 2005.
- [67] A. Milad, I. Adwan, S. A. Majeed, N. I. M. Yusoff, N. Al-Ansari, and Z. M. Yaseen, "Emerging Technologies of Deep Learning Models Development for Pavement Temperature Prediction," *IEEE Access*, Vol. 9, p. 23840-23849, 2021.
- [68] Y. Hsieh and Y. J. Tsai, "Machine Learning For Crack Detection: Review And Model Performance Comparison," *Journal of Computing in Civil Engineering*, Vol. 34, No. 5, p. 04020038, 2020.
- [69] F. Alharbi, "Predicting Pavement Performance Utilizing Artificial Neural Network (ANN) Models." Graduate Theses and Dissertations, 16703, 2018.
- [70] X. Luo, F. Wang, H. Gong, J. Tao, X. Qiu, and N. Wang, "Effectiveness Evaluation of Preventive Maintenance Treatments on Asphalt Pavement Performance Using LTPP Data." *International Journal of Pavement Research and Technology*, p. 1-16, 2021.

- [71] S. Amarasiri and B. Muhunthan, "Evaluating Performance Jumps for Pavement Preventive Maintenance Treatments in Wet Freeze Climates Using Artificial Neural Network." *Journal of Transportation Engineering, Part B: Pavements*, 148(2), p. 04022008, 2022.
- [72] Y. Jia, J. Wang, Y. Gao, M. Yang, and W. Zhou, "Assessment of Short-Term Improvement Effectiveness of Preventive Maintenance Treatments on Pavement Performance Using LTPP Data." *Journal of Transportation Engineering, Part B: Pavements*, 146(3), p. 04020048, 2020.
- [73] Y. Jia, S. Wang, J. Peng, Y. Gao, M. Liu, W. Zhou, "Characterization of Rutting on Asphalt Pavement in Terms of Transverse Profile Shapes Based on LTPP Data." *Construction and Building Materials*, 269, p. 121230, 2021.
- [74] Q. Zhou, E. Okte, and I. L. Al-Qadi, "Predicting Pavement Roughness Using Deep Learning Algorithms." *Transportation Research Record*, 2675, 11, p. 1062-1072, 2021.
- [75] S. Amarasiri and B. Muhunthan, "Evaluating Cracking Deterioration of Preventive Maintenance-Treated Pavements Using Machine Learning." *Journal of Transportation Engineering, Part B: Pavements*, 148(2), p. 04022014, 2022.
- [76] H. Ziari, J. Sobhani, J. Ayoubinejad, and T. Hartmann, "Prediction of IRI in Short and Long Terms for Flexible Pavements: ANN and GMDH Methods." *International Journal of Pavement Engineering*, 17(9), p. 776-788, 2016.
- [77] O. Kaya, H. Ceylan, S. Kim, D. Waid, and B. P. Moore, "Statistics and Artificial Intelligence-Based Pavement Performance and Remaining Service Life Prediction Models for Flexible and Composite Pavement Systems." *Transportation Research Record*, 2674(10), p. 448-460, 2020
- [78] R. Martinek, Kelnar M., Vanus J., Bilik P., and Zidek J., "A Robust Approach for Acoustic Noise Suppression in Speech Using ANFIS." *Journal of Electrical Engineering*, 66(6), p. 301-310, 2015.
- [79] J. Vanus, T. Weiper, R. Martinek, J. Nedoma, M. Fajkus, L. Koval, and R. Hrbac, "Assessment of the Quality of Speech Signal Processing within Voice Control of Operational-Technical Functions in the Smart Home by Means of the PESQ Algorithm." *IFAC-Papers online*, 51(6), p. 202-207, 2018.

- [80] S. Kumarganesh and M. Suganthi, "An Enhanced Medical Diagnosis Sustainable System for Brain Tumor Detection and Segmentation Using ANFIS Classifier." *Current Medical Imaging*, 14(2), p. 271-279, 2018.
- [81] M.A. Khan and F. Algarni, "A Healthcare Monitoring System for the Diagnosis of Heart Disease in the IoMT Cloud Environment Using MSSO-ANFIS." *IEEE Access*, 8, 122259-122269, 2020.
- [82] S. Terzi, "Modeling for Pavement Roughness Using the ANFIS Approach." *Advances in Engineering Software*, 57, p. 59-64, 2013.
- [83] M. Ghariieb, T. Nishikawa, S. Nakamura, K. Thepvongsa, "Application of Adaptive Neuro-Fuzzy Inference System for Forecasting Pavement Roughness in Laos." *Coatings*, 12(3), 380, 2022.
- [84] S. Karahancer, E. Eriskin, N. Morova, M. Saltan, S. Terzi1, "Pavement Performance Assessment by ANFIS Approach Using Marine Corps Air Station Cherry Point, North Carolina Data." 8th International Advanced Technologies Symposium IATS. Vol. 17. 2017.
- [85] H. Ziari, J. Sobhani, J. Ayoubinejad, and T. Hartmann, "Analysing the Accuracy of Pavement Performance Models in the Short and Long Terms: GMDH and ANFIS Methods." *Road Materials and Pavement Design*, 17(3), p. 619-637, 2016.
- [86] N. Talpur, M. N. Salleh, and K. Hussain, "An Investigation of Membership Functions on Performance of ANFIS for Solving Classification Problems." *IOP Conference Series: Materials Science and Engineering*. Vol. 226. No. 1. IOP Publishing, 2017.
- [87] G. Biau and E. Scornet, "A Random Forest Guided Tour," *Test*, Vol. 25, p. 197-227, 2016.
- [88] L. Breiman, "Random Forests," *Machine Learning*, Vol. 45, p. 5-32, 2001.
- [89] V. Svetnik, A. Liaw, C. Tong, J. C. Culberson, R. P. Sheridan, and B. P. Feuston, "Random Forest: A Classification and Regression Tool for Compound Classification and QSAR Modeling," *Journal of Chemical Information and Computer Sciences*, Vol. 43, No. 6, p. 1947-1958, 2003.

- [90] F. Zhang and L. J. O'Donnell, "Support Vector Regression," *Machine Learning*, p. 123-140, 2020.
- [91] Louisiana Department of Transportation and Development. "2022 Federal NHS Transportation Asset Management Plan." 2022.
- [92] The Mathworks, Inc., "AI, Data Science, and Statistics (R2022a)." 2022.

Appendix A

The specific weight and bias values for the developed ANN cracking prediction models listed in Table 9 through Table 11 are presented below:

(A) The developed ANN model parameters for Asphalt Pavements (ASP)

Functional Class No.	Roadway Category	Weight (iw)	Bias ($b1$)	Weight (lw)	Bias ($b2$)
01	Interstate Rural	$iw_{01(asp)}$	$b1_{01(asp)}$	$lw_{01(asp)}$	$b2_{01(asp)}$
02	Principal Arterial Urban	$iw_{02(asp)}$	$b1_{02(asp)}$	$lw_{02(asp)}$	$b2_{02(asp)}$
11	Interstate Urban	$iw_{11(asp)}$	$b1_{11(asp)}$	$lw_{11(asp)}$	$b2_{11(asp)}$
12	Freeway Urban	$iw_{12(asp)}$	$b1_{12(asp)}$	$lw_{12(asp)}$	$b2_{12(asp)}$
14	Principal Arterial Urban	$iw_{14(asp)}$	$b1_{14(asp)}$	$lw_{14(asp)}$	$b2_{14(asp)}$
16	Minor Arterial Urban	$iw_{16(asp)}$	$b1_{16(asp)}$	$lw_{16(asp)}$	$b2_{16(asp)}$

- **Function Class No. = 01**

$$iw_{01(asp)} = [8 \times 5] =$$

1.053699515 1.755481155 -0.312824039 -0.091241531 -1.061294433
 0.987116191 1.199858643 0.996056665 0.544340538 -1.093503543
 -1.23715647 -0.557744176 0.758864639 0.309993888 -1.21802477
 1.235528161 1.180908678 0.305587883 -0.026143953 0.534241888
 0.029317903 1.763821811 1.008421206 0.446747654 0.852315783
 -1.211842075 -0.296484983 -1.52190556 -0.7741759 -0.252429035
 -0.74485554 0.453905391 0.960410298 0.586535839 1.59603166
 0.09069055 -0.897825286 1.048783329 -0.860227347 -1.411669801

$$b1_{01(asp)} = [8 \times 1] =$$

-1.86576492
-1.412137958
0.905929056
0.496057541
0.176609796
-0.88249823
-1.516169135
2.119398457

$$iw_{01(asp)} = [1 \times 8] = [0.500128232 \quad -0.39082904 \quad -0.27559375 \quad 0.45846716 \\ -0.514368719 \quad -0.495842001 \quad -0.371093497 \quad -0.22523529]$$

$$b2_{01(asp)} = [1 \times 1] = -0.260763044$$

- **Function Class No. = 02**

$$iw_{02(asp)} = [7 \times 5] =$$

0.025247634 -0.618406913 1.527798957 -2.314662987 -1.433732234
0.227172836 0.373184075 -0.614258538 -0.101909034 0.092675031
0.172147949 0.073746169 1.101994896 0.871451755 0.590222768
-0.081657182 -0.258230424 -0.017235637 -0.968008782 -0.570693258
-0.08347096 0.717527695 2.978094164 -1.277145163 0.488701211
-0.294514003 -0.050316073 -0.315059077 -0.629912142 -0.443485446
-4.000696515 0.023059125 0.385632547 -0.525590413 0.330120363

$$b1_{02(asp)} = [7 \times 1] =$$

1.466719342

-0.291775505

1.476450838

-0.597914379

0.942140656

-0.213708577

-5.300564726

$$lw_{02(asp)} = [1 \times 8] = [0.530392266 \quad 1.563671014 \quad 1.233340924 \quad 1.974541241 \\ -0.410394668 \quad -1.951905455 \quad -1.580960224]$$

$$b2_{02(asp)} = [1 \times 1] = -1.814255436$$

- **Function Class No. = 11**

$$iw_{11(asp)} = [2 \times 5] =$$

0.45945151 0.260747176 -0.459883557 1.081220919 2.363395101

0.733280784 -0.300857729 0.565356962 -0.937861637 -2.084966413

$$b1_{11(asp)} = [2 \times 1] =$$

3.129860622

-2.226821494

$$lw_{11(asp)} = [1 \times 2] = [0.496238877 \quad 1.034454519]$$

$$b2_{11(asp)} = [1 \times 1] = -0.451019641$$

- **Function Class No. = 12**

$$i\mathbf{w}_{12(\text{asp})} = [3 \times 4] =$$

1.3069213 1.694850263 -1.734671309 0.009611953
 0.431834875 0.047992353 -0.046252939 0.032720437
 -0.348664622 -2.564990347 -0.859783782 0.461337666

$$b\mathbf{1}_{12(\text{asp})} = [3 \times 1] =$$

-0.612305906
 0.467205418
 -1.989658342

$$i\mathbf{w}_{12(\text{asp})} = [1 \times 3] = [-0.408212931 \quad 3.89173946 \quad 0.105976779]$$

$$b\mathbf{2}_{12(\text{asp})} = [1 \times 1] = -1.299575778$$

- **Function Class No. = 14**

$$i\mathbf{w}_{14(\text{asp})} = [4 \times 5] =$$

0.709574849 0.282267907 -0.136285271 -1.592699908 -1.680582968
 0.681710817 -0.063444727 0.285895071 0.266028644 0.379628139
 -0.090779894 0.148322811 -1.994452953 -0.287582381 -0.190932587
 1.321740072 -0.040472509 0.282077943 0.317756289 0.284851016

$$b\mathbf{1}_{14(\text{asp})} = [4 \times 1] =$$

-0.429549422
 -0.293798532

-0.295132597

2.114468334

$$lw_{14(asp)} = [1 \times 4] = [0.301108436 \quad 1.111348084 \quad 0.285209939 \quad 1.288802613]$$

$$b2_{14(asp)} = [1 \times 1] = -0.733100242$$

- **Function Class No. = 16**

$$iw_{16(asp)} = [2 \times 3] =$$

0.293518166 0.002842591 -0.574578113

5.56410423 -0.019840265 3.500922141

$$b1_{16(asp)} = [2 \times 1] =$$

-0.219206619

2.938146015

$$lw_{16(asp)} = [1 \times 2] = [3.794560636 \quad 1.920407647]$$

$$b2_{16(asp)} = [1 \times 1] = 0.71346133$$

(B) The developed ANN model parameters for Composite Pavements (COM)

Functional Class No.	Roadway Category	Weight (<i>iw</i>)	Bias (<i>b1</i>)	Weight (<i>lw</i>)	Bias (<i>b2</i>)
01	Interstate Rural	<i>iw</i> _{01(com)}	<i>b1</i> _{01(com)}	<i>lw</i> _{01(com)}	<i>b2</i> _{01(com)}
02	Principal Arterial Urban	<i>iw</i> _{02(com)}	<i>b1</i> _{02(com)}	<i>lw</i> _{02(com)}	<i>b2</i> _{02(com)}
11	Interstate Urban	<i>iw</i> _{11(com)}	<i>b1</i> _{11(com)}	<i>lw</i> _{11(com)}	<i>b2</i> _{11(com)}
12	Freeway Urban	<i>iw</i> _{12(com)}	<i>b1</i> _{12(com)}	<i>lw</i> _{12(com)}	<i>b2</i> _{12(com)}

Functional Class No.	Roadway Category	Weight (iw)	Bias ($b1$)	Weight (lw)	Bias ($b2$)
14	Principal Arterial Urban	$iw_{14(\text{com})}$	$b1_{14(\text{com})}$	$lw_{14(\text{com})}$	$b2_{14(\text{com})}$
16	Minor Arterial Urban	$iw_{16(\text{com})}$	$b1_{16(\text{com})}$	$lw_{16(\text{com})}$	$b2_{16(\text{com})}$

- **Function Class No. = 01**

$$iw_{01(\text{com})} = [7 \times 5] =$$

0.269177228 0.634588088 -0.619313821 -1.40899347 1.255907864
0.678686722 1.381213404 -1.573440524 -0.864257723 -0.519584337
-1.472345911 -2.572031772 1.458563056 1.741746182 0.911298691
2.504221237 -0.074747011 0.132455108 0.782342542 -0.933577645
-0.774007813 -1.692108058 1.229768929 1.117719696 0.626766694
1.240715946 -1.356731064 2.01206133 3.517563452 -0.188159803
-0.615382518 -0.242299159 -0.076041652 0.542046772 1.144862984

$$b1_{01(\text{com})} = [7 \times 1] =$$

-0.162232732
-0.411985263
0.657449657
2.427986768
0.634808303
1.666552687
1.018027499

$$lw_{01(\text{com})} = [1 \times 7] = [0.724615615 \quad 1.453422056 \quad -1.875174536 \quad 0.51980295$$

3.555328156 0.330652006 -0.747213811]

$$b2_{01(\text{com})} = [1 \times 1] = -0.337234831$$

- **Function Class No. = 02**

$$iw_{02(\text{com})} = [5 \times 5] =$$

1.411448153 -0.377868991 -0.092303345 0.078370299 -0.119961504

0.428332602 0.528182832 1.678707034 1.388774026 -1.70234599

-0.475130701 -2.343144722 0.155010599 -0.35351921 -0.514824194

0.478515935 -0.515538021 -0.047124579 -0.229324961 0.056733842

3.719963778 0.294047946 0.073497855 0.319061184 -0.283921476

$$b1_{02(\text{com})} = [5 \times 1] =$$

-0.150810116

-2.096614308

0.920942613

1.508484904

4.254576295

$$lw_{02(\text{com})} = [1 \times 5] = [0.405855953 \quad 0.098902316 \quad -0.331197361 \quad 1.71304983 \\ 0.73376092]$$

$$b2_{02(\text{com})} = [1 \times 1] = -2.040683413$$

- **Function Class No. = 11**

$$iw_{11(\text{com})} = [5 \times 5] =$$

4.164973314 1.667796049 -0.659888848 -0.581522041 -2.752903745
3.8577821 0.450397044 1.774800176 1.130291499 -1.150580048
-3.525833139 -0.457798656 0.244575426 1.997281005 2.517404487
2.202342684 6.417253949 3.830429881 0.995728254 -1.568911034
0.168770712 7.621388276 -1.572815093 -1.174435855 1.124377965

$$b1_{11(\text{com})} = [5 \times 1] =$$

-2.437167956
2.37413695
1.652892303
-2.164617051
9.48600954

$$iw_{11(\text{com})} = [1 \times 5] = [0.26337031 \quad 0.445388007 \quad -0.31154564 \quad -0.153811092 \\ 0.416050488]$$

$$b2_{11(\text{com})} = [1 \times 1] = -0.548216269$$

- **Function Class No. = 12**

$$iw_{12(\text{com})} = [2 \times 5] =$$

0.534204669 0.087737794 -0.065992316 0.065636395 0.312847561
0.979844591 -0.088288919 -0.033188884 -0.028929095 -0.298626356

$$b1_{12(\text{com})} = [2 \times 1] =$$

0.055410547

0.073156626

$$lw_{12(\text{com})} = [1 \times 2] = [0.604754022 \quad 0.961319246]$$

$$b2_{12(\text{com})} = [1 \times 1] = -0.049597858$$

- **Function Class No. = 14**

$$iw_{14(\text{com})} = [3 \times 5] =$$

0.551764848 -0.003884088 0.005264446 -0.012630488 0.029465243
14.55702543 0.004420367 -0.50209711 -12.05339232 -4.639821474
-5.762054359 0.116385526 0.102411995 0.082842069 0.540654015

$$b1_{14(\text{com})} = [3 \times 1] =$$

-0.080408165
3.193114169
-5.17036189

$$lw_{14(\text{com})} = [1 \times 3] = [1.743582922 \quad 0.026716733 \quad -0.129765977]$$

$$b2_{14(\text{com})} = [1 \times 1] = 0.084412457$$

- **Function Class No. = 16**

$$iw_{16(\text{com})} = [1 \times 5] =$$

[-2.207724159 -0.692095736 -0.409775912 0.626647328 0.508499662]

$$b1_{16(\text{com})} = [1 \times 1] = [-0.344154739]$$

$$lw_{16(\text{com})} = [1 \times 1] = [-0.46849547]$$

$$b2_{16(\text{com})} = [1 \times 1] = [-0.525449568]$$

(C) The developed ANN model parameters for Jointed Concrete Pavements (JCP)

Functional Class No.	Roadway Category	Weight (iw)	Bias ($b1$)	Weight (lw)	Bias ($b2$)
01	Interstate Rural	$iw_{01(Jcp)}$	$b1_{01(Jcp)}$	$lw_{01(Jcp)}$	$b2_{01(Jcp)}$
02	Principal Arterial Urban	$iw_{02(Jcp)}$	$b1_{02(Jcp)}$	$lw_{02(Jcp)}$	$b2_{02(Jcp)}$
11	Interstate Urban	$iw_{11(Jcp)}$	$b1_{11(Jcp)}$	$lw_{11(Jcp)}$	$b2_{11(Jcp)}$
12	Freeway Urban	$iw_{12(Jcp)}$	$b1_{12(Jcp)}$	$lw_{12(Jcp)}$	$b2_{12(Jcp)}$
14	Principal Arterial Urban	$iw_{14(Jcp)}$	$b1_{14(Jcp)}$	$lw_{14(Jcp)}$	$b2_{14(Jcp)}$

• **Function Class No. = 01**

$$iw_{01(Jcp)} = [4 \times 5] =$$

3.332207403 0.425195148 -0.194392242 -0.539810969 -1.165240673
 2.751362105 -0.647659708 -0.119853335 -0.45627788 -1.382604122
 2.944147049 -1.443683461 -0.144823992 -0.363579587 -1.427395561
 4.204190848 2.833010774 0.461479853 0.491777699 -0.998897896

$$b1_{01(Jcp)} = [4 \times 1] =$$

0.43282688
 0.357866437
 -0.107679128
 -1.665206304

$$lw_{01(Jcp)} = [1 \times 4] = [1.122333368 \quad -2.270068136 \quad 1.984396286 \quad 0.796987606]$$

$$b2_{01(Jcp)} = [1 \times 1] = 0.615018113$$

- **Function Class No. = 02**

$$iw_{02(Jcp)} = [5 \times 5] =$$

1.603774614 -0.906286204 -1.1416795 -0.840786008 0.983522952
 1.141565099 -0.273351019 0.467779771 0.07629874 -0.545729543
 -0.375890502 0.281525188 0.277894576 -0.124170639 0.22140033
 1.023200206 0.626843646 0.360412157 -0.217767071 0.410895043
 -0.072484183 1.289496311 1.042001152 0.642788045 0.177904104

$$b1_{02(Jcp)} = [5 \times 1] =$$

-1.615531207
 -0.335873206
 -0.585218371
 0.504437875
 2.681810917

$$lw_{02(Jcp)} = [1 \times 5] = [0.11510969 \quad 0.408260858 \quad -0.980752183 \quad 0.667040412 \\ -0.298127129]$$

$$b2_{02(Jcp)} = [1 \times 1] = -0.19332537$$

- **Function Class No. = 11**

$$iw_{11(Jcp)} = [5 \times 5] =$$

0.62652813 -0.013100234 0.002184099 0.014856307 -0.005967983
 4.965532491 -0.296397207 -1.775587429 -4.542047402 0.306935041
 -25.50795386 -0.749641689 1.517467616 5.428977207 -0.112877996

3.854940237 3.440065769 -1.428428069 1.971456871 3.462942978
7.192784215 1.103652877 -2.370667267 10.23288213 -1.216030308

$$b1_{11(Jcp)} = [5 \times 1] =$$

0.51904898
1.880108128
-22.12856046
5.0843082
8.409800346

$$lw_{11(Jcp)} = [1 \times 5] = [2.138092076 \quad 0.020316049 \quad 0.010790832 \quad 0.032166761 \\ -0.016078518]$$

$$b2_{11(Jcp)} = [1 \times 1] = -0.766553002$$

- **Function Class No. = 12**

$$iw_{12(Jcp)} = [1 \times 4] =$$

0.227179874 -0.001792371 0.004232937 0.00101699

$$b1_{12(Jcp)} = [1 \times 1] = 0.4137024$$

$$lw_{12(Jcp)} = [1 \times 1] = 5.292764017$$

$$b2_{12(Jcp)} = [1 \times 1] = -1.935001527$$

- **Function Class No. = 14**

$$iw_{14(Jcp)} = [1 \times 5] =$$

-0.533834085 0.001887079 -0.000476969 0.001294354 -0.001856218

$$b1_{14(Jcp)} = [1 \times 1] = -0.278844494$$

$$lw_{14(Jcp)} = [1 \times 1] = -2.104845728$$

$$b2_{14(Jcp)} = [1 \times 1] = -0.464208275$$